THE DESIGN OF A RESIDUAL GAS ANALYSER BASED ON A TIME-OF-FLIGHT MASS SPECTROMETER

A thesis for the degree of

MASTER OF SCIENCE

Presented to

DUBLIN CITY UNIVERSITY

By

JOHN GERARD O'DWYER B.Sc.
THE SCHOOL OF PHYSICAL SCIENCES
DUBLIN CITY UNIVERSITY

Research supervisor

DR. JOSEPH FRYAR B.Sc. Ph.D.

July 1990

DECLARATION

This thesis is based on my own work.

This thesis is dedicated to my parents, **Sean** and **Lillian**

CONTENTS

THE DESIGN OF A RESIDUAL GAS ANALYSER BASED ON A TIME-OF-FLIGHT MASS SPECTROMETER

JOHN O DWYER

ABSTRACT

A residual gas analyser is an instrument which, by ionising the ambient gas under low pressure ($<10^{-7}$ atm), enumerates the different atomic elements in the gas and measures their relative abundance. The analysis of the gas is done using a mass spectrometer, which identifies the atomic elements by separating the atoms, group of atoms or molecules according to their *mass to charge ratio*. Mass spectrometers are classified on the basis of how the atomic mass separation is accomplished. In a time-of-flight mass spectrometer the mass separation is achieved by injecting a mono-energetic ion beam, into a long electric/magnetic field free tube. The time taken to reach the end of the tube depends on the square root of the ions mass to charge ratio and so by observing the output times of whatever ions are present, the different atomic elements are revealed. The relative abundance of the elements is simply the ratio of the number of ions egressing the tube at the specific times.

This thesis describes the work carried out on the development of a new type of time-of-flight mass spectrometer for the purposes of residual gas analysis and was funded by Eolas, the Irish science and technology agency. Like the conventional type it uses a field free flight tube, however the tube is used more as a delay line rather than as the mass separator. The mass separation is achieved using a combination of time varying accelerating / decelerating electric fields at the start and end of the tube. The voltages producing these electric fields are between 0 and -200 volts D.C. and between 100 and 300 volts peak to peak A.C. at a frequency of 40 to 50kHz. The resolution obtained with the mass spectrometer is approximately ± 0.5 atomic mass units.

TERMINOLOGY

Ions: Ions are positively or negatively charged atoms, groups of atoms or molecules. They become charged by losing or gaining one or more of their electrons. Although both positive and negative ions can be studied by mass spectrometry, only positive charged ions will be dealt with, since the ion source produces them in larger quantities than negative ions by a factor of $\approx 10^3$. For the rest of this thesis "ions" denotes positive ions unless stated otherwise.

Mass to Charge Ratio: The mass to charge ratio ,m/ne, is the ratio of the mass, m, of the ion to the number, n, of electric charges, e, lost during ionization.

Mass: The mass of a body is generally understood to be a measure of matter the body contains and in physics is defined as a measure of inertia, i.e., a property of a body that determines the acceleration it will experience when acted upon by a given force. In mass spectrometery the term "mass" has several connotations which require qualification.

When equations are derived in mass spectrometery, m means mass measured in kg. For purposes of analysis, comparing masses of ions to each other is more useful than than knowing their absolute mass, therefore, a more convenient unit for mass in this case is the *atomic mass unit, u* or amu, which is defined as exactly one twelfth the mass of a $^{12}_{6}C$ atom. This second standard of mass is needed because present laboratory techniques permit comparisons of atomic masses to each other with greater precision than comparing them to the standard kilogram. The relationship is approximately

$$1 \text{ amu} = 1.66043 \text{ X } 10^{-27} \text{ kg}$$

In mass spectrometry the term "mass" or "m/e value" refers to the sum of the mass numbers of the individual atoms composing a particular ion. Although the majority of ions in a mass spectrometer are singly charged, atoms and certain molecules may loose more than one electron without disintegration. Doubly charged ions exhibit an apparent mass exactly one half that of the corresponding singly charged ion. For example, doubly charged carbon dioxide (CO_2^{2+}) appears at mass 22, triply charged argon (Ar^{3+}) at mass 13⅓. (See appendix A for a copy of the periodic table and a note on the convention for chemical symbols.)

Mass Spectrum: The mass spectrum of a sample reveals in a graphical or tabular form the measured mass to charge ratios of the separated ions and their corresponding intensities. The knowledge of the mass to charge ratios of the ions determines *what* is present, while the measured ion intensities determines *how much* is present.

Chapter 1
INTRODUCTION

In this chapter the major types of mass spectrometers are briefly described with a view to introducing the wide and varied types that have been developed over the years and to give some prospective of the place the new type described in this thesis will take. In general the mass spectrometer is used in identifying all the atoms and molecules that comprise gases, liquids and solids. Even the so-called fourth and fifth states of matter, plasmas and clusters, can be characterised by mass spectroscopic techniques [1]. They have found applications in physics, chemistry, biology, pharmacology, agriculture, geology, metallurgy, environmental science etc. and are therefore quite an important instrument to science. Mass spectrometers are usually classified on the basis of how the mass separation is accomplished, whether it is by using magnetic and/or electric fields.

MAGNETIC ANALYSERS

180° sector

This device, originally reported by Dempster in 1918 [2] and still widely used, is shown in figure 1.1 overleaf. The basic principle of operation is as follows; ions given a certain initial velocity are injected into a magnetic field B perpendicular to their velocity vector. The ions will be deflected into a circular orbit which, assuming the ions are singly charged, is given by

$$Be\nu = \frac{M\nu^2}{R} \qquad \text{or} \qquad R = \frac{M\nu}{Be}$$

where R is the radius of curvature, e is the electric charge, ν is the velocity of the ions and M represents

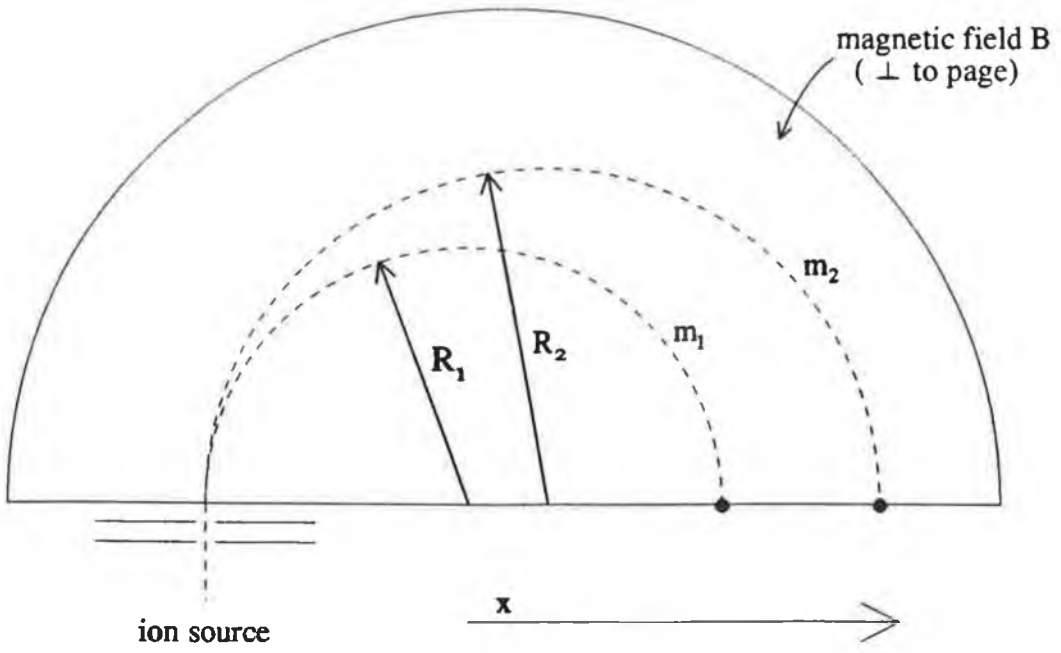

Figure 1.1
Ion trajectories in a homogeneous magnetic field 180° sector

their mass. Keeping ν and B constant the radius and hence the position along the x axis which the ions reach, depends on the mass to charge ratio of the ions.

There are several desirable features of this spectrometer. The ion trajectories lie completely within the analysing B field so there are no field boundary or edge effects to account for. Ions of all masses are deflected onto the 180° plane so that the simultaneous readout of the mass spectra can be recorded. In fact, work by Bainbridge on the reaction $^{1}H + {}^{7}Li \rightarrow 2\,{}^{4}He$ using this spectrometer provided the first experimental proof of the Einstein mass-energy relationship [3].

There are however limitations with this arrangement particularly with the sharpness of the line image arising from the divergence angle of the input ions. To overcome this problem the ions have to be restricted to small angles.

The 60° sector

The 60° magnetic sector proposed by Nier in 1940 [4] is shown in figure 1.2. The underlying principle, of deflecting the ion beam by a magnetic field is the same as

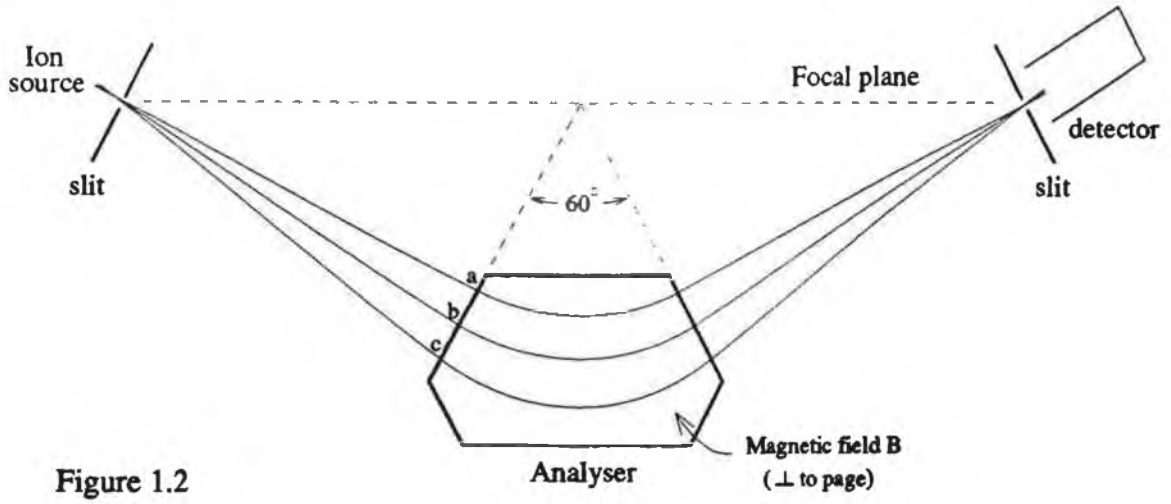

Figure 1.2
The 60° Magnetic sector

the 180° sector above, but in addition it provides a sharper focusing effect, removing the limitations due to using a diverging ion beam. The focusing occurs because ions entering at point a spend less time in the B field than ions entering at point c and so are deflected less. The geometry is such that ions of the same mass entering the spectrometer at different angles all converge at one point on the focal plane. By either altering the position of the detector along the focal plane or varying the magnetic field strength, the different ion masses are selected.

This configuration was used in many of the instruments built by General Electric for the Oak Ridge National Laboratory in the US during World War II [1] and for several decades after was the standard in hundreds of commercial instruments.

The 90° sector

This is another useful configuration popular for its small radius of curvature (≈5cm) and has found extensive use as partial pressure gas analysers, leak detectors, breath analysers etc. [1] because of its small size. Figure 1.3 shows the layout. Its operation is similar to that of the 60° sector. Corrections must be made to the object and image distances to account for the fringing field in order to focus the ions properly. Often this is

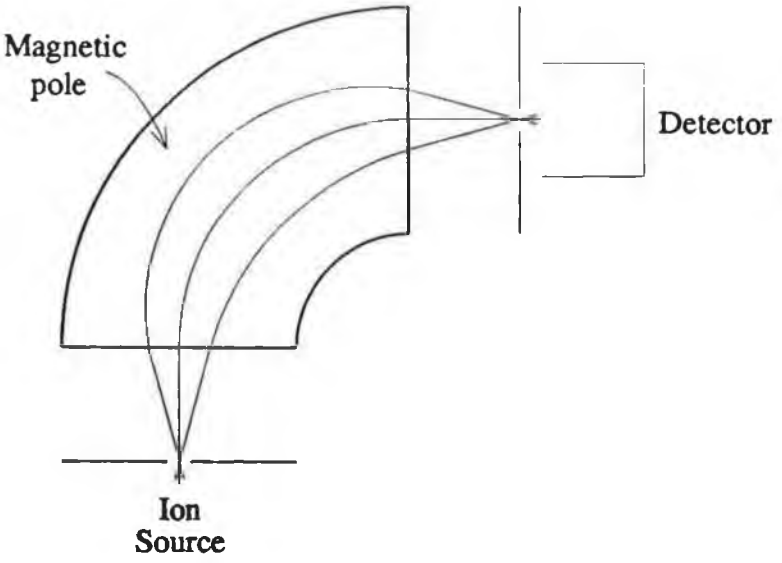

Figure 1.3
The 90° magnetic sector

done experimentally with the magnet being displaced in small steps with respect to the analysing tube. This type of analyser was used by Davis in 1962 to measure the partial pressure of gases down to 10^{-16} mbar [5]. Such a pressure corresponds to a density approximating only 1 molecule per cm^3, a pressure presumed comparable to that of outer space!

There is no reason why sector magnets of any angle cannot be constructed, but the 180°, 60° and 90° ones have become somewhat standard. In modern instruments ion entrance angles and trajectories are determined by fringe field mapping and computer calculations.

ELECTROSTATIC ANALYSERS

Quadrupole mass filter

The quadrupole is termed as a mass filter rather than a spectrometer because it transmits ions having only a narrow range of mass to charge values and attenuates all others rather like an electrical bandpass filter. It can be used as a spectrometer by varying the electrical parameters to vary the mass to charge ratio which it will transmit, with a trade-off made between transmission and resolution. Figure 1.4 shows the analysing section of the

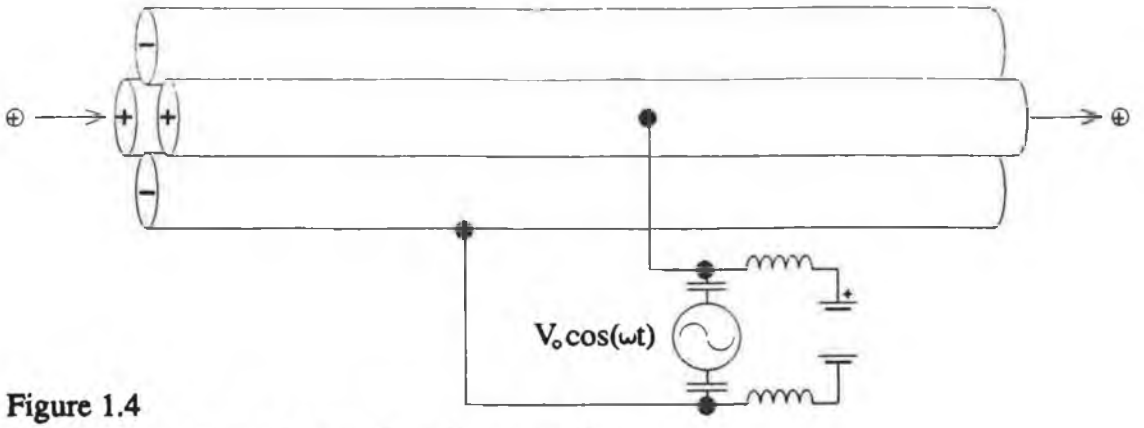

Figure 1.4
Analysing section of a quadrupole mass filter

quadrupole. Ideally the electrodes should be of hyperbolic cross-section, however cylindrical rods are easier to manufacture and are satisfactory provided they are spaced correctly. The rods are typically 8mm in diameter and 200mm long with a 7mm separation between opposite rods [6]. By proper selection of potentials and frequency, an ion of desired mass can be made to pass through the system, while unwanted masses will undergo an oscillating trajectory of increasing amplitude perpendicular to the major axis so that they will ultimately be collected on one of the electrodes. Values of the supply voltages range from 0 to 800v p-p for the radio-frequency source and 0 to -140v for the D.C. source. Frequencies are typically between 3 and 4 MHz [6].

In practical quadrupoles there is a limit on the angular divergence of an entering ion and the performance is also dependant upon the fringing fields at the entrance and exit apertures. There are also strict mechanical and electrical requirements for good resolution. The electrode rods must have an extremely uniform cross-section and must be positioned parallel to each other with a tolerance of only a few microns. The amplitudes of the voltages must, at least, be stable to 1 part in 10^5 and stability must be 1 part in 10^3 for frequency [6].

Its main advantages are: (1) independence from the energy distribution of the ion beam (below a limiting value), (2) high transmission rate (particularly at low

resolution), and (3) opportunity for fast scanning.

Energy balance spectrometer

The Bennett rf spectrometer [7] was one of the first energy balance type developed. Its operation is similar to a linear accelerator and is shown in figure 1.5. Ions of a known energy are drawn into the first stage, which consists of three grids all at the same dc potential. An additional rf component is added to the middle grid G_2 so that equal and opposite rf fields are established between grids G_1,G_2 and G_2,G_3. Only ions which take exactly one cycle to transverse between G_1 and G_3 and which enter when the rf voltage is changing polarity, will lose no energy. In addition, the ions whose time of flight in the field free region is equal to an integral multiple of the rf period (adjusted by $-V_{dc}$) will remain at the same energy as they progress toward successive stages and so mass separation will be improving. A retarding grid G_r at the end of the tube allows only the highest energy ions to reach the detector.

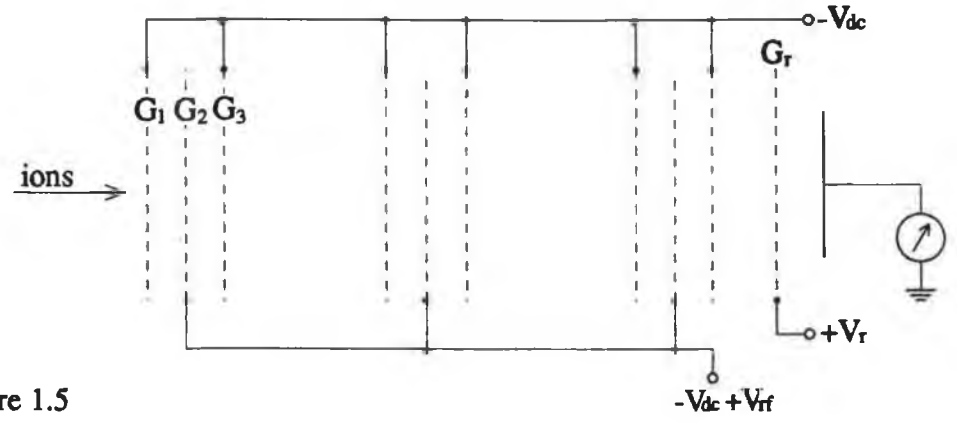

Figure 1.5
Bennett rf mass spectrometer

The main advantages of this spectrometer are absence of a magnet and the general simplicity making it ideal for use in upper atmosphere research. Other applications include residual gas analysis and analysis of ions in flames [6].

Time of flight spectrometer

The principle of the time-of-flight (TOF) mass spectrometer was first proposed by Stephens in 1946 [8] and a commercial prototype was subsequently developed by Wiley and M^{c}Laren in 1955 and manufactured by the Bendix Corporation [9].

The TOF spectrometer is rather straightforward and is shown in figure 1.6. The ions, generated in packets, are accelerated by passing them through a fixed electric potential into a time of flight tube. The energy gained

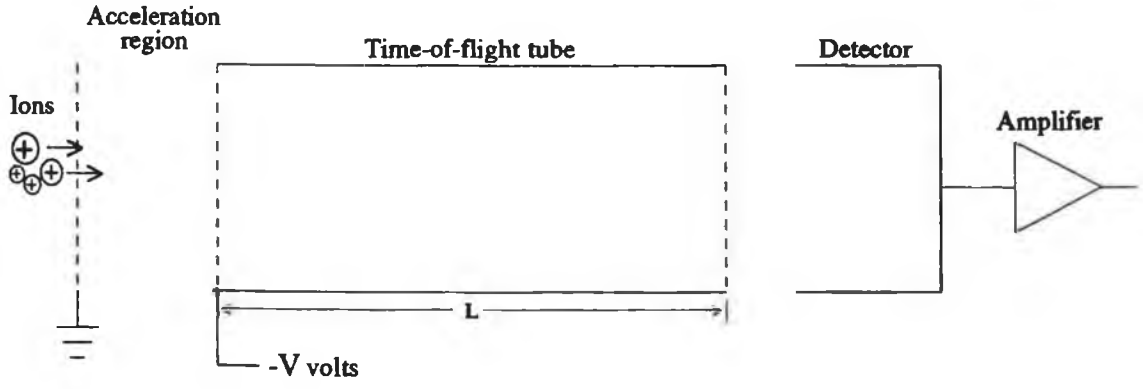

Figure 1.6
Schematic diagram of conventional time-of-flight mass spectrometer

by a singly charged ion passing through the electric field is

$$\text{Energy Gained} = eV$$

where e is the charge on the electron and V is the potential difference through which the ion passes. Assuming that the initial energy of the ion is close enough to zero to be ignored this expression represents the total kinetic energy of the ion i.e.

$$K.E._{ion} = eV$$

$$\Rightarrow \quad \tfrac{1}{2}mv^2 = eV$$

$$\Rightarrow \quad v = \sqrt{\frac{2eV}{m}}$$

where m is the mass of the ion (in kg) and v is the final

ion velocity. The ion velocity is inversely proportional to the square root of the ion's mass, so light ions travelling into the time of flight tube have a higher velocity than heavier ones, therefore they arrive at the end of the tube first at a time given by

$$t = \frac{L}{v}$$

$$\Rightarrow \quad t = \sqrt{\frac{L^2}{2V} \cdot \frac{m}{e}}$$

where L is the length of the tube. By timing the emergence of the ions a complete mass spectrum can be drawn up. The timings between the different ion bunches will depend on the tube length, the accelerating voltage and on the ion masses, however it is desirable to have the time differences large in order to improve resolution and to avoid the problems involved with using ultra high speed electronics for the detection of the ions. Typically the accelerating voltage is ≈3kV with a tube length of ≈1 meter [6], so in order to have a resolution of 1 amu at 100 amu, ion bunches of approx. 65nS apart need to be resolved. Clearly the ion packets, injected into the time of flight tube at the start, should be kept as short as possible so that the mass separated ion bunches at the detector are equally as short. The reason such a high tube voltage is used, is because the ion energy spread going into the tube will be a smaller percentage of the total energy than if a lower tube voltage was used, thus reducing the spread in arrival times for individual ion bunches.

Chapter 2
THEORY

This chapter will describe the operation of the new mass spectrometer, beginning with a simple account in the following section and introducing more detail later.

Theory of operation

The new mass spectrometer differs from the conventional type in three respects. Firstly, and most importantly the tube voltage is time dependant. It's general form is

$$V = F(t) = A + B\cdot\cos(2\pi ft)$$

where f is the alternating frequency, B is the peak A.C. voltage, and A is a D.C. component. Secondly the ions, instead of travelling directly to the detector after leaving the tube, are decelerated by a grid at ground potential placed between the tube and the detector. Thirdly the ions may be injected into the time of flight tube at any time i.e. the mass spectrometer will accept a continuous input ion beam. Figure 2.1 outlines the basic structure.

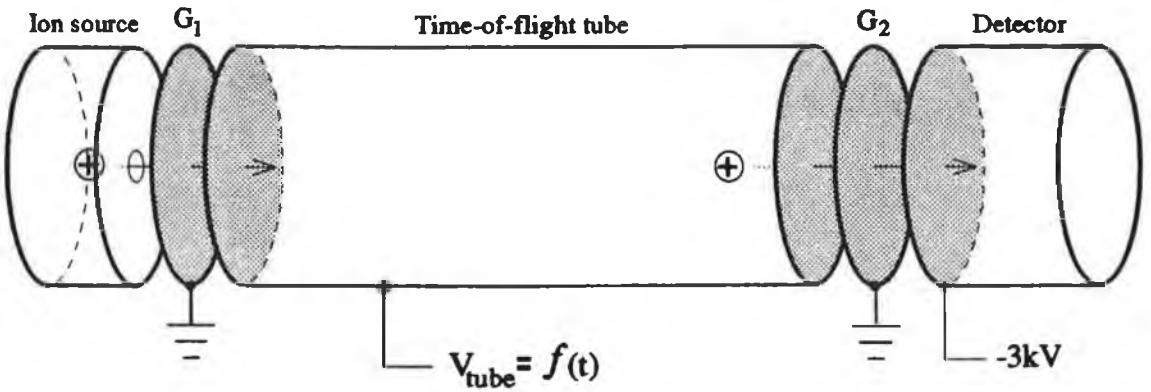

Figure 2.1
Basic diagram of new mass spectrometer

Its operation is as follows: Ions emerge from the source through the grounded grid G_1 and enter the tube with an energy in electron-volts equivalent to the tube voltage at that time (ignoring any initial ion energy). They travel down the tube and arrive at the far end after a time t_{tof} similar to that of the conventional time of flight, namely

$$t_{tof} = \sqrt{\frac{L^2 m}{2Ve}}$$

but within this time the tube voltage will have altered and depending on whether it is larger or smaller will decide whether the ion will pass grid G_2 or not. To clarify this, figure 2.2 below shows the times of flight for ions (a),(b) and (c), of equal mass, starting out from grid G_1 at different times.

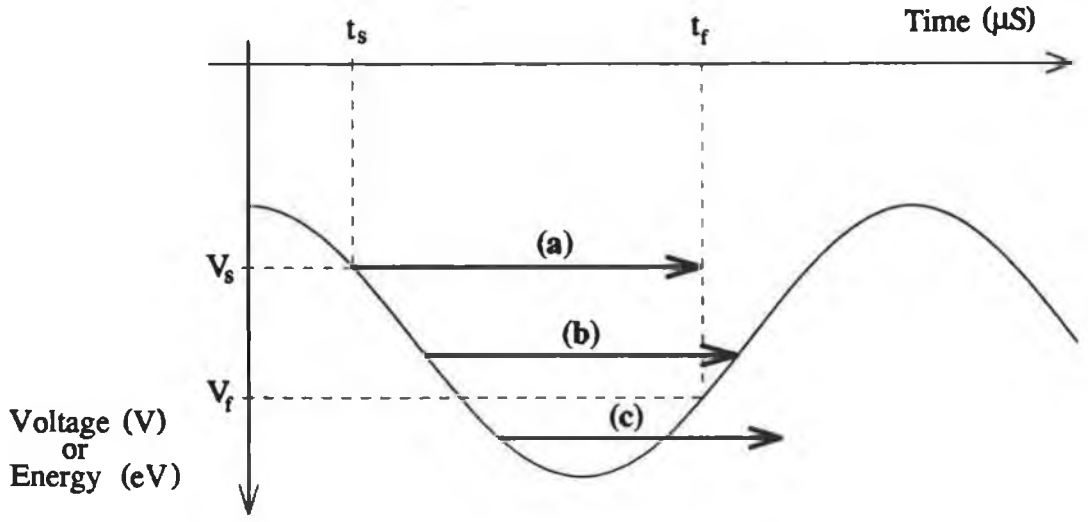

Figure 2.2
Diagram to demonstrate tube voltage/ion energy *vs* time, for a number of ion starting times

Concentrating on ion (a), it can be seen that starting at a time t_s, it enters the tube with an energy of V_s electron-volts. It travels down the tube and arrives at the far end after a certain time indicated by the length of the arrow. At time t_f the voltage on the tube is V_f, thus any ion which is to pass grid G_2 at this time must possess a kinetic energy equal to or in excess

of V_f electron-volts. Since V_f is larger in magnitude than V_s the ion is accelerated back into the tube and lost. In the case of ion (b), V_f is equal to V_s and so the ion's axial velocity is unaltered by the passage between G_1 and G_2 and once passed G_2 is accelerated towards the detector. V_f for ion (c) is less in magnitude than V_s and consequently the ion has more than enough energy when it arrives at the end of the tube to overcome the retarding electric field and pass G_2.

Figure 2.3 below shows the locus of all the t_f,V_f points for a continuous ion beam.

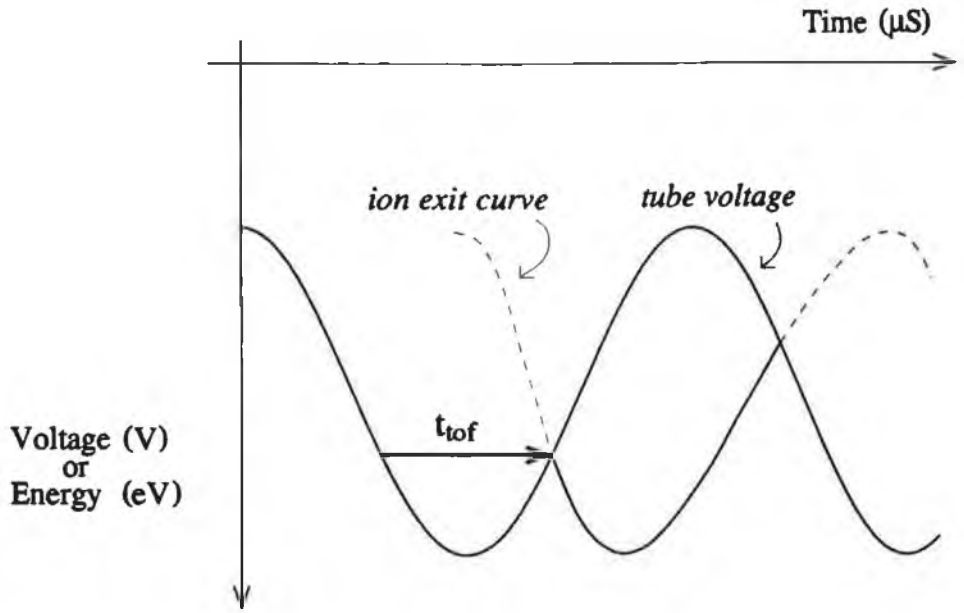

Figure 2.3
Typical ion exit curve

It is essentially a graph of the energy of the ion within the tube *vs* the time it arrives at the end of the tube. The dashed line indicates that the ion does not pass grid G_2. The point at which the ions start to cross G_2 occurs when the ion's time of flight across the tube corresponds to the time it takes the voltage on the tube to decrease to a minimum and rise back to the same value it was at when the ion entered, indicated as t_{tof}. This observation allows the calculation of the time at which the ions first appear at the detector relative to time zero at the crest of the a.c. tube voltage. Designating t_s as the ion entry time and t_f as the ion exit time, at the breakthrough time

the following equation holds;

$$V(t_s) = V(t_f)$$

$$\Rightarrow \quad A + B\cos(\omega t_s) = A + B\cos(\omega t_f)$$

$$\Rightarrow \quad \cos(\omega t_s) = \cos(\omega t_f)$$

Solving this equation between 0 and 2π, knowing $t_s \neq t_f$, yields the solution: $t_f = T - t_s$, where T is the AC period. Now,

$$t_{tof} = t_f - t_s \quad \text{and} \quad t_{tof} = \sqrt{\frac{L^2 m}{2eV}}$$

$$\Rightarrow \quad \sqrt{\frac{L^2 m}{2eV}} = t_f - t_s$$

$$= 2t_f - T$$

$$\Rightarrow \quad \frac{L^2 m}{2eV} = (2t_f - T)^2$$

but $V = A + B\cos(\omega t_f)$

$$\Rightarrow \quad \boxed{\cos(\omega t_f) = \frac{L^2 m}{2eB(2t_f - T)^2} - \frac{A}{B}}$$

This equation can only be solved by using numerical techniques. One such technique is to approximate a value of t_f, fit it into the equation and by comparing both sides, successive values of t_f are determined which after several iterations converge to the correct value. This value is then the "time of flight" for an ion of mass m with respect to the peak of the cosinsoidal tube voltage.

As can be seen in figure 2.3 the exit curve of the ion crosses back across the tube voltage curve approximately half a period later and the process is repeated, but it should be noted that the exit curve is not sinusoidal since the time of flight of ions starting at low values of V_s will be longer than those starting at larger values. Ions of different atomic mass will have different exit curves. Figure 2.4 (a) overleaf illustrates this for two masses M_1 and M_2. Figure 2.4 (b)

shows the ion current that reaches the detector, with, as an example, ions of mass M_2 being twice as numerous as those of mass M_1. Figure 2.4 (c) shows the differentiated ion current at the detector (ignoring negative peaks).

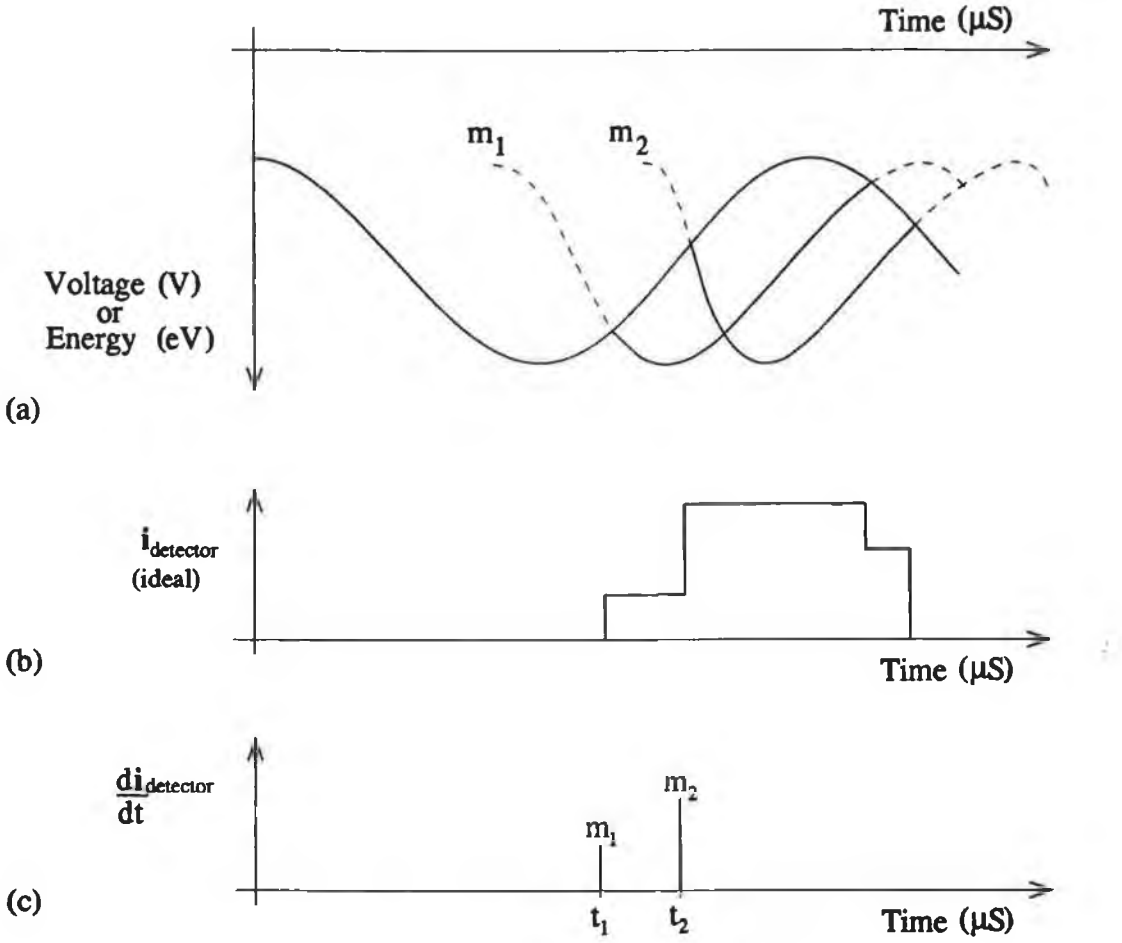

Figure 2.4

Diagram showing the sequence of events leading to a mass spectrum

Differentiating the detector current will therefore yield a time resolved mass spectrum with the lighter ions appearing first and the height of the peaks indicating their relative abundance. Since the a.c. component of the tube voltage is alternating at typically 45kHz, a mass spectrum is produced forty five thousand times a second. Time zero is chosen arbitrarily at the crest of the tube a.c. voltage and all timings henceforth are given relative to this point.

Refinements to the model

The description given above has not addressed two important factors which are needed for calculating the timing of the mass peaks accurately. The first of these is the finite time taken by the ions to cross between the grids and the time-of-flight tube. Because the tube voltage is time dependant, the voltage changes while the ion is being accelerated with the result that the ion's energy in electron-volts will not equal the tube voltage at the time it enters the tube (except at two discrete points). Similarly the ion energy (in eV) which is required to pass grid G_2 will not equal the tube voltage at the time it leaves the tube. The second factor that must be accounted for is the initial energy of the ion that has been up to now ignored for the purposes of illustration. This initial energy or velocity will also alter the energy of the ion entering the tube at a given time.

Consider the situation depicted in figure 2.5.

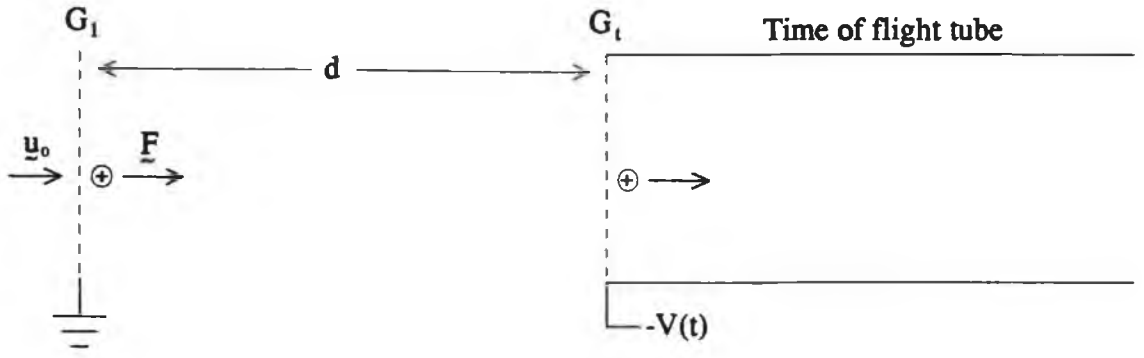

Figure 2.5
Ion acceleration region

An ion crosses grid G_1 at time t_o with an initial velocity U_o. It experiences a force F towards grid G_t which is given by

$$F = - \frac{eV(t_o)}{d}$$

where $V(t_o)$ is the tube voltage at time t_o, d is the separation between the grids and e is the charge on the electron. The instantaneous acceleration experienced by

the ion of mass m, at time t_o, is therefore

$$a_o = - \frac{eV(t_o)}{dm}$$

As the ion is in transit between the grids this acceleration is changing and by time t_e, the time it reaches grid G_t, the acceleration will be

$$a_e = - \frac{eV(t_e)}{dm}$$

It is possible to calculate the ion's velocity on reaching grid G_t directly from integration of Newton's 2nd law which gives impulse of force equals change in momentum, however in order to keep the same format of calculation throughout this section it is preferable to calculate the velocity from first principles. The first step is to fragment the time taken to cross between the grids into increments of time, Δt, then calculate the velocity after each Δt and take the limit as Δt tends towards zero. The velocity of the ion after the first increment is given by

$$U_1 = U_o + a_o \Delta t$$

Similarly the velocity after the second and third increment are, respectively

$$U_2 = U_1 + a_1 \Delta t = U_o + a_o \Delta t + a_1 \Delta t$$
$$U_3 = U_2 + a_2 \Delta t = U_o + a_o \Delta t + a_1 \Delta t + a_2 \Delta t$$

Thus the velocity after the nth increment is

$$U_n = U_o + a_o \Delta t + a_1 \Delta t + \cdots\cdots + a_{n-2} \Delta t + a_{n-1} \Delta t$$

$$\Rightarrow \quad U_n = U_o + \sum_{k=0}^{n-1} a_k \Delta t$$

Taking the limit as Δt tends towards zero between the limits t_o and t_e, the final velocity is then

$$V = U_o + \int_{t_o}^{t_e} a(t)\, dt$$

given that $a(t) = -\frac{eV(t)}{dm} = -\frac{e}{dm}\left(A+B\cos(\omega t)\right)$

$$\Rightarrow \quad V = U_o - \frac{eA}{dm}\int_{t_o}^{t_e} dt \; - \; \frac{eB}{dm}\int_{t_o}^{t_e} \cos(\omega t)\, dt$$

$$\Rightarrow \quad \boxed{V = U_o - \frac{eA}{dm}(t_e - t_o) - \frac{eB}{dm\omega}\left(\sin(\omega t_e) - \sin(\omega t_o)\right)}$$

This expression has to be solved numerically. It gives a value of ion velocity crossing into the time of flight tube provided the initial ion velocity (U_o), the time the ion crosses grid G_1 (t_o) and the time the ion reaches grid G_t (t_e) are known. In order to find the latter, which itself depends on t_o and U_o we have to consider the equation for distance travelled under acceleration i.e.

$$s = ut + \tfrac{1}{2}at^2$$

$$s+\Delta s = u(t+\Delta t) + \tfrac{1}{2}a(t+\Delta t)^2$$

$$\Delta s = \left(u + at + \tfrac{1}{2}a\Delta t\right)\Delta t$$

Again breaking the transit time into increments of Δt, the distance covered during the first increment is

$$\Delta S_1 = \left(U_o + \tfrac{1}{2}a_o\Delta t\right)\Delta t$$

and the distances covered during the second and third increment are, respectively

$$\Delta S_2 = \left(U_o + a_o\Delta t + \tfrac{1}{2}a_1\Delta t\right)\Delta t$$

and $$\Delta S_3 = \left(U_o + a_o\Delta t + a_1\Delta t + \tfrac{1}{2}a_2\Delta t\right)\Delta t$$

so, the distance covered after the nth increment is

$$S_n = \Delta S_1 + \Delta S_2 + \cdots\cdots + \Delta S_{n-1} + \Delta S_n$$

i.e.

$$S_n = \sum_{k=1}^{n}(U_o\Delta t) + \sum_{k=1}^{n}\left\{\sum_{j=0}^{k-1} a_j \Delta t\right\}\Delta t + \frac{1}{2}\sum_{k=0}^{n}\left(a_k \Delta t\right)\Delta t$$

again taking the limit as Δt tends towards zero between the limits t_o and t_e, the total distance covered by the ion is

$$S = U_o\int_{t_o}^{t_e} dt + \int_{t_o}^{t_e}\int_{t_o}^{t} a(t)\, dt\, dt$$

Note: the third term in the equation for S_n disappears in the limit. Substituting the expression for acceleration into the above equation gives

$$S = U_o\int_{t_o}^{t_e} dt - \int_{t_o}^{t_e}\int_{t_o}^{t} \frac{e}{dm}\left(A + B\cos(\omega t)\right)dt\, dt$$

$$S = U_o(t_e - t_o) - \frac{eA}{2dm}(t_e^2 - t_o^2) + \frac{eAt_o}{dm}(t_e - t_o) + \frac{eB}{dm\omega^2}\left(\cos(\omega t_e) - \cos(\omega t_o)\right) + \frac{eB\sin(\omega t_o)}{dm\omega}(t_e - t_o)$$

Again numerical techniques are required to solve this equation, so by successively approximating t_e, knowing t_o and that S should equal d, t_e may be evaluated. This value can then be used to estimate the ion's final velocity.

Knowing the ion's velocity into the tube the time of flight along the tube is simply

$$t_{tof} = \frac{L}{V}$$

where L is the length of the tube.

On emerging out of the far end of the tube, the ion is subjected to a time dependant electric field in the opposite direction. The equations to calculate whether the ion has enough energy to cross the final grounded grid (G_2 in figure 2.1) are much the same as above except the

acceleration is negative. The equations for Δs are

$$\Delta S_1 = \left(V - \frac{1}{2} a_o \Delta t\right)\Delta t$$

$$\Delta S_2 = \left(V - a_o \Delta t - \frac{1}{2} a_1 \Delta t\right)\Delta t$$

$$\Delta S_2 = \left(V - a_o \Delta t - a_1 \Delta t - \frac{1}{2} a_2 \Delta t\right)\Delta t$$

etc..

Where V is the velocity of the ion within the tube. This leads to the equation for distance between the tube and G_2

$$S = U_o(t_e - t_o) + \frac{eA}{2dm}(t_e^2 - t_o^2) - \frac{eAt_o}{dm}(t_e - t_o) - \frac{eB}{dm\omega^2}\left(\cos(\omega t_e) - \cos(\omega t_o)\right) - \frac{eB\sin(\omega t_o)}{dm\omega}(t_e - t_o)$$

this is the same as before apart from the changes in sign of some of the terms. The times t_o and t_e refer now to the time the ion emerges from the tube and the time it reaches G_2 respectively. Again t_e is determined by successively approximating it, knowing t_o and that S should equal the distance between the tube and grid G_2. If the ion has insufficient kinetic energy to cross G_2 then S will never equal this distance and will go negative for large enough values of t_e.

The breakthrough time is then given as the earliest time the ions start to cross G_2 (plus the time required to travel between G_2 and the detector). The computer programs used to calculate these times are given in appendix D. It must be said however that the breakthrough times are generally not linear with time or TOF tube voltage and the degree of non-linearity depends on the TOF tube parameters such as frequency, the magnitude of the AC and DC voltages, tube length etc. The solution to this is to either choose tube parameters to reduce the non-linearity to a minimum or to adjust the spectrum data after it has been gathered.

Changing the parameters

Up to now the mass spectrometer basically consisted of a grounded grid, a time-of-flight tube followed by a second grounded grid all between an ion source and detector, and this was indeed how the first version of the mass spectrometer looked. The ion source was a commercial electron bombardment type, the detector an electron multiplier and the time-of-flight tube was a spare piece of copper plumbing pipe! In this section the upgraded version of this first model is introduced, including such additions as electrostatic focusing and field penetration cancellation. The dependence of the spectrum on various parameters such as tube length, A.C. frequency, A.C. amplitude, D.C. bias voltage etc. are also investigated.

The ions generated in the source have a certain axial velocity on leaving, U_o in the previous section, however the ions will also have a certain radial velocity ranging from zero upwards and the effect of this is that the ion beam diverges as it travels outward from the source. For the mass spectrometer to function as best as possible it is desirable to have a parallel beam of ions or at least keep the divergence low enough so that the beam "spot size" doesn't grow larger than the active surface area of the detector by the time it reaches it (see figure 2.6 below).

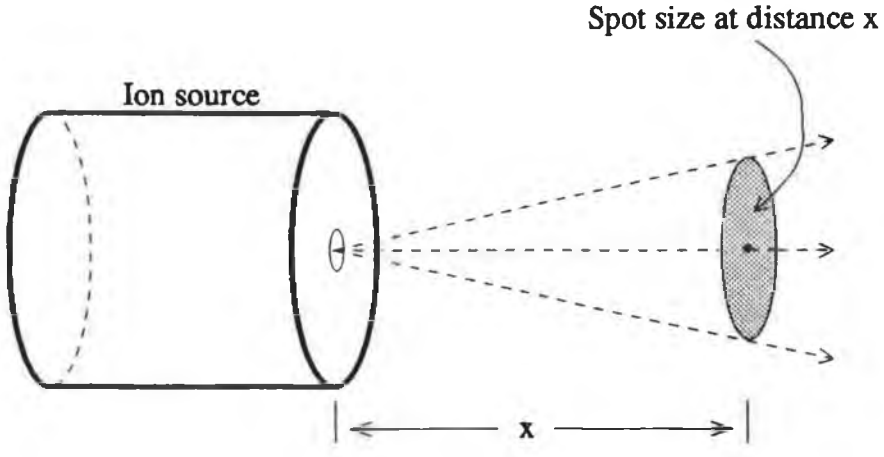

Figure 2.6
Divergence of the ion beam (not drawn to scale)

This requirement is hindered by the fact that the voltage on the tube is varying, since this will tend to cause a time dependent focusing effect, modulating the spot size at the frequency of the tube voltage. For this reason, instead of the grounded grid immediately after the ion source (G_1) and a grid on the input of the time-of-flight tube, a three element electrostatic lens is fitted, using the time-of-flight tube as the final element (see figure 2.7).

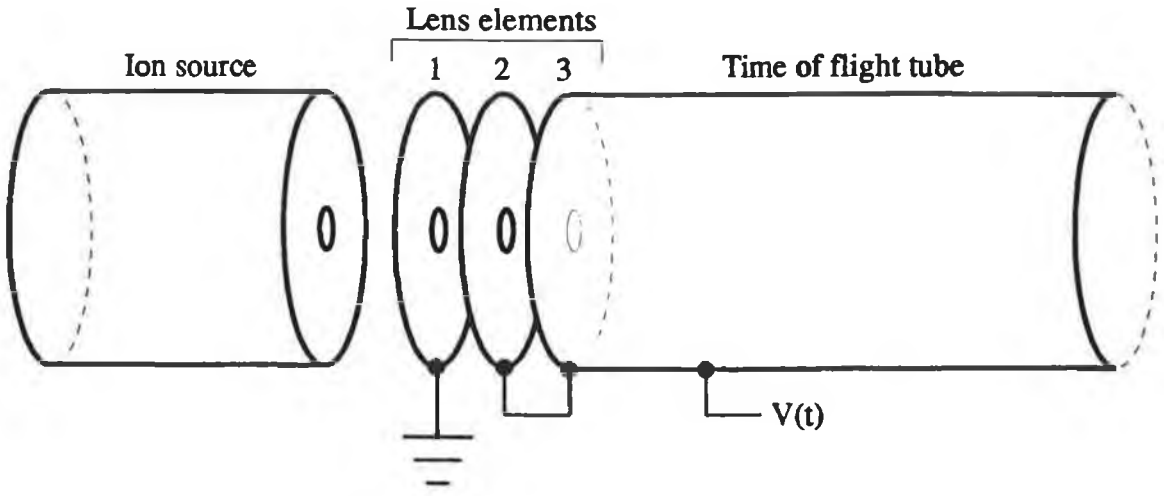

Figure 2.7

The electrostatic lens at the entrance of the TOF tube

The physical dimensions of the lens elements were worked out using graphs and tables of standard lens systems [10]. The analysis given in the previous section for calculating the (axial) velocity of the ions entering the tube still holds when using the lenses, with the distance between element 1 and 2 replacing the distance between the grids.

The second modification made to the original design is at the far end of the time-of-flight tube. The electron multiplier, used to detect the ions, operates at a bias potential of -3kV and the time-of-flight tube at a potential in the region of -100V to -200V. Because of the large difference between the electric fields on each side of G_2 and the finite size of the grid spacings, a certain amount of field penetration occurs. This leads to non-uniformities in the electric field between the time-of-flight tube and grid G_2 leading to a possible

degradation of the mass spectrum. In order to overcome this problem an additional grid is placed between G_2 and the electron multiplier tube at the same potential as the time-of-flight tube (see figure 2.8). This will reduce the amount of field penetration into the spacing d_1 while having no effect on the operation of the mass spectrometer. It will however affect the flight time between G_2 and the electron multiplier and will of course have to be taken into account in calculating the detection times of the mass peaks.

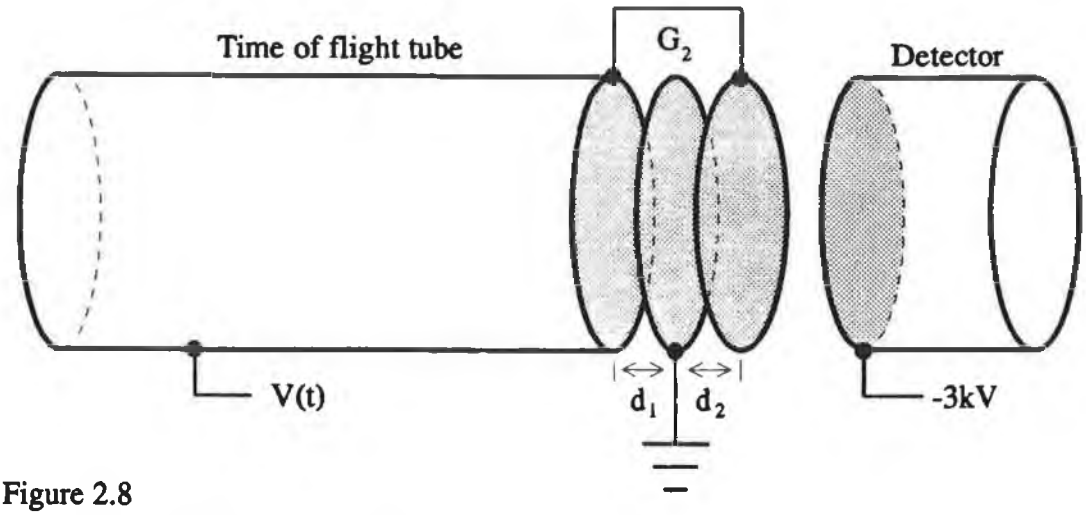

Figure 2.8

Schematic diagram showing the grids at the end of the TOF tube

The dependence of the mass spectrum on the various different parameters, such as tube voltage, tube length etc., is best shown by example. Take N_2^+ with an atomic mass of 28 amu. Figure 2.9 overleaf shows a computer printout of the calculated exit curve for the parameters shown. The jump in the exit curve occurs because the computer program plots the time the ion either comes to rest or is detected. Since it has to travel an extra distance once it makes it past G_2 the exit curve must jump at this point to accommodate this. The exit curve is mapped 10V higher than its real position for clarity (the initial ion energy of 10eV means that the maximum and minimum exit energy of the ions is 110eV and 210eV respectively).

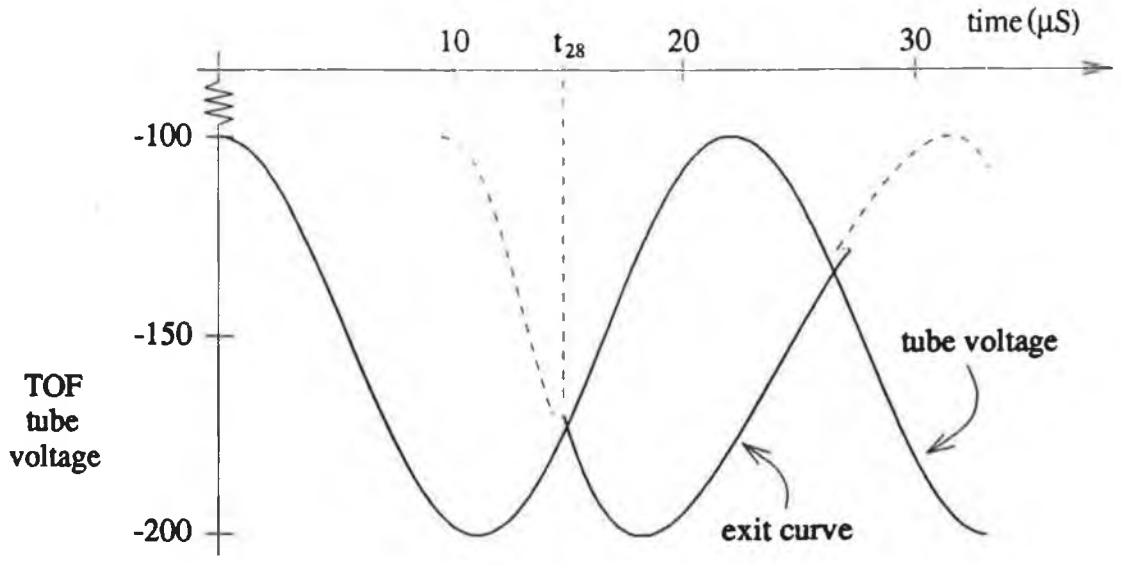

F_{tube} = 45kHz , L_{tube}=25cm

Figure 2.9
Computer simulation of N_2^+ exit curve

Figure 2.10 below is a table showing the effects of varying the different parameters on the breakthrough time i.e. the mass peak time indicated as t_{28} in figure 2.9. The table demonstrates that varying any of the parameters has an effect, to various degrees, on the breakthrough time of the ion, however none of the parameters is

Tube parameters					Breakthrough time for N_2^+ (t_{28}) (in μS)
Frequency (kHz)	AC amplitude (V_{p-p})	DC magnitude (V)	Length (mm)	tube to G_2 spacing (mm)	
45	100	-150	250	4	14.96
50	100	-150	250	4	13.95
45	200	-150	250	4	14.85
45	100	-200	250	4	14.83
45	100	-150	260	4	15.12
45	100	-150	250	5	15.00
45	100	-173	260	4	14.96
45.5	120	-140	250	4	14.96
43.3	100	-152	200	3.5	14.96

Figure 2.10

critical since if one varies the others can be adjusted to give the same result. This is illustrated at the bottom of the table, with t_{28} remaining the same for the three sets.

Ion breakthrough current

All the discussion so far has centered on the timing of the mass peaks and on the detection of particular ionic species, however there is another important parameter of any mass spectrometer; that is the measurement of the relative abundance of the different ions. At first glance it may seem simply a matter of measuring the relative heights of the mass peaks, however a closer look will reveal that this is not so. Figure 2.11 (a) overleaf is a computer simulation of the exit curves of ions of mass 10 and 100 amu under the given parameters and part (b) shows the calculated detector current that should appear, assuming both ion masses are equally abundant. The detected ion current can be obtained from the slope of the ion exit curve (solid line only), a larger slope generally indicating a larger ion current. The precise relationship between the two is

$$I_{detected} = I_{in} \left| \frac{M_{slope}}{-\omega B.\sin(\omega t_{in})} \right|$$

where I_{in} is the input ion current into the mass spectrometer (assumed constant), M_{slope} is the slope of the ion exit curve at a particular point, and t_{in} is the time an ion would have to enter the spectrometer in order to arrive at the point of interest on the ion exit curve. As can be seen the detected current depends not only on the slope of the exit curve but also on the tube voltage at the time the ion enters. The derivation of this equation is given in appendix F.

Differentiating the current to obtain mass peaks is therefore going to indicate a larger abundance of 100 amu ions than 10 amu ions. The solution to this is to multiply each peak by a correcting or adjustment factor to compensate for the difference, making all the peaks the

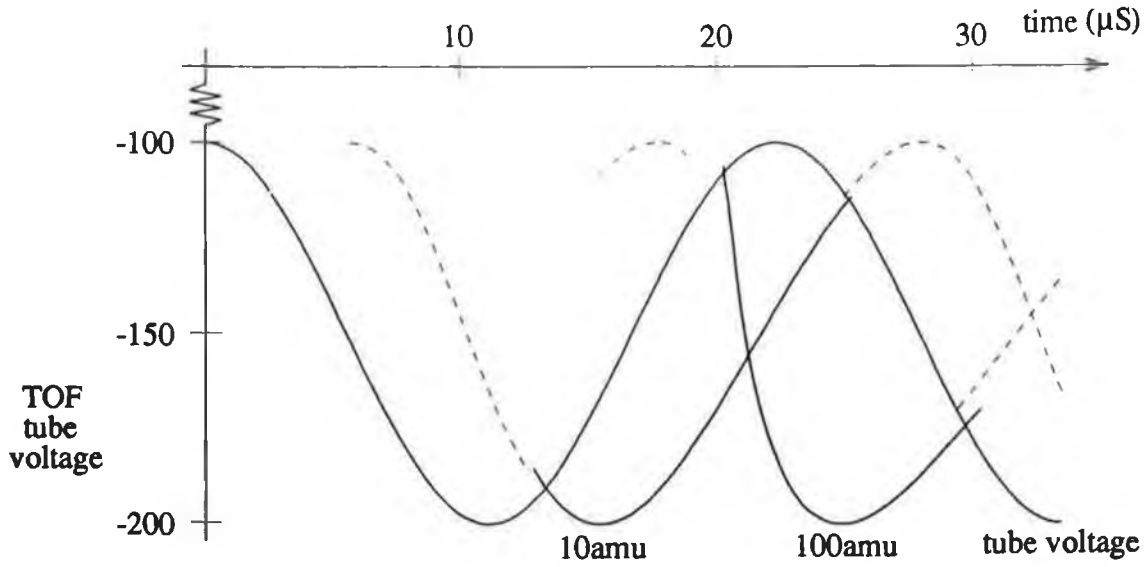

F_{tube} = 45kHz , L_{tube} =25cm

(a) **Computer simulation of exit-curves for masses 10 and 100 amu**

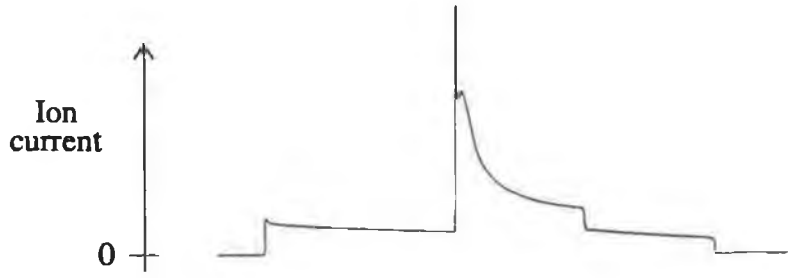

(b) **Computer simulated detected current for the same 10 and 100 amu masses, of equal abundance**

Figure 2.11

same height for equal quantities of each ion mass. This has been done using the computer simulations but has never been tested experimentally. Figure 2.12 overleaf shows a graph of the height adjustment factor (HAF) versus atomic mass.

If $H(m)$ is the height of the mass peak for an ion of mass m then the true height of the peak is

$$h(m) = HAF(m) \cdot H(m)$$

This product can be easily calculated using a computer equipped with a look-up table of values for HAF(m). The HAF will be different for different TOF tube parameters.

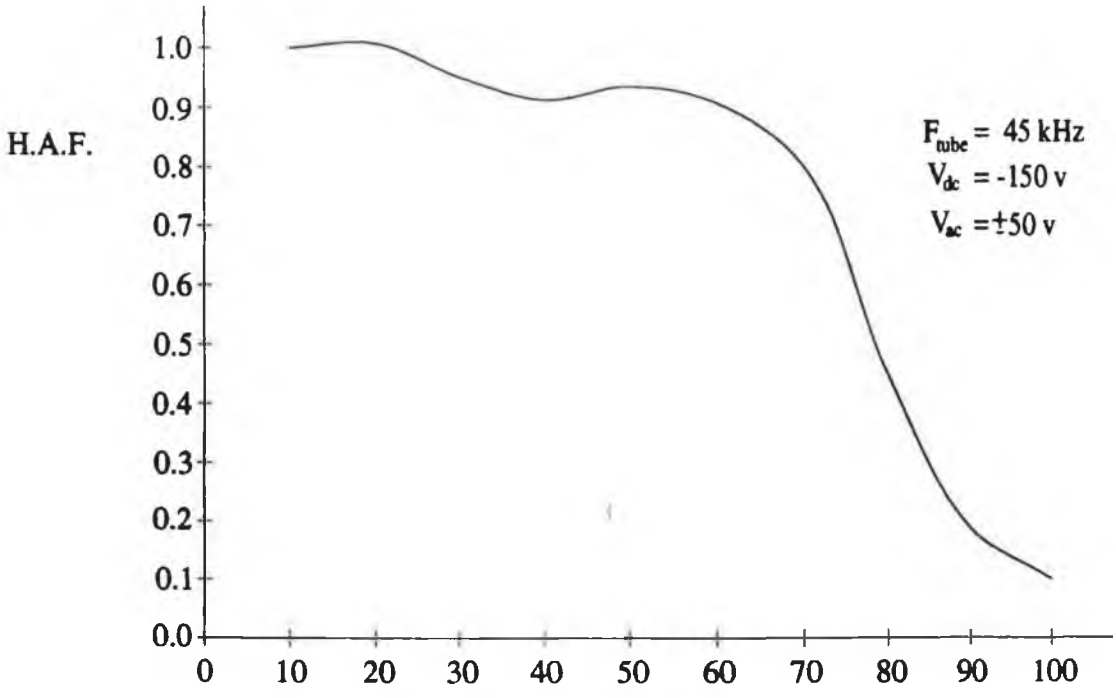

Figure 2.12
Graph of height adjustment factor *versus* atomic mass

Ion bunching

If the AC amplitude is made comparable to or larger than the D.C. voltage an interesting effect occurs. The voltage on the TOF tube varies at a large enough rate such that, during a certain period of time, the ions that enter the tube late receive a large enough difference in energy to ions that entered earlier such that they "catch up" with the earlier ones at the end of the TOF tube. This bunching of the ions leads to a large detector current at breakthrough time. Figure 2.13 (a), again a computer simulation, shows this effect for ions of N_2^+ and 2.13 (b) shows the ideal detector current that should result from this arrangement. Obviously since a large number of ions emerge at the same time this will give rise to a very large peak dying away rapidly. Again the heights of the peaks depend on mass and a height adjustment factor is needed.

This leads to the question: What would happen if the TOF tube voltage was triangular or some other shape besides cosinsoidal? It happens that a sinusoidal shape is the best all-round for observing the complete spectrum together (not to mention the easiest to work with). It is

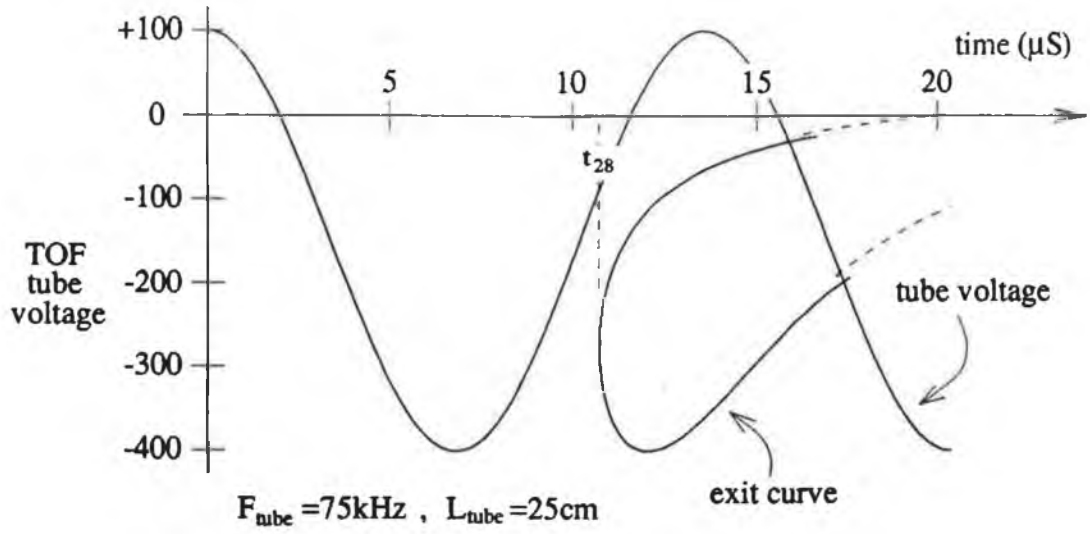

(a) Computer simulation of N_2^+ exit curve showing ion bunching

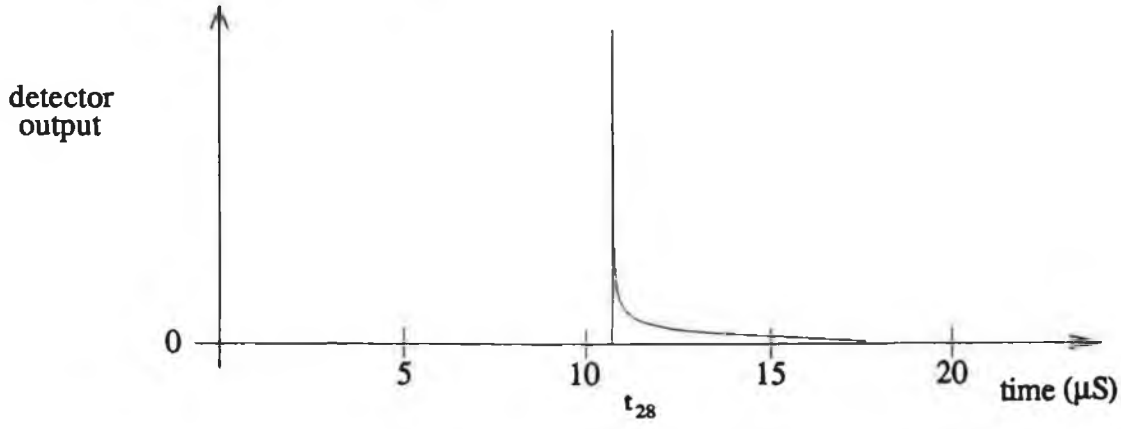

(b) Corresponding calculated detector current for a mono-energetic ion beam
Figure 2.13

conceivable that a triangular shape wave at a particular frequency, AC amplitude and DC offset will allow all the ions of one particular mass entering the TOF tube during the first half of the cycle to exit at the same time, but it would not suit any other mass because of the square root dependence of the time-of-flight with mass.

Figure 2.14 overleaf is a graph of the breakthrough time versus atomic mass for a 45kHz cosinsoidal tube voltage with an amplitude of 300 V_{p-p} and a dc offset of -50 V (similar to the parameters in figure 2.13 above). A straight line is added to the diagram to outline the slightly curved shape, indicating that mass peaks in the region 70 to 90 amu will be spaced closer together than those in the range 10 to 30 amu, for instance. As

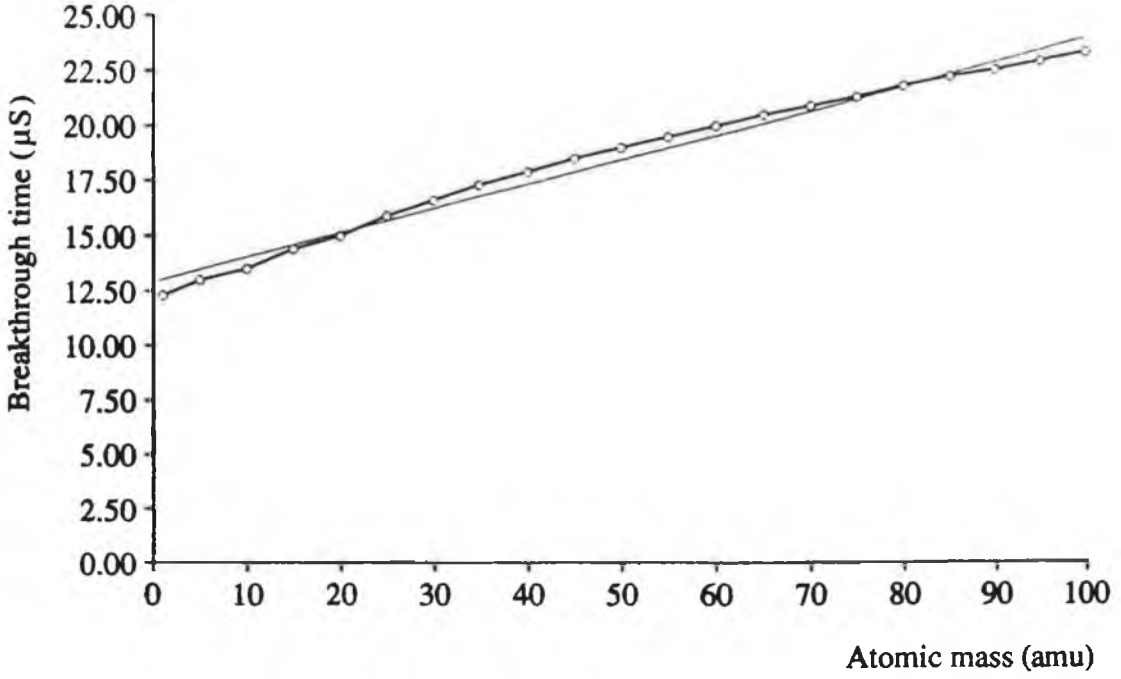

Figure 2.14
Graph of breakthrough time *versus* atomic mass

mentioned earlier the mass scale is generally not linear with either time or TOF tube voltage but the non-linearity in this case is tolerable, especially for a restricted mass range and the mass spectra presented in chapter 4 are all obtained using these parameters.

Very Heavy Ions

Ions of mass greater than about 300amu or so will pose difficulties for the mass spectrometer because of their very long flight time. Figure 2.15 below shows the exit curve of an ion of atomic mass 414 amu as an example. Its breakthrough time, t_b, coincides with that of an ion of mass 28 amu (N_2^+). Even though its flight time is very long it will appear within each cycle of the tube voltage, the ions that exit the tube at any time having entered it in the previous cycle. As a result, for example, a peak at 28 amu may indicate ions of atomic mass 28 or 414 amu.

A possible way of unveiling these rogue peaks is to adjust one of the parameters (tube voltage for example) and observe the new spectrum. A peak of 28 amu will keep its correct position relative to the other peaks around it, whereas a 414 amu peak will move to some other

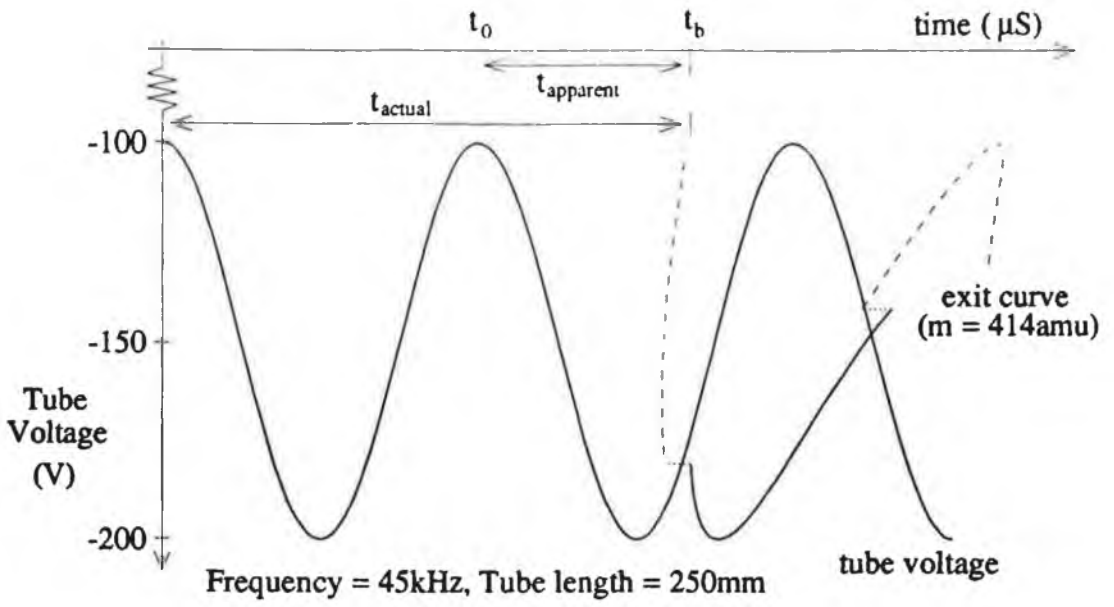

Figure 2.15
Exit curve for an ion of atomic mass = 414 amu

un-correlated position. This is demonstrated in figure 2.16 below. If there are no other peaks to compare with the suspect peak position, then a comparison of the two different calculated and observed breakthrough times should identify the peak. For the mass spectra presented in this thesis, where the ions are produced from the ambient air, there was no traces of any very heavy ions.

Parameters: TOF tube length = 250mm, Frequency = 45kHz

AC voltage = 100 V_{p-p}, DC voltage = -150 V

Mass (amu)	Breakthrough time (μS)
18	14.79
28	14.96
40	15.94
414	14.96

AC voltage = 200 V_{p-p}, DC voltage = -200 V

Mass (amu)	Breakthrough time (μS)
18	13.67
28	14.75
40	15.17
414	15.96

Figure 2.16
Table showing the shift of a 414 amu peak from the 28 amu position with a change in TOF tube voltage

Chapter 3
EQUIPMENT

THE VACUUM SECTION

The first part of this chapter describes the various vacuum components of the mass spectrometer. As shown in the previous chapter, the mass spectrometer consists of an ion source, electrostatic lens, the TOF tube and an electron multiplier. Neither the ion source or the electron multiplier can operate at pressures greater than $1x10^{-4}$ mbar and so a medium to high vacuum is needed for operation. A vacuum is also required so that the ions mean free path is long enough to avoid collisions as they progress along the length of the spectrometer.

A rotary pump, diffusion pump combination provides a pressure of approximately $1x10^{-5}$ mbar in the vacuum chamber, to which the mass spectrometer is connected, enough to allow it to function and this pressure is monitored using an ion gauge which automatically shuts the spectrometer down should the pressure rise above $1x10^{-4}$ mbar due to a power failure or mechanical fault. A liquid nitrogen trap, placed between the vacuum chamber and the diffusion pump, is used to prevent any hot oil vapour from the diffusion pump reaching the mass spectrometer by presenting it with vacuum chamber walls at a temperature below -196°C. The spectrometer's key parts are described below.

The ion source and electrostatic lens

The ion source is an electron bombardment type manufactured by VG Quadrupoles ltd. [11], designed for use in a quadrupole mass filter and, together with the electrostatic lens, is outlined in figure 3.1 overleaf. It consists of a Rhenium filament, a grid cage and an electrostatic lens assembly. Electrons are obtained by

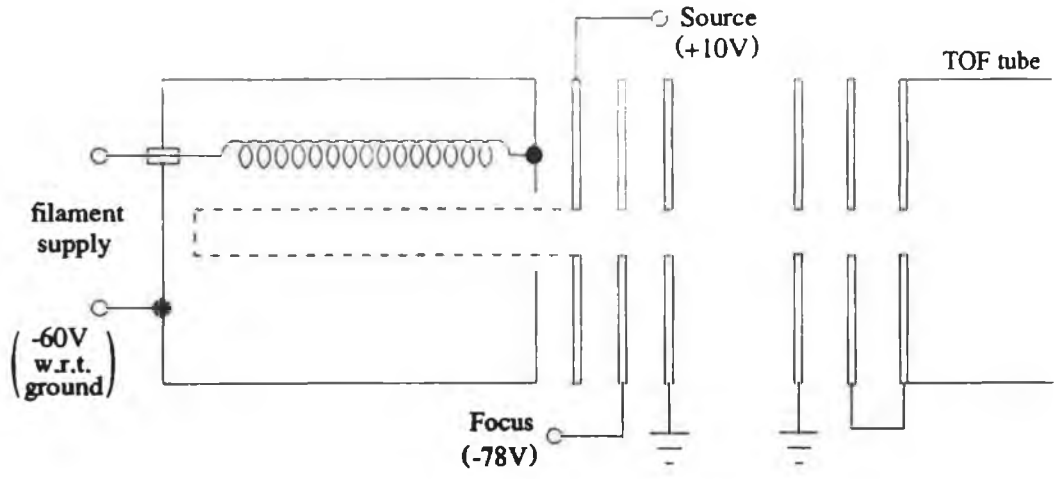

Figure 3.1

thermionic emission from the heated filament and accelerated towards the grid. The high transmittance of the grid allows most of these electrons to cross through and ionise the gas inside the grid cage. Because of the large mass difference between electrons and the target molecules, the latter will acquire only a small energy increment on impact and the energy spread can be as low as 0.1eV or less. The manufacturers of the ion source quote an energy spread of 0.2eV at an electron emission current of 30μA and 0.8eV at 500μA, at a pressure of $1x10^{-7}$ mbar.

The ion source's built-in electrostatic lens consists of three elements. The first is connected to the grid cage and its potential (+10V) determines the energy at which the ions emerge from the source. The second element is biased negative to draw the ions out of the grid region and to focus the ion beam in front of the source. The final element is connected to ground.

In order to accelerate the electrons from the filament to the grid cage, a potential difference must be applied across this region. It might be presumed that the energy of the ionisation electrons need only exceed the first ionisation or appearance potential of the sample gas to produce ions. For achieving the maximum ionisation efficiency, however, the electron energy must always substantially exceed this value. Figure 3.2 overleaf indicates the relative yield of ions as a function of

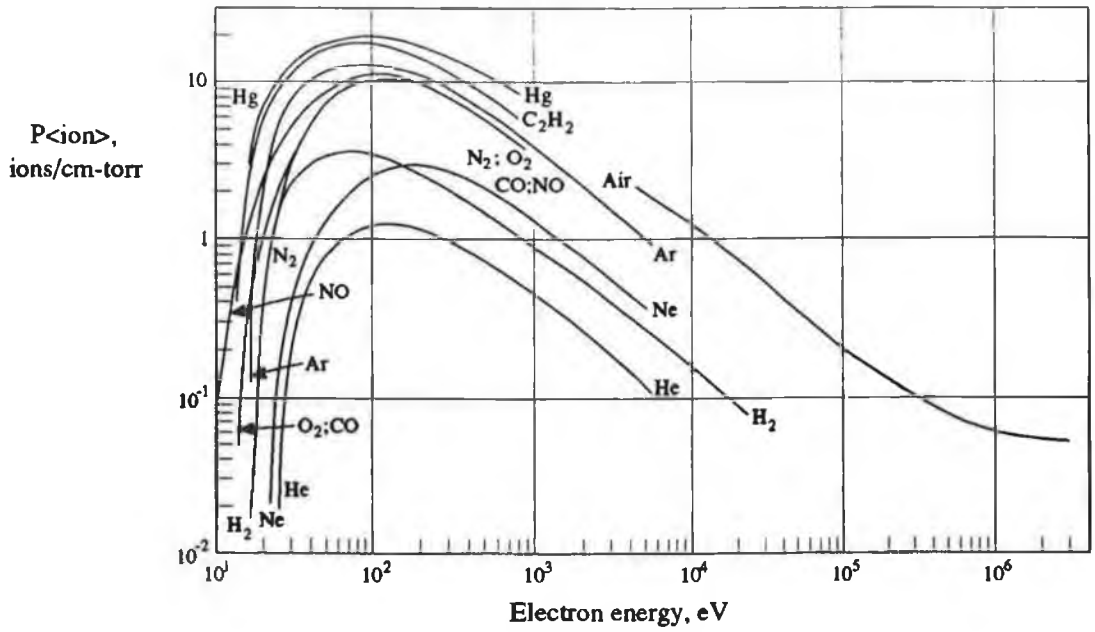

Figure 3.2

Ionisation efficiency curves for inorganic gases

(R. Jaeckel, "Allgemeine Vakuumphysik", in *Handbuch der Physik*, Vol. 12, S. Flügge, Ed., Springerverlang, Berlin 1958, p. 535.)

electron energy and it is seen that the maxima of the curves is located at the same energy level (≈70eV) for most gases. Thus the body of the ion source is biased to -60V giving an overall potential between grid and filament of 70V. The vertical scale in the figure is the *probability of ionisation* which is defined as the number of collisions which result in ion production per centimeter of electron path through a gas at a pressure of 1 torr (1.333 mbar) at 0°C.

In addition to the built-in lens an external lens was added to provide a parallel beam of ions for the TOF tube. It also consisted of three elements, the first at ground potential and the last two connected to the TOF tube supply. The lens plates, made from 0.5mm thick stainless steel, are separated by a spacing of 4.5mm. The diameter of the elements was limited by the vacuum chamber housing to 35mm with a aperture diameter of 10mm. The parameters of the lens were chosen from a book of pre-calculated sample lenses [10], but since only a limited amount of information was available about the ion source, the ion focal point etc., the external lens was limited in its

effectiveness. Figure 3.3 is a graph of the electron multiplier anode current versus the voltage on the time of flight tube, showing how variation in the tube voltage affects the focusing and hence the number of ions reaching the detector. Ideally the ion current should be independent of tube voltage, so the variations will have to be taken into account when determing the relative peak heights.

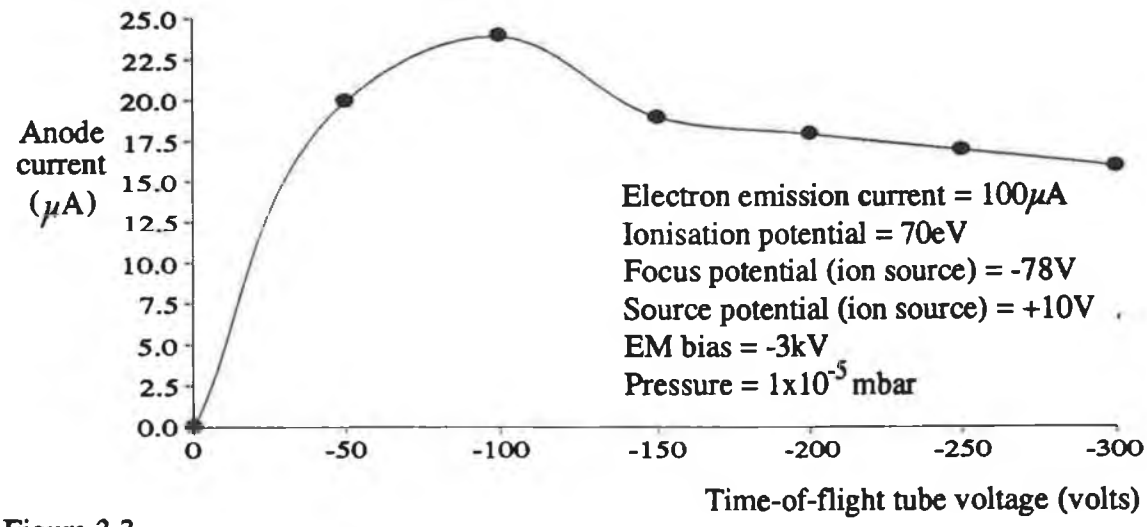

Figure 3.3
Detector current as a function of focusing voltage

A diagram of the vacuum mounting of the ion source and electrostatic lens is shown in figure 3.4. The pumps are situated directly below the gas inlet and in front of the ion source so that once the inlet has been shut off, the gas clears in a matter of seconds.

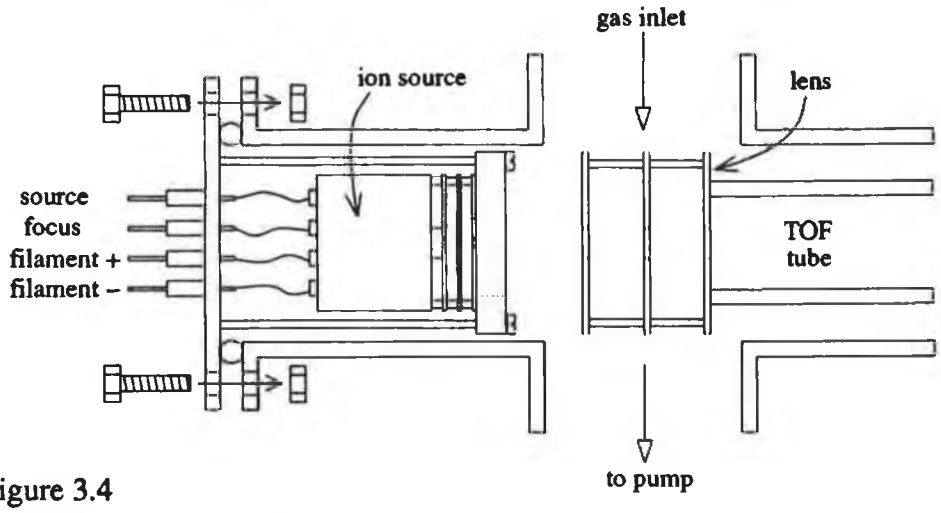

Figure 3.4
Vacuum mounting of the ion source

The time-of-flight tube

The structure of the tube is very straightforward. It is 250mm long, 30mm in diameter and made of copper. Its job is to provide a field free region, blocking out any external electric fields that would affect the trajectory of the ions. Irrespective of its potential with respect to its surroundings , the electric field everywhere inside the tube (with no charges present) is zero. Electrical contact is made at the center of the tube so that any time delay due to the propagation of the electric field to the ends is equal in both directions (≈ 0.5nS each way) and hence cancels out, but this is not really of any significance. The tube itself forms one plate of a capacitor with respect to the vacuum chamber walls with a value close to 300pF and requires a special circuit to drive this capacitance at the frequencies and voltages required. The grid at the end of the tube and the grounded grid are separated by 4.0mm, followed by spacing of 3.5mm between the grounded grid and the final grid. These consist of a fine wire mesh with wires of 20 micron diameter and 500 micron separation.

Electron multiplier

Electron multipliers are based on a phenomenon called secondary electron emission, where a number of electrons are ejected from a surface, bombarded by an energetic particle. They utilise this for detecting ions in two ways: First, the ion current is "converted" into an equivalent electron current on the first electrode or dynode of the multiplier (see figure 3.5 overleaf). The secondary electron emission current is then amplified as it becomes the primary electron current for the second dynode and so on. The obvious requirement of the dynode material is that the values of the secondary electron emission coefficients for ion and primary electron bombardment be as large as possible.

The electron multiplier used in the mass spectrometer was a Thorn EMI EM642/3B, 18 stage venetian blind type with a typical gain of 5×10^6 at a supply voltage of -3kV (voltage on the first dynode with respect to the anode).

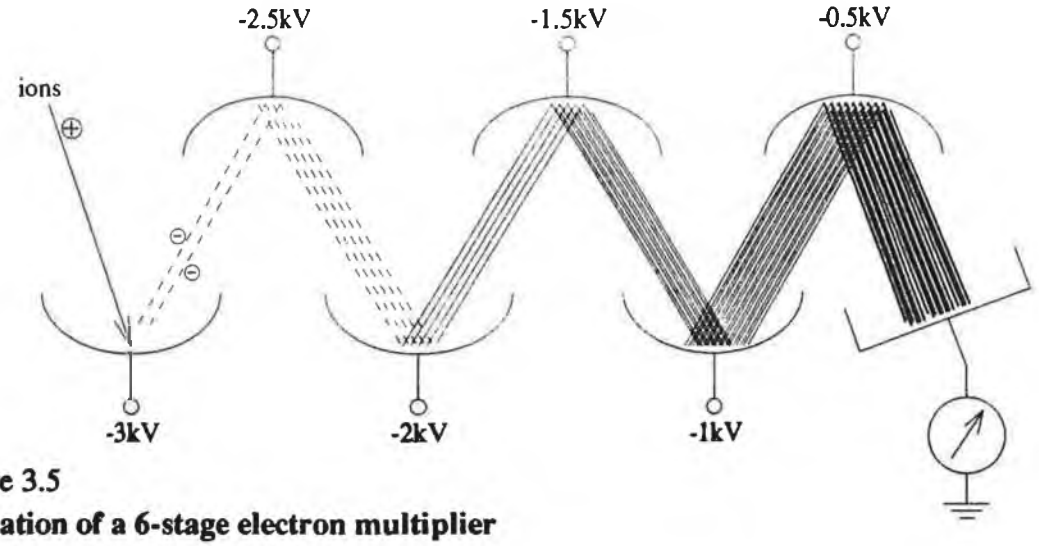

Figure 3.5
Operation of a 6-stage electron multiplier

The detection efficiency for ions is not specified at ion impact energies of 3keV but is approximately 60% at 6keV and 85% at 18keV and is not greatly affected by ion mass [12]. The transit time (the time between ion impact and electrons reaching the anode) is not specified either but the manufacturer Philips [13] give a value of 30nS at a supply voltage of -3kV for a similar type. The pulse rise time is given as 5nS and is more than adequate for the purpose required.

The electron multiplier (enclosed in a glass envelope) is mounted in the vacuum chamber as shown in figure 3.6.

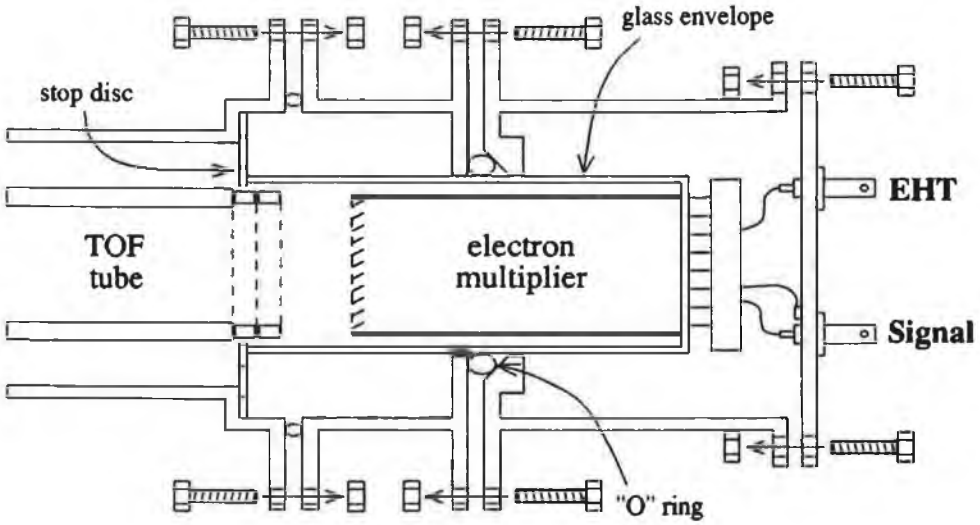

Figure 3.6
A section of the vacuum chamber containing the electron multiplier

A rubber "O" ring, seals the chamber at a point along the glass tube and a metal stop disk is used to prevent the multiplier from being pushed into the chamber by the pressure differential, equivalent to 196 Newtons (the weight of a 20kg mass!). Ordinary non-vacuum connections can then be used to power up and receive signals from the multiplier tube.

THE ELECTRONICS SECTION

The electronic section of the mass spectrometer can be divided into 3 main parts. The first section is the amplification of the tiny ion currents reaching the detector, most of which is done by the detector itself, an electron multiplier. The second is the manipulation of the signal to extract a mass spectrum from it and to plot the spectrum out on some easily readable way and the third and final section deals with the supporting circuits. Not all the circuits are given in this chapter but any that are not shown here are given in appendix C. The detection, amplification and processing circuits are all necessarily high speed since the mass spectrum occurs during the second half of the TOF tube cycle (typically 10μS). If 100 mass peaks are to be accommodated within this time each peak has to be, at most, 100nS wide for 1 amu resolution, however this represents the lower limit of resolution and it is preferable to aim for higher than this. All this being considered the circuits must be able to deal with frequencies in the range 10 to 100 MHz. The final part of this section looks at the possibility of micro-processor/ computer control.

Supporting circuits

The circuits covered in this section are, the TOF tube driver and to a limited extent the ion source power supply which is a commercial type with a few minor modifications.

The time-of-flight tube driver has the task of providing the time dependant accelerating/decelerating electric fields which are fundamental to the operation of the spectrometer. It supplies the DC and AC voltages to

the time-of-flight tube together with a smaller replica of the signal to the data processing circuit. The driver circuit was built to provide a DC potential of 0 to ±200V with a superimposed AC potential of 0 to ±200V_{p-p}. Fortunately the circuit was relatively simple since the capacitance, formed between the tube and the walls of the vacuum chamber, grids, etc., was reasonably small, about 300pF. This capacitive load on the circuit has a reactance of approximately 10kΩ at typical tube frequencies of around 50kHz. The circuit is shown in figure 3.7.

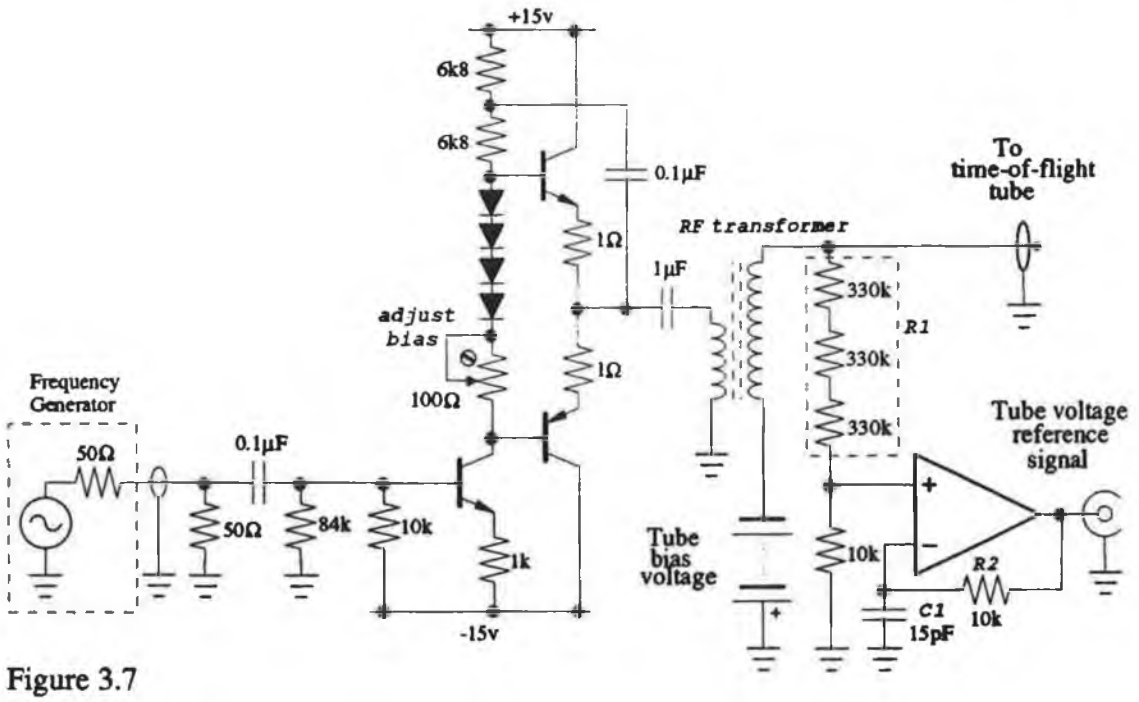

Figure 3.7
Time of flight tube driver circuit

The central component is the purpose wound RF transformer. It has a flat response over a large range of tube frequencies (see appendix E) and requires a primary voltage of only ±12V to achieve the maximum ±200V output required at the secondary. The circuit driving the primary is a standard class AB power amplifier [14], designed to operate over the same frequency range as the transformer. Because of the considerable and variable phase shift of the whole circuit with frequency, the reference signal is tapped directly off the output of the transformer. Three resistors are used for R_1 to minimise

phase shifts caused by stray capacitances within the resistors themselves. R_2 and C_1 provide compensation for the small amount that does occur due to other factors. The linearity of the mass scale of the spectrum with respect to the tube voltage depends on accurate timing of the reference signal. It is therefore important to keep the reference as accurately in phase as possible. The values of R_2 and C_1 were chosen to achieve a phase shift of less than 0.18° (10nS at 50kHz). The op amp eliminates the need to compensate for cable capacitance by providing a very low driving impedance while buffering the reference signal.

The ion source power supply consists essentially of a medium power voltage source to supply the filament, a low power voltage source to provide the ionising and focusing potentials and a current source to set the electron emission current. It was this latter part that was modified as shown in figure 3.8. The addition to the

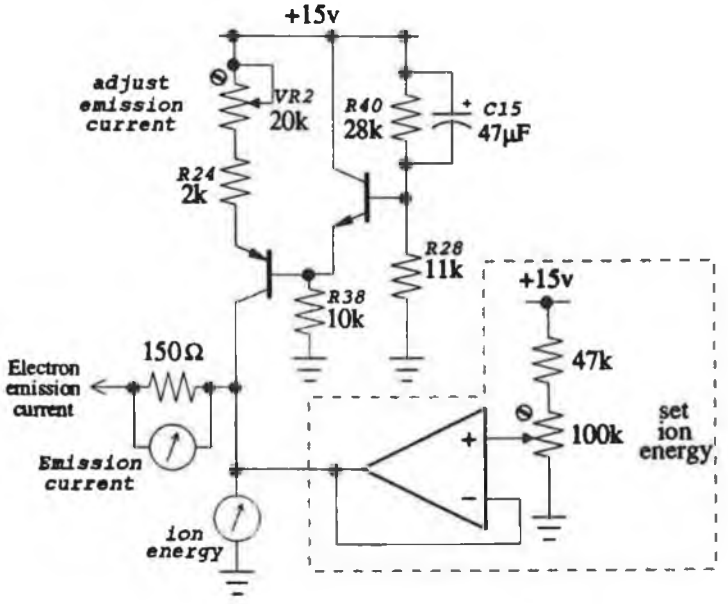

Figure 3.8
Initial ion energy adjustment circuit

circuit is outlined by the dashed box. Its purpose was to provide a means to vary or trim the initial energy of the ions entering the time of flight tube, between 0 and 10 electron-volts, so that its value could be set and known exactly as required.

The rest of the circuitry is involved with the actual ion signal, and as mentioned above is segregated into two sections;

Signal amplification

The major part of the signal amplification is done by the electron multiplier used to detect the ions. The minute ion current, less than 0.0005μA $_{RMS}$ at 2×10^{-5}mbar, striking the front end of the multiplier appears as a current of approximately 10μA $_{RMS}$ at the anode end. A complete diagram of the amplifier is shown in figure 3.9.

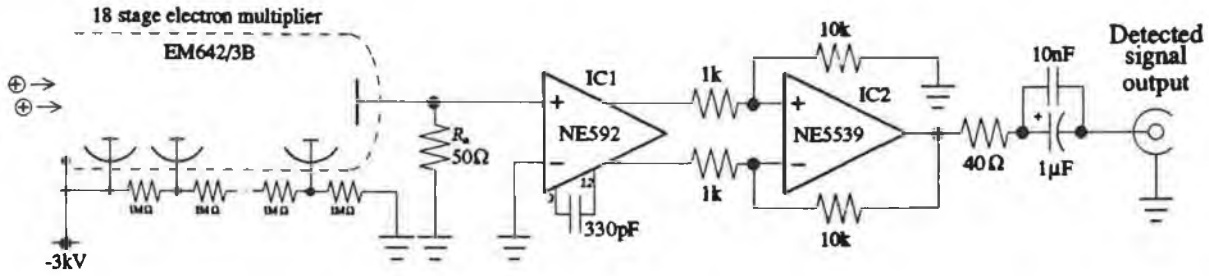

Figure 3.9
Ion detection and amplification circuit

The multiplier provides an excellent method of amplification in terms of low noise and wide bandwidth. In order to preserve the higher frequency components of the signal the anode resistor, R_a, needs to be kept small, otherwise together with any stray capacitance, including the input capacitance of the following amplifier (≈7pF in total), it will act as a low pass filter with a -3dB point at a frequency given by

$$f_{-3dB} = \frac{1}{2\pi R_a C_s}$$

where C_s is the stray capacitance. In order to keep this -3dB point above 100MHz, R_a must be at most 220Ω. R_a also determines the signal voltage at the anode since the anode looks electrically like a current source. It was found that putting R_a=220Ω gave too large a signal and overloaded IC1. An R_a of 50Ω was found satisfactory as well as giving the added advantage of making the circuit compatible with other 50Ω high speed amplifiers.

IC1 is an integrated circuit designed for video signals up to 200MHz and gives a gain of 200 in the wiring configuration shown. IC2 is an ultra high speed op-amp and in this circuit is designed to give an overall gain of 5 and to drive a cable and load terminated in the standard 50Ω. In the construction of the circuit, while not being terribly important, some consideration must be given to the layout of the printed circuit tracks in terms of capacitive coupling, inductance etc. because of the high frequencies involved. The signal level at the output is in the order of 100's of millivolts at a pressure of $1x10^{-5}$ mbar, substantial enough to observe a mass spectrum without difficulty on an oscilloscope (figure 3.10), but as discussed in chapter 2 this is the "raw" data and the peak heights need to be adjusted for correct relative abundance measurements and also the timings of the peaks will not be linear with time.

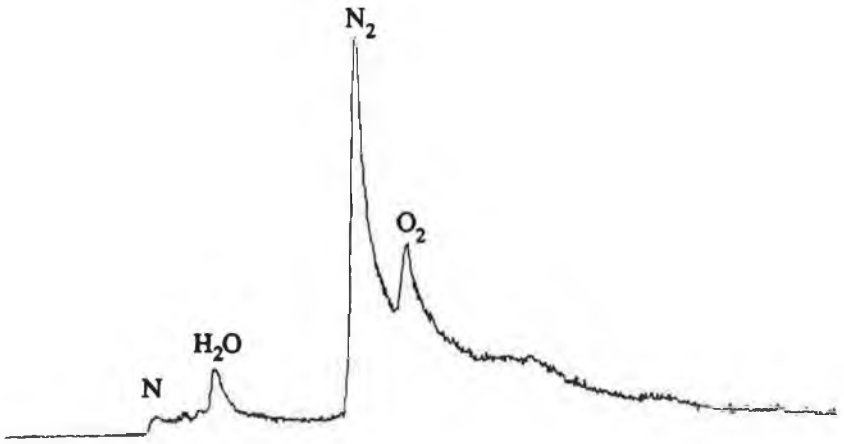

(a) undifferentiated

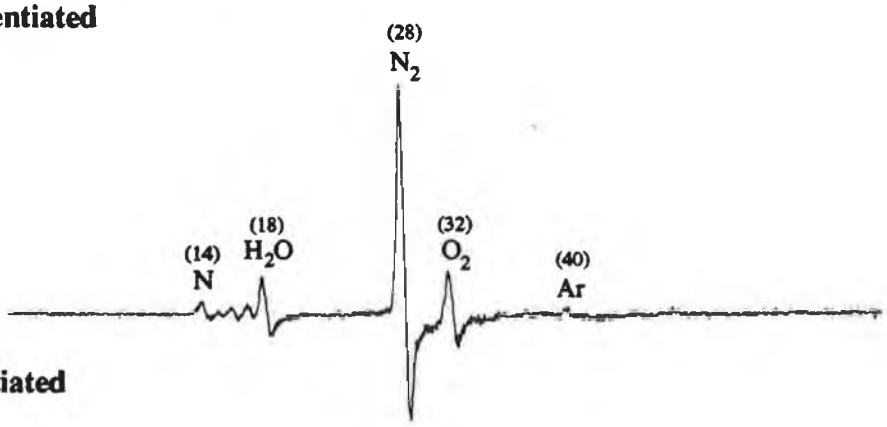

(b) differentiated

Figure 3.10
Oscilloscope trace showing the mass spectrum of air at a pressure of $1x10^{-5}$ mbar.

Signal processing

Examining the mass spectrum on the screen of an oscilloscope, besides the difficulties mentioned above, is marred by two other problems, the first being that the noise on the signal obscures the smaller peaks and makes the full spectrum difficult to observe and measurements difficult to obtain and the second being that there is no permanent record of the mass spectrum. It was decided that the best and quickest way to overcome this problem was to build a device to average the signal over a number of tube cycles, in order to rescue the smaller peaks from noise and to plot the resultant mass spectrum on a plotter or chart recorder. The averaging part of this device is shown in figure 3.11. The central component is the

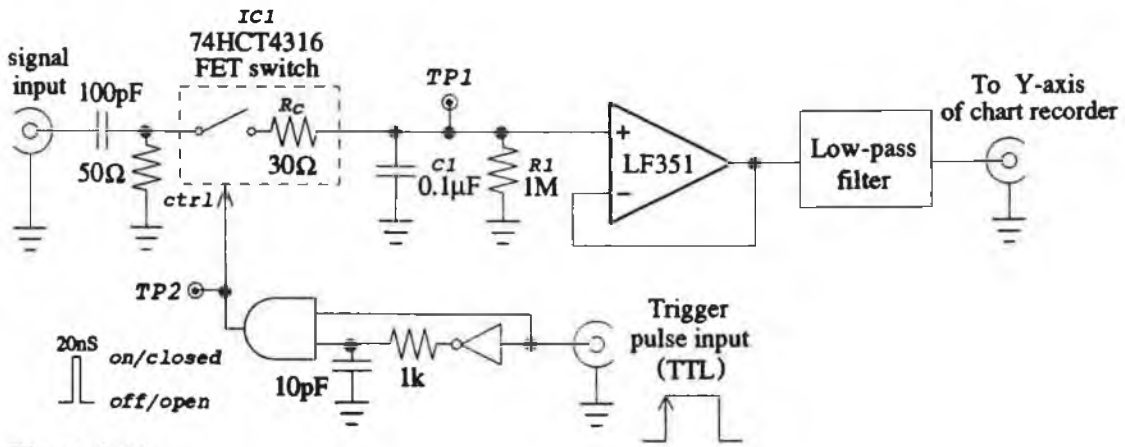

Figure 3.11
The averaging section of the data processing circuit

74HCT4316 (IC1), an electronic FET switch capable of switching a signal in and out in the order of 10 nanoseconds. The circuit operation is as follows:

The logic gates are triggered by the rising edge of a pulse supplied to the trigger input and produces ≈20nS pulse at test point 2 (tp2) in the circuit, the moment it is triggered. This pulse is simply supplied to the control pin of one of IC1's four FET switches (the other three are unused). The front end of the switch is connected to the differentiated incoming signal. The back end is connected to a capacitor (C_1) and resistor (R_1) connected in parallel to ground and from there into an op-amp. The op-amp merely buffers the voltage across C_1

into a X-Y plotter via a low-pass filter, used to eliminate any high frequency noise from the switch control, power supplies etc.

When a trigger pulse is supplied, the FET switch conducts for ≈20nS. This switching time was considered sufficiently short to preserve the shape of the mass peaks accurately enough. While the switch is conducting the signal driver will charge the capacitor through the switch. The capacitor will initially only charge to 0.66% of the signal value during the first 20nS sample, but if a trigger pulse is received at the same time every tube cycle then the voltage across the capacitor C_1 will, after a number of periods, reach the average value of the signal voltage at that time of the cycle. Therefore scanning the arrival time of the trigger pulse slowly over the period of the tube voltage will produce an averaged mass spectrum at the output of the circuit. If this output is connected to the Y axis of a plotter and the X axis scanned at the same rate as the trigger pulse, then the averaged mass spectrum will be plotted out. R_1 is there to provide bias to the op-amp when no trigger pulses are being received (before and after a scan) and it also provides a shunt to ground for the FET leakage current.

The second part of the signal processor generates the trigger pulse needed above and the circuit is shown in figure 3.12 overleaf. This circuit consists of, input amplifiers for the reference voltage, a ramp generator and a comparator.

The ramp generator's job is to provide a slowly increasing DC voltage over a set period of time, and is achieved by using IC4 as an integrator and supplying it with a constant voltage. The rate of increase of the output voltage can be adjusted and mostly it is set around 1 volt per 5 to 6 seconds. The generator's output is connected directly into the input of a comparator (IC5) and is also used to drive the X axis of the plotter.

The reference voltage amplifier is built in three stages using IC1,2 & 3. The first stage is used to provide a phase lead in order to compensate for delays in the processing and switching circuits and to adjust the

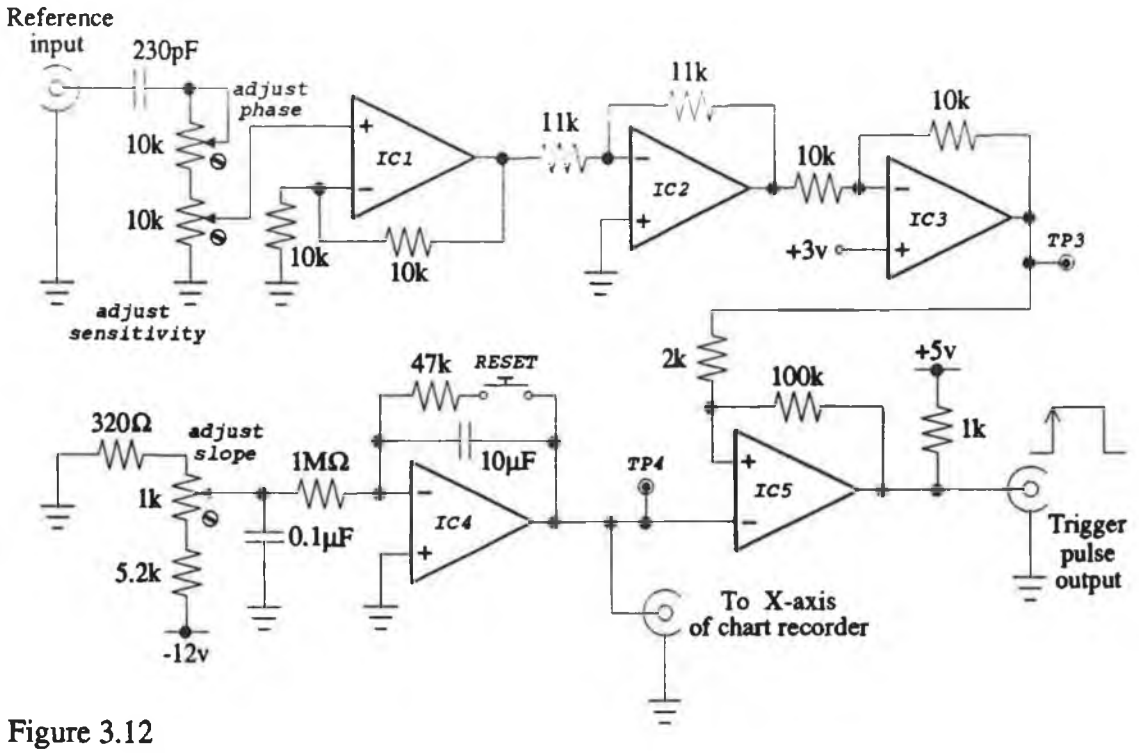

Figure 3.12
The time-of-flight tube signal processing circuit

amplitude so that, for reasons presented shortly, it is reduced to $3v_{p-p}$. The second stage inverts the signal and the third stage re-inverts it again but also adds +3v DC so that the signal at tp3 ranges from 0 to 6v. This signal is compared with the DC ramp voltage (tp4) using IC5 and the output becomes the trigger pulse for the averaging circuit in figure 3.11.

Justification for the rather contrived circuit in figure 3.12 is contained in figure 3.13 overleaf. In part (a) the reference voltage at tp3 is shown superimposed over the DC ramp voltage at tp4 at a particular point during the ramping period. The comparator output is shown in part (b). Recalling that the mass spectrum appears during the second half of the tube period it can be seen that the rising edge of the pulse from the comparator appears during this time. As the DC ramp voltage increases with time from 0V to 6V, this rising edge moves along the time axis between $\frac{1}{2}\tau$ and τ, where τ is the tube voltage period. In this way the sampling "window" of the averaging circuit, which occurs at the rising edge of the trigger pulse, scans across the spectrum.

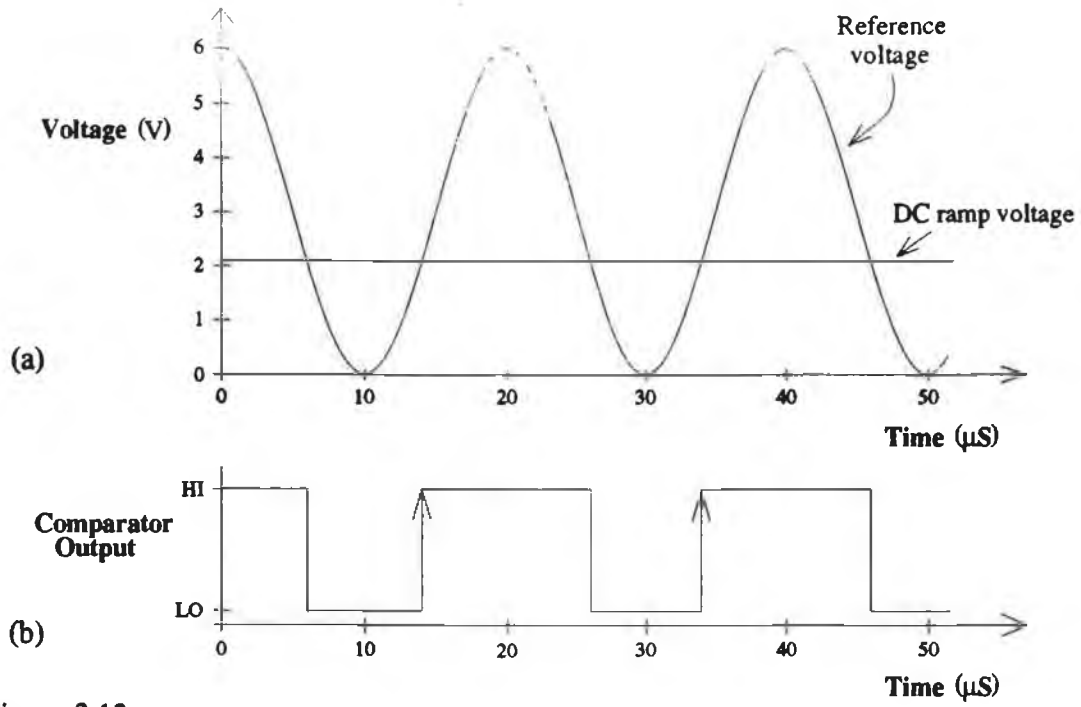

Figure 3.13
Comparison of reference and ramp voltages

Overshoot compensation

For reasons of clarity, a small addition to the averaging circuit was omitted up to now. Although this additional circuit doesn't affect the operation of the above circuits it does have an effect on the quality of the plotted mass spectrum. The differentiation of the detected ion current produces negative overshoots or "tails" in the mass peaks. It is not enough to simply clip out these negative tails with say a diode or something similar since this could reduce the height or even obscure a small peak if it was close enough to be caught in the tail of a large peak. For this reason a special circuit is required to cancel out the tails of the peaks and this section describes such a circuit.

The tail of the peak is to a good approximation exponential. The principle of operation of the compensation circuit is that it adds to the signal an exponentially decaying pulse with the same height and time constant as the tails of the peaks but of the opposite

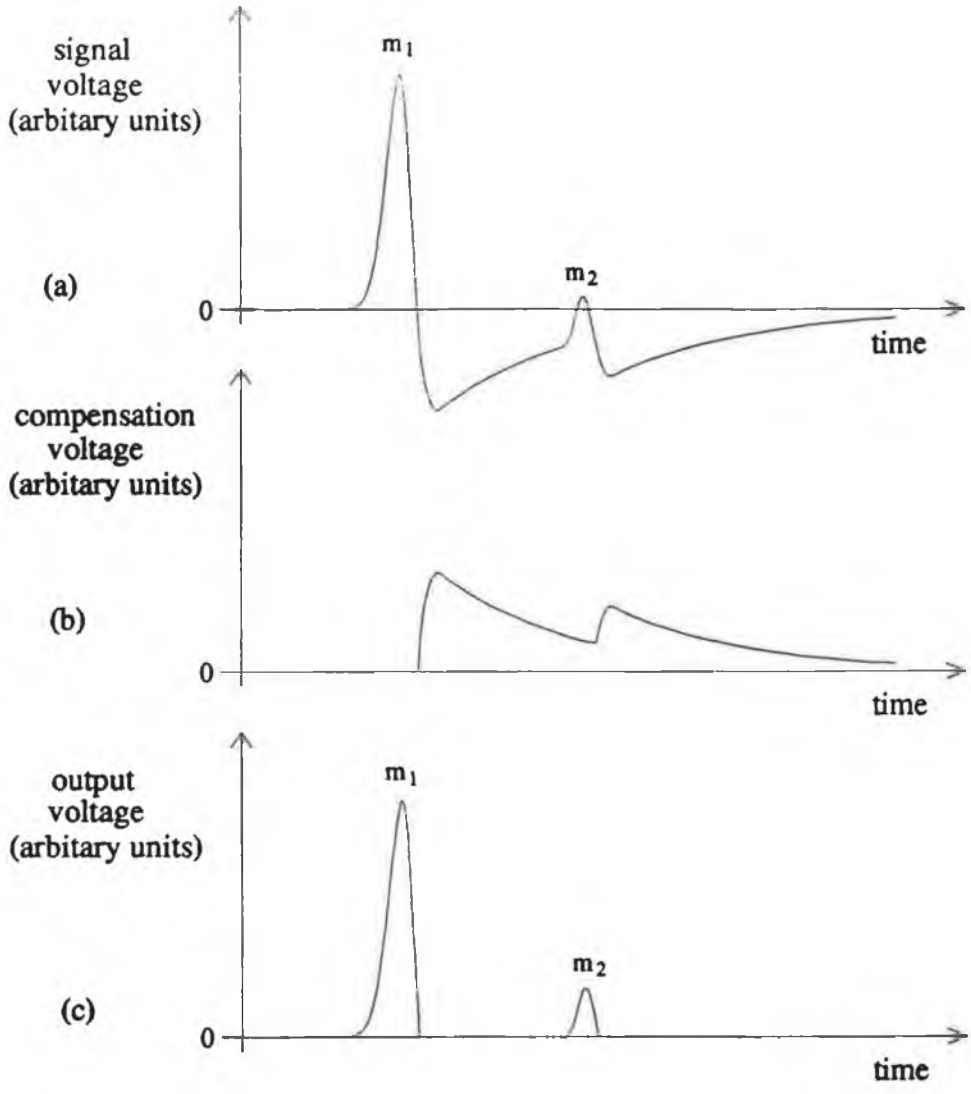

Figure 3.14
Overshoot compensation

polarity. Figure 3.14 above shows the progression of events within the circuit. Part (a) shows the input signal, consisting of two mass peaks M_1 and M_2 close to each other such that the height of M_2 is reduced by the tail of M1, relative to zero volts. Part (b) shows the internally generated compensation signal that the circuit produces from the negative part of the input signal and part (c) shows the summation of part (a) and part (b) which is the correctly compensated signal, i.e. the height of M_2 is independent of the presence of M_1.

The circuit diagram is shown in figure 3.15 overleaf. The section within the dashed box is the part that generates the compensation signal. The rest of it is simply the adder circuit (IC4 adds the two signals and

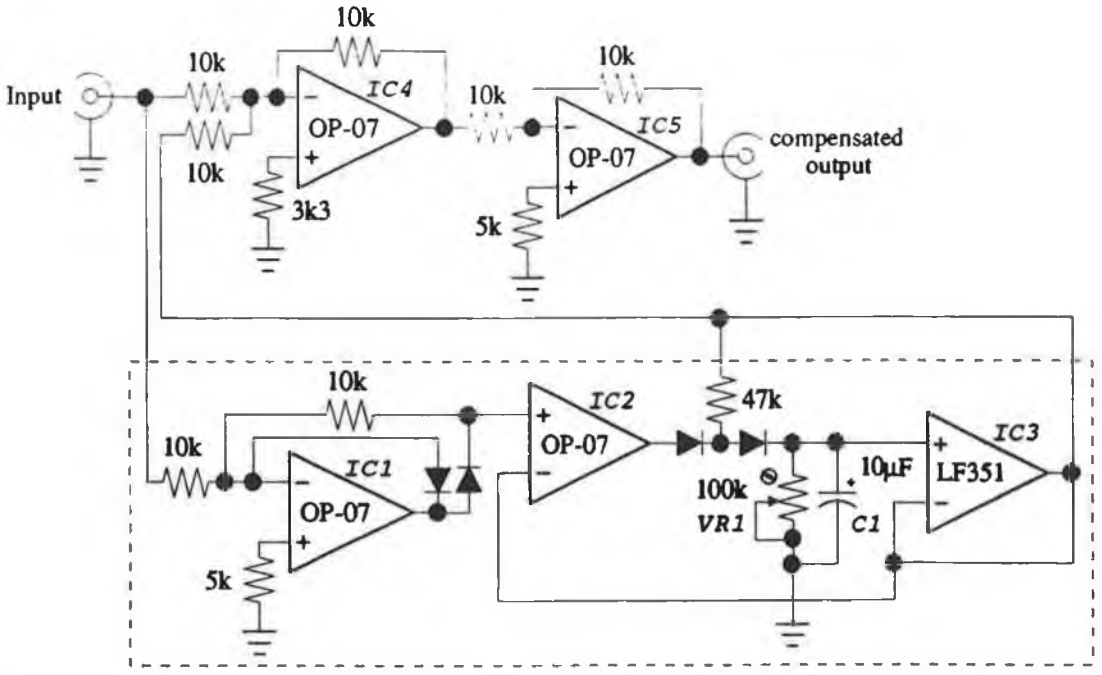

Figure 3.15
Overshoot compensation circuit

inadvertently inverts them in the process so IC5 re-inverts them to the correct polarity for output to the X-Y plotter). The compensation signal generator works as follows: IC1 serves a dual purpose, it inverts the polarity of the input signal and rectifies it so that only the part of the original signal that was negative appears at IC2 but as a positive replica. The combination of IC2, IC3, C_1 and the diodes act as a peak hold amplifier and if VR1 was not present would hold the value of the largest input voltage that was applied to IC2, at the output of IC3 indefinitely (assuming ideal components). Instead the existence of VR1, adjusted so that the product of VR1 times C_1 matches the time constant of the peak tails, causes the output to decay exponentially once the input voltage to IC2 has dropped from its maximum value. If VR1 is adjusted correctly this decay should match the decay in the input signal and since it is positive, when added to the input signal will cancel out the peak tails.

If during the decay another peak occurs, like in figure 3.14, the input to IC2 will drop to zero but the output of IC3 will still be positive and continue to decay exponentially, so when added to the input signal will "lift" the second peak M_2 up to its correct position on

the voltage scale. When the tail of M_2 occurs, the voltage at IC2's input will exceed the voltage at IC3's output at which stage IC2 will charge up C_1 to the new maximum input value and when this voltage starts to decline again, IC3's output will start to drop exponentially as before.

It should be noted that while IC2 is charging up C_1, the output of IC3 is just a replica of the input, giving a "dead time" after each peak, during which, the output is held at zero volts. This is not a problem as long as the "dead time" is over before the appearance of the next peak.

Computer control

The simplest way to provide computer control for the above circuits is to use a digital to analogue converter (DAC) instead of the ramp generator to provide the DC ramp voltage and to use an analogue to digital converter (ADC) at the output of the averaging circuit to read the averaged signal. This way by continually incrementing the DAC, to provide the rising DC ramp voltage, and reading the ADC after every increment the mass spectrum can be stored as a series of numbers. This would make the processing of the data, such as adjusting and comparing peak heights a trivial matter. It would also allow the data to be adjusted easily for any non-linearity in the mass axis and so would permit the use of a wide range of working parameters for the TOF tube voltage, frequency etc..

The circuit diagrams for a more detailed digital system are given in appendix C. These circuits were designed for an experimental device and allow the computer to control a wide variety of parameters such as TOF tube AC amplitude,frequency & waveform, the number of samples per point on the mass spectrum etc. and is thus far more complicated than is needed on a working model as described above.

Also contained in appendix C is an alternative circuit for generating the trigger pulse, to the one given in the previous section, which produces a mass spectrum

with the mass scale linear with respect to time as opposed to TOF tube voltage.

COMPUTER ALGORITHM

This section describes the algorithm behind the computer programs used throughout the thesis, for drawing the ion exit curves, comparing the calculated and experimental breakthrough times etc.. The programs are listed in full in appendix D and are written in the high level language "C". Some of the programs require quite a substantial length of time to run (a matter of days on a PC) and for this reason they were written on a very high speed computer; the Acorn Archimedes 440 with a math co-processor installed. Even so, longer programs like the height adjustment factor program take just over 2.5 hours to complete.

All the programs concerned, use the equations given in chapter 2 for the velocity of an ion after acceleration, V, and distance travelled by an ion under acceleration, S, namely;

$$V = U_o - \frac{keA}{dm}(t_e - t_o) - \frac{keB}{dm\omega}\left(\sin(\omega t_e) - \sin(\omega t_o) \right)$$

and

$$S = U_o(t_e - t_o) - \frac{keA}{2dm}(t_e^2 - t_o^2) + \frac{keAt_o}{dm}(t_e - t_o) + \frac{keB}{dm\omega^2}\left[\cos(\omega t_e) - \cos(\omega t_o)\right] + \frac{keB\sin(\omega t_o)}{dm\omega}(t_e - t_o)$$

respectively, where k=+1 for an accelerating electric field and k=-1 for a decelerating field. As a reminder, A is the magnitude of the DC component of the tube voltage, B is the peak AC amplitude, ω is equal to twice pi times the frequency of the AC voltage, e is the charge on the electron, m is the mass of the ion, d is the separation across the acceleration region and the time the ion enters the electric field is given by t_o. V and S may then be calculated for any time t_e during the accelerating process.

These two equations, along with the basic equations

for straight line motion with constant acceleration, form the basis of the computer programs. Everything else in the programs, such as drawing graphics etc., including differences between the programs are peripheral to the simulation of the physical events undergone by the ions and for this reason are not dealt with in this text.

The above two equations need to be solved numerically. Figure 3.16 shows the algorithm used to calculate the velocity of the ion entering the TOF tube.

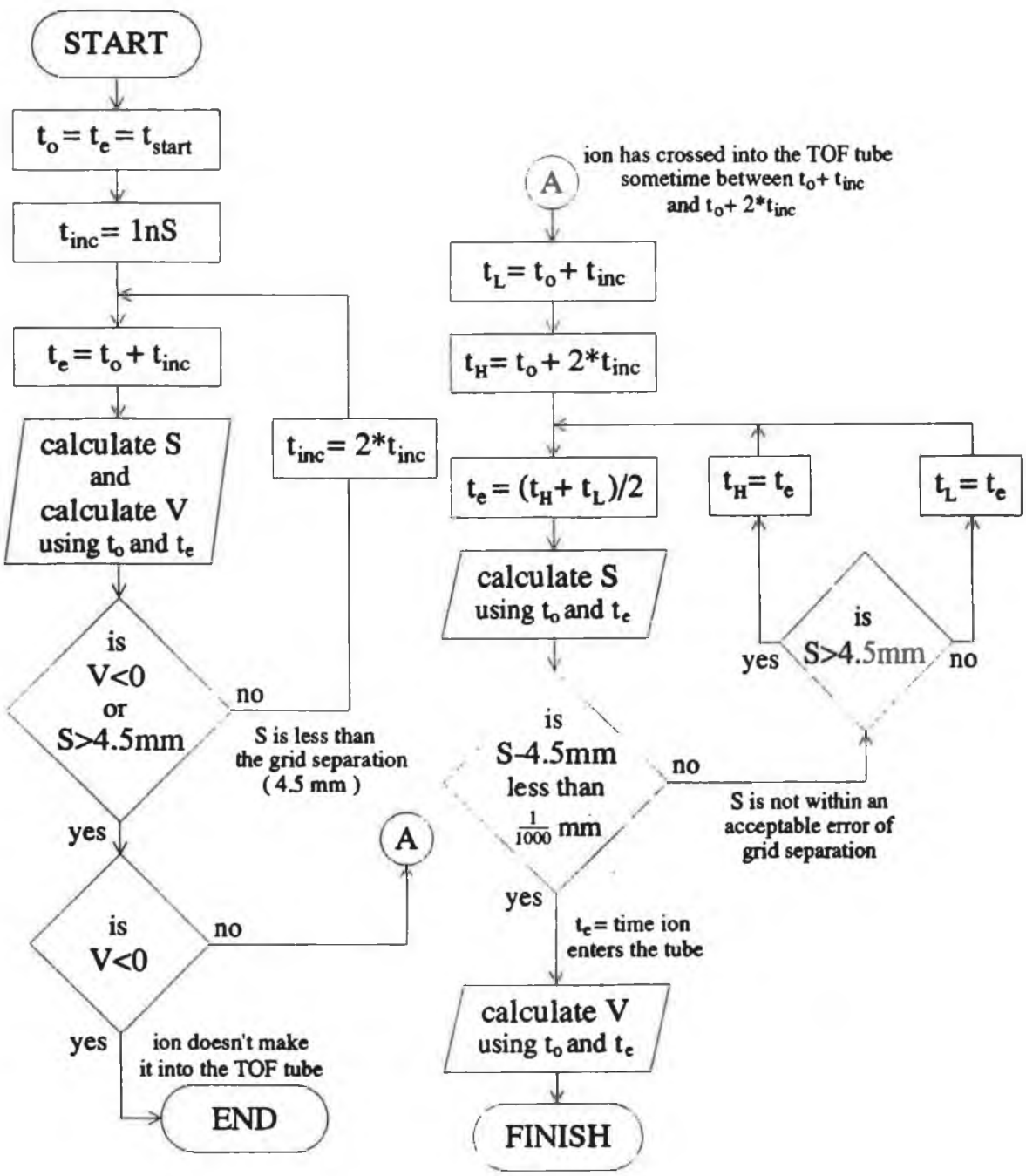

Figure 3.16

Algorithm flow chart for acceleration of ions into the TOF tube

The grid separation referred to in the figure is simply the distance across the acceleration region which in fact in the actual spectrometer is the distance between the first two lens elements. The calculating of the ions velocity entering the tube is a very small part of the algorithm (the last block before FINISH), the rest of the algorithm is taken up in determing the value of t_e. The problem, and the reason why an equation for S is needed at all, is that the time the ion takes to cross the acceleration region (t_e-t_o) depends on the starting time t_o, the initial ion velocity U_o and on all the parameters of the tube voltage. Thus t_e depends on a lot of factors and the most convenient way to calculate it is to use an equation for the distance covered by the ion while accelerating, knowing that this should equal the grid separation at the correct value of t_e.

The first section of the algorithm, on the left hand side of figure 3.16, calculates a "window" of time that t_e should lie within, this window being necessary if the *bisection method* is to be used to converge to a value for t_e.

The bisection method is shown in the right hand side of figure 3.16. A lower and higher limit on t_e, t_L and t_H respectively are defined and t_e is set to half way between the two. S is calculated and compared with the actual distance (4.5mm in this case). If the difference is not below about 1 micron, this error being decided on after a number of trial runs, then t_e is revised. If S is larger than 4.5 mm then t_e must lie somewhere between its present value and t_L, therefore the higher time limit t_H is set equal to t_e and the new value of t_e is again chosen half way between t_H and t_L. The process is repeated a number of times (about 10 on average) until S eventually converges to a value within 1 micron of 4.5 mm. The value of t_e at this stage can be considered as the true value and it is then a simple matter of calculating V.

From the value of V, the time to travel the length of the tube L, can be calculated from

$$t_{tof} = \frac{L}{V}$$

A similar algorithm is then applied for the de-acceleration of the ion as it leaves the TOF tube, and for the re-acceleration of the ion if it passes the grounded grid. Once it passes the final grid the acceleration towards the electron multiplier is again determined by the variation on the TOF tube but to a lesser extent because of the large bias on the front of the multiplier, of -3kV.

Chapter 4
MASS SPECTRA

In this chapter several mass spectra, from a working model of the mass spectrometer, are presented. They include spectra of the ambient air, and of known mixtures of other gases. Before looking at these in detail, it is necessary to clarify some of the terms used as well as looking at the structure of air in order to identify the different peaks in the spectra.

Resolution

The resolving power is a measure of the smallest increment in mass that can be identified in the mass spectrometer output. By convention, this is defined in terms of $m/\Delta m$, where m is the mass of the observed peak and Δm is the amount by which the mass of another peak of equal intensity must be smaller or larger in mass than the observed peak in order that the height contribution of one to the other becomes negligibly small. This is normally accepted as the point where the valley between the two peaks is 10% of the peak height i.e. $h/H = 0.05$ in figure 4.1 overleaf.

A measure of resolution may also be obtained from a single peak if the shape is approximately Gaussian. The mass difference Δm, calculated above, is equal to the width of a single Gaussian peak at 5% of its height and equal to 2.08 times the full width at half maximum (FWHM). If Δm remains constant over the mass range of the spectrometer, the resolution may also be quoted as simply Δm atomic mass units.

When peaks have long "tails", extending much beyond the nominal mass number, there may be considerable addition or subtraction to the top of one peak from the tail of another (figure 4.2). This can be a particular problem in trace analysis where small peaks must be

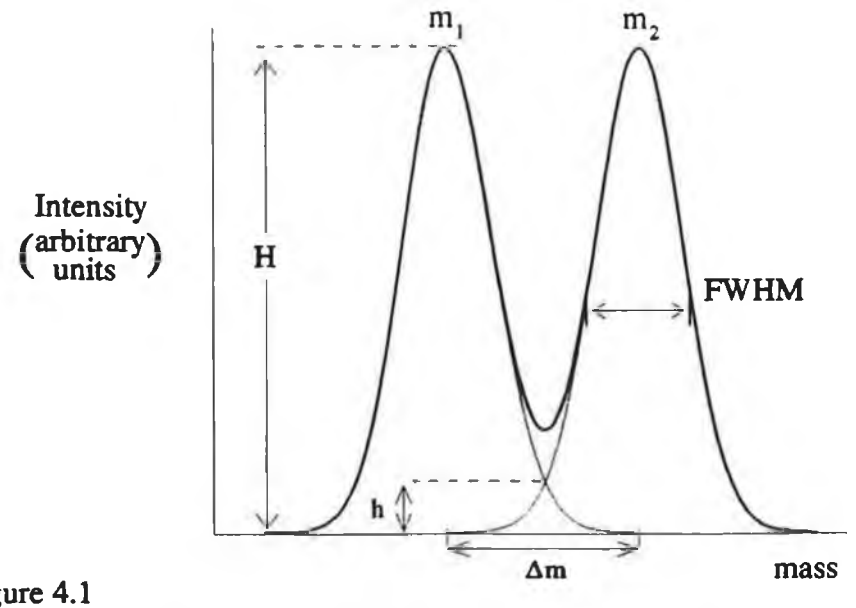

Figure 4.1
Two mass peaks of equal intensity, seperated by Δm atomic mass units

assertained in the presence of large ones and also in the determination of low abundance isotopes adjacent to masses of high abundance. The ability of a mass spectrometer to handle such a problem is measured by the *abundance sensitivity* whose magnitude is given by the ratio of peak ion current at mass m to the "background current" at adjacent mass spectral positions m±1. The background current is considered to be the absolute value of the difference in height of a peak, at either m±1, due to the presence of the peak at mass m.

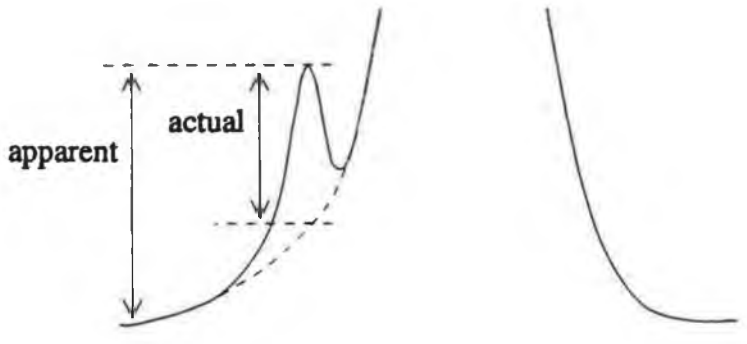

Figure 4.2
Diagram showing the distortion of the height of a small peak in the presence of a large peak close by

For Quadrupole mass filters, transmission of the ion beam through the filter and resolution are complimentary parameters. Typically a resolution of 100 at 100 amu (Δm = 1amu) is achieved at a transmission of 10% with resolution dropping to 35 at 100 amu (Δm = 2.8 amu) for transmission of 100% [6]. For a conventional time-of-flight mass spectrometer the resolution is dependant on the speed of response of circuitry rather than on geometric factors. Present commercial instruments have a resolution of around 300 with a mass range up to 1500 amu (Δm = 5 amu) [6].

Mass spectral patterns

The ionisation source in most mass spectrometers operates at an ionisation potential somewhat in excess of what is needed for parent ion formation i.e. singly charged replica of the ambient atoms or molecules. This results in the appearance in the spectra of doubly, triply, etc. charged ions in addition to the isotope peaks. The array of peaks in the complete spectrum of a pure substance is referred to as a *cracking pattern*. Peak heights in a spectrum are usually normalised by taking the largest peak in the spectrum, called the base peak, and allotting it a height of 100 units. Part (a) of figure 4.3 overleaf shows the cracking patterns, in tabular form, of the three most abundant elements in air (excluding water vapour). Cracking patterns have three important properties:

(1) Every chemical compound has its own distinctive cracking pattern or "fingerprint"
(2) Cracking patterns are constant as long as experimental parameters are kept unchanged
(3) When two or more components are present at the same time, each will produce its own cracking pattern and the resultant spectrum is produced by simply adding the components.

Therefore a list of cracking patterns for different compounds or compilations of compounds can be stored and used to identify or remove the presence of particular atoms or molecules from a mass spectrum.

Element	Percent by Volume
N_2	78.08
O_2	20.95
Ar	0.934
CO_2	0.033
Ne	1.8×10^{-3}
He	5.2×10^{-4}
CH_4	2.0×10^{-4}
Kr	1.1×10^{-4}
N_2O	5.0×10^{-5}
H_2	5.0×10^{-5}
Xe	8.7×10^{-6}
O_3	7.0×10^{-6}

Cracking patterns

m/e	% abundance
13	0.01
20	19.10
36	0.36
38	0.08
40	100.00

m/e	% abundance
12	0.12
16	8.96
28	3.40
32	100.00
33	0.10
34	0.40

m/e	% abundance
14	6.85
27	0.96
28	100.00
29	0.89

(a) Components of atmospheric air (excluding water vapour)

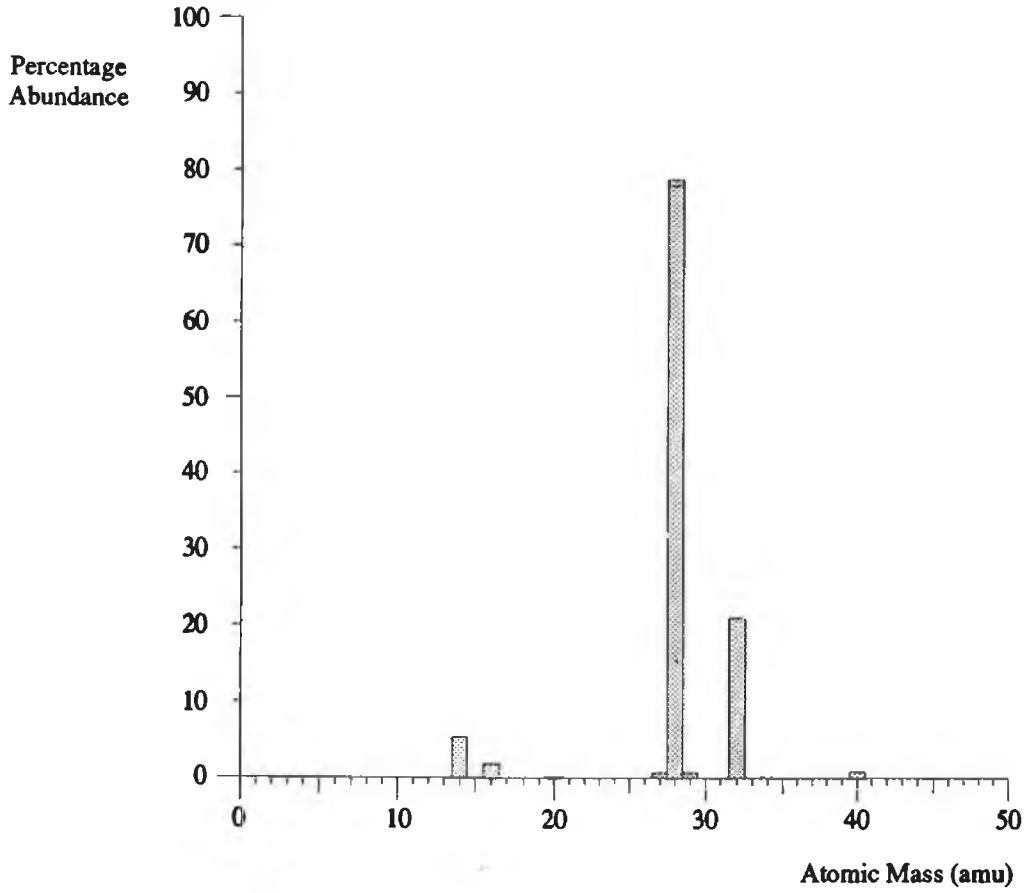

(b) Expected mass spectrum of air (excluding water vapour)

Figure 4.3

Electron impact phenomena

When electrons collide with neutral particles the collisions may be elastic or inelastic. If the electrons are travelling at a low velocity, elastic collisions occur with no change in the internal energy of the atom. If the velocity is increased, the collisions become inelastic when excited species are produced. The excess energy gained by the atom is eventually dissipated as radiation. At even higher energies many configurational changes are possible. At electron energies of 25-30eV, stripping of two valence electrons becomes possible, producing doubly charged ions and when the energy available becomes equal to the dissociation energy in one of the ion's degrees of freedom, fragment ions appear.

The typical components of atmospheric air are given in part (a) of figure 4.3. The bar graph in part (b) is a convenient way of showing the expected spectrum. A table of the nuclidic masses and relative abundances of the isotopes of the most common elements of air is given in appendix A

Mass spectra

After examining what is to be expected for the mass spectrum, it is now appropriate to look at some of the recorded spectra.

Figure *spectrum # 1* (page 57) shows the mass spectrum obtained for residual air inside the vacuum system at a pressure of $1x10^{-5}$ mbar. It shows all the major peaks as expected; nitrogen, oxygen, etc., as well as a water vapor peak. Fragment peaks of water vapor, OH, and single oxygen and nitrogen are also distinctly visible. Argon and a rather large carbon dioxide also appear and the isotopes of N_2 appear in approximately the correct proportions at 27 and 29 amu. There are a number of small peaks notably at atomic mass numbers 15,26,42 and ≈50 upwards which cannot be easily explained and are more than likely due to pollution in the air, fragmented pump oil contaminants, noise or a combination of these. The following is a list of the additional spectra and what they represent:

*spectrum # 2....*Helium & air

*spectrum # 3....*Methane & air

*spectrum # 4....*Argon & air

*spectrum # 5....*Nitrogen & air

*spectrum # 6....*90% Ar, 10% CH_4 & air

*spectrum # 7....*Butane/Propane (domestic gas) & air

Each scan took approximately 20 seconds to record and the N_2 peak represents a signal voltage of approximately 3.5V (at a pressure of $3x10^{-5}$mbar). The mass scale on these spectra are not linear for reasons mentioned in chapter 2, however it is possible to adjust the scale so that the mass increments are of equal length, by using a computer, provided it can predict accurately when the mass peaks are to be expected. The computer algorithm shown in the previous chapter was written for this purpose and it's predictions along with the experimentally measured breakthrough times are given in table 4.1 below. A comparison shows that the computer can predict the timings of the peaks down to at least 0.6% accuracy and indicates that the computer model fits well with the actual spectrometer.

Parameters: f_{tube} = 45.00 kHz, V_{ac} = 300 v_{p-p}, Initial ion energy = 10 eV

		V_{dc} = -50v		V_{dc} = 0v	
Element	Mass No.	Measured time (μS)	Calculated time (μS)	Measured time (μS)	Calculated time (μS)
N	14	14.2	14.22	15.15	15.16
CH_3	15	14.3	14.37	15.37	15.39
CH_4	16	14.4	14.46	15.59	15.61
H_2O	18	14.79	14.73	16.07	16.04
Ar^{2+}	20	15.05	15.05	16.47	16.44
N_2	28	16.33	16.31	17.87	17.85
O_2	32	16.91	16.87	18.51	18.47
Ar	40	17.89	17.89	19.6	19.59

Table 4.1

Comparison between measured and calculated values of breakthrough times

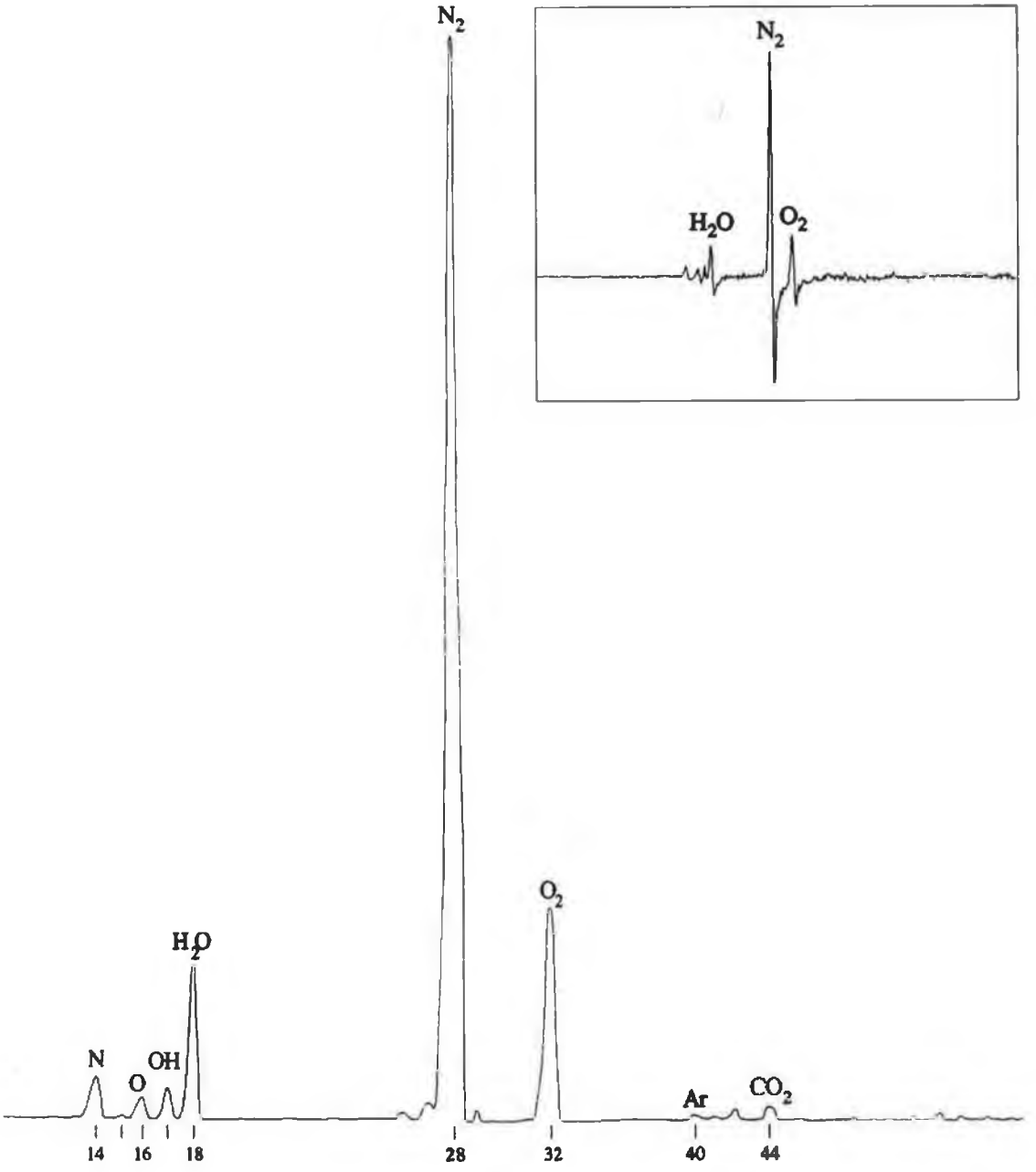

Spectrum # 1

The recorded mass spectrum of Air at $1x10^{-5}$ mbar

(inset: oscilloscope trace of same spectrum)

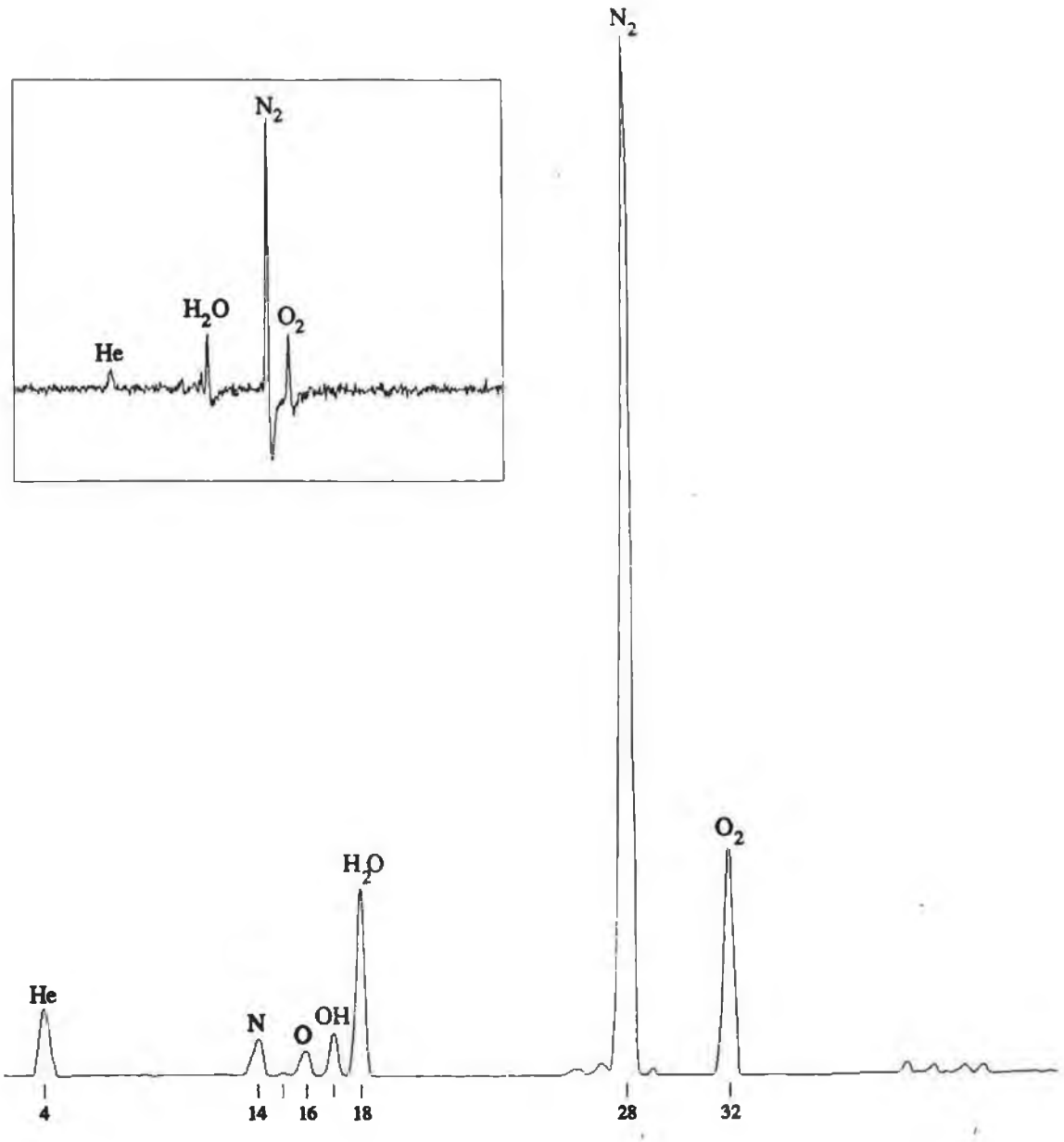

Spectrum # 2

The mass spectrum of Helium & air at $3x10^{-5}$ mbar

(inset: oscilloscope trace of same spectrum)

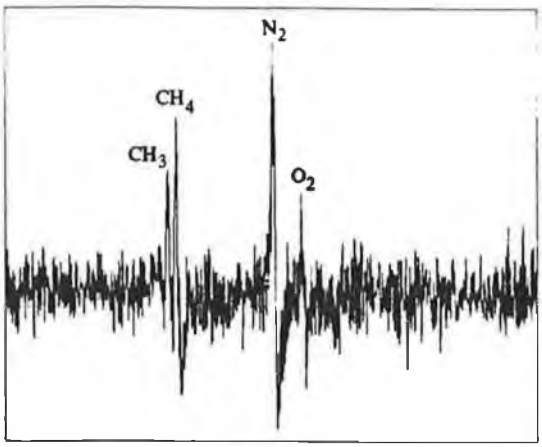

oscilloscope trace

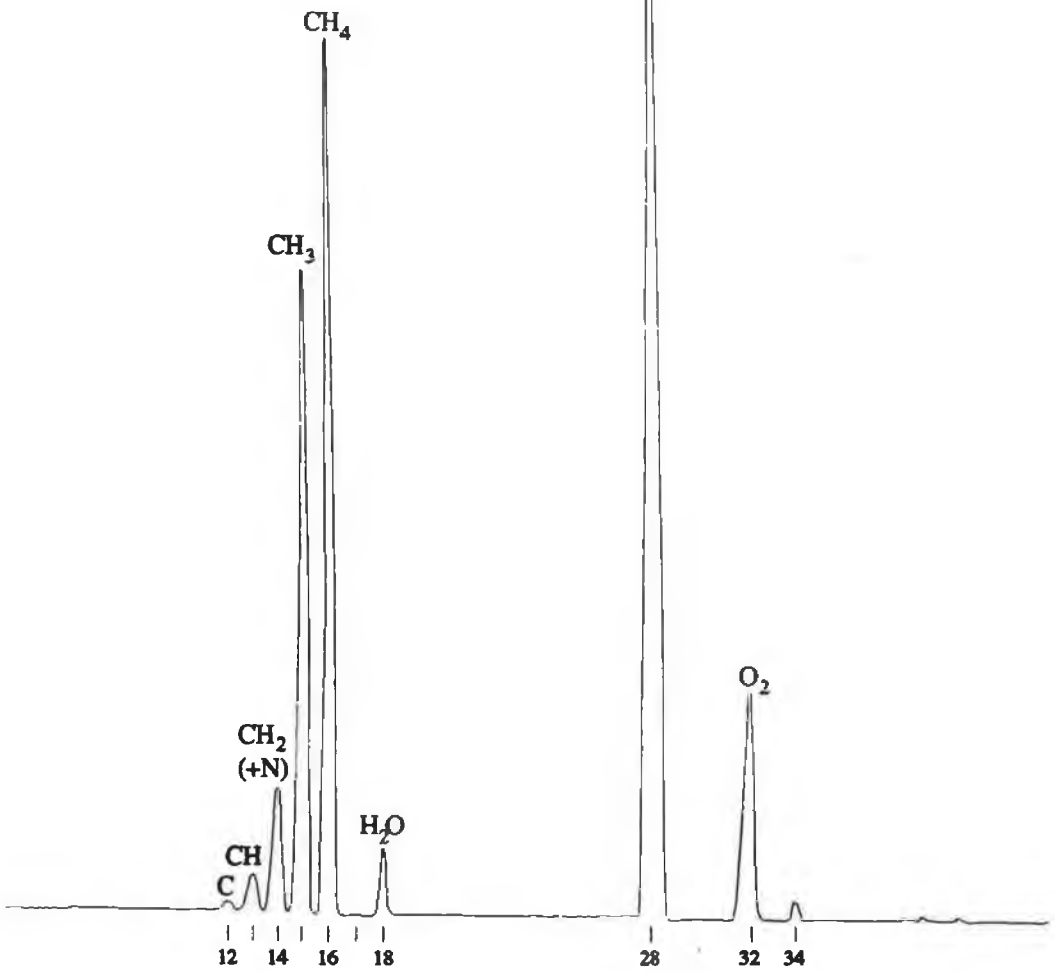

Spectrum # 3

The mass spectrum of Methane and air at $3x10^{-5}$ mbar

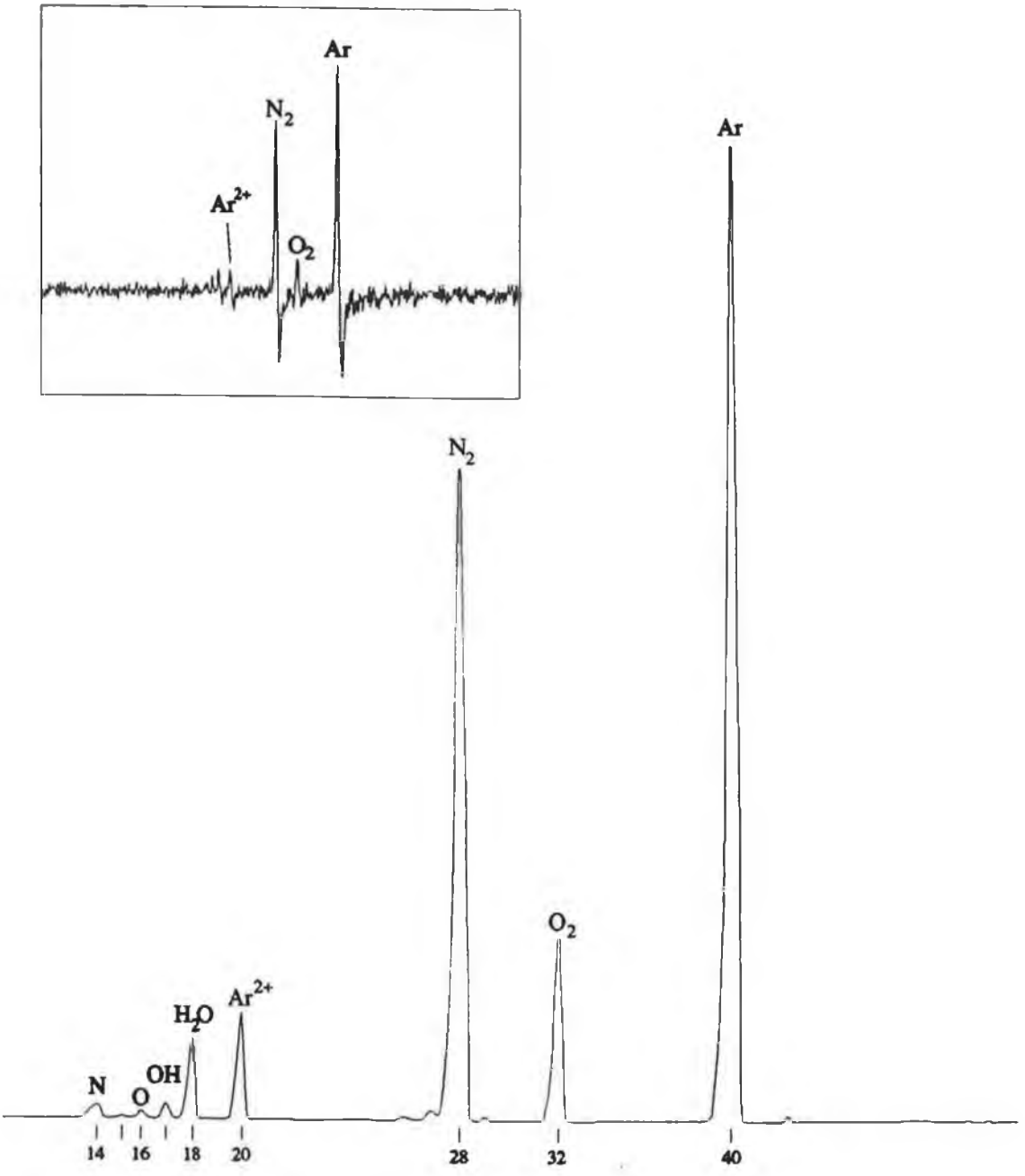

Spectrum # 4

The mass spectrum of Argon and air at $3x10^{-5}$ mbar

(inset: oscilloscope trace of same spectrum)

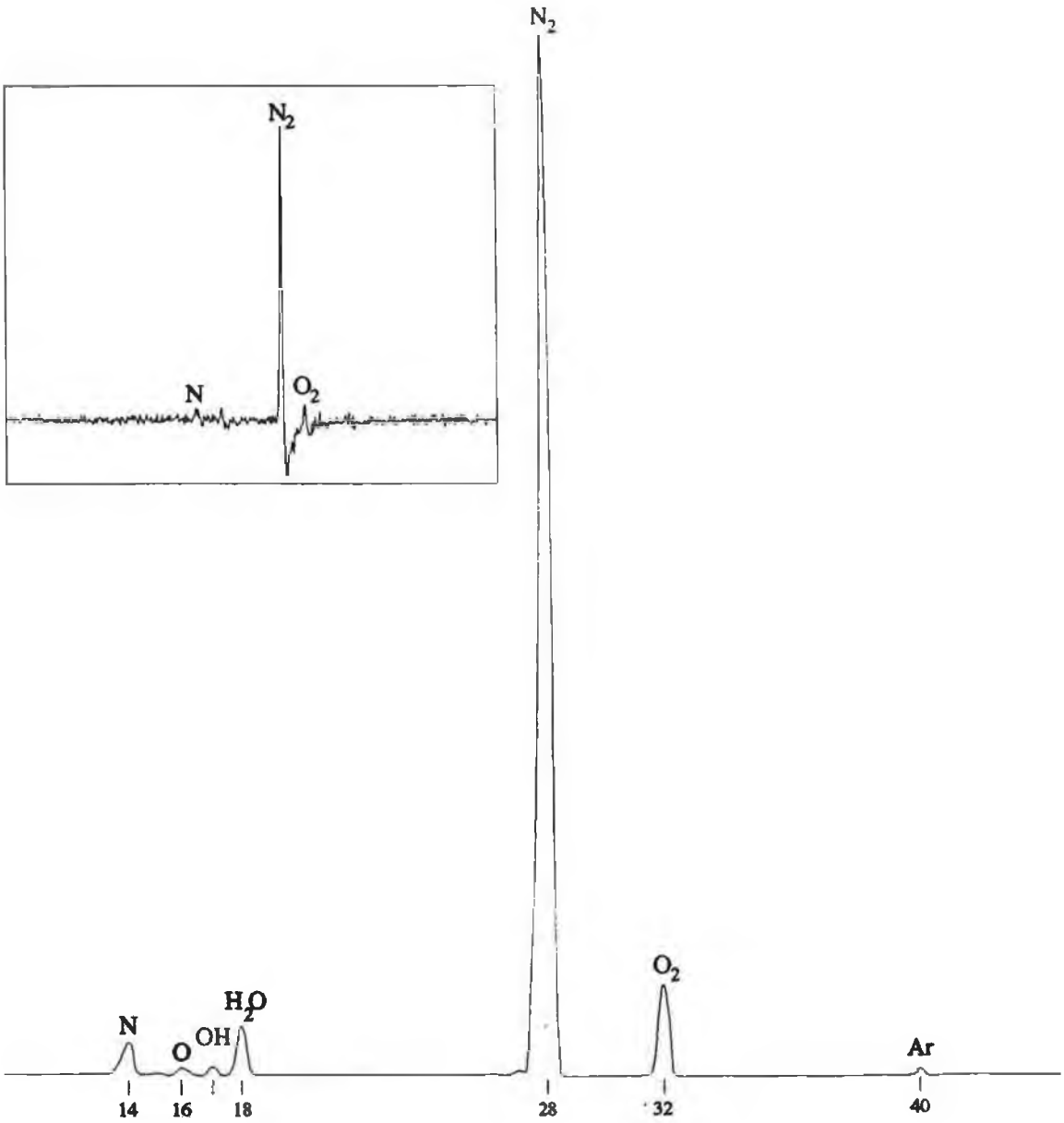

Spectrum # 5

The mass spectrum of Nitrogen and air at $3x10^{-5}$ mbar

(inset: oscilloscope trace of same spectrum)

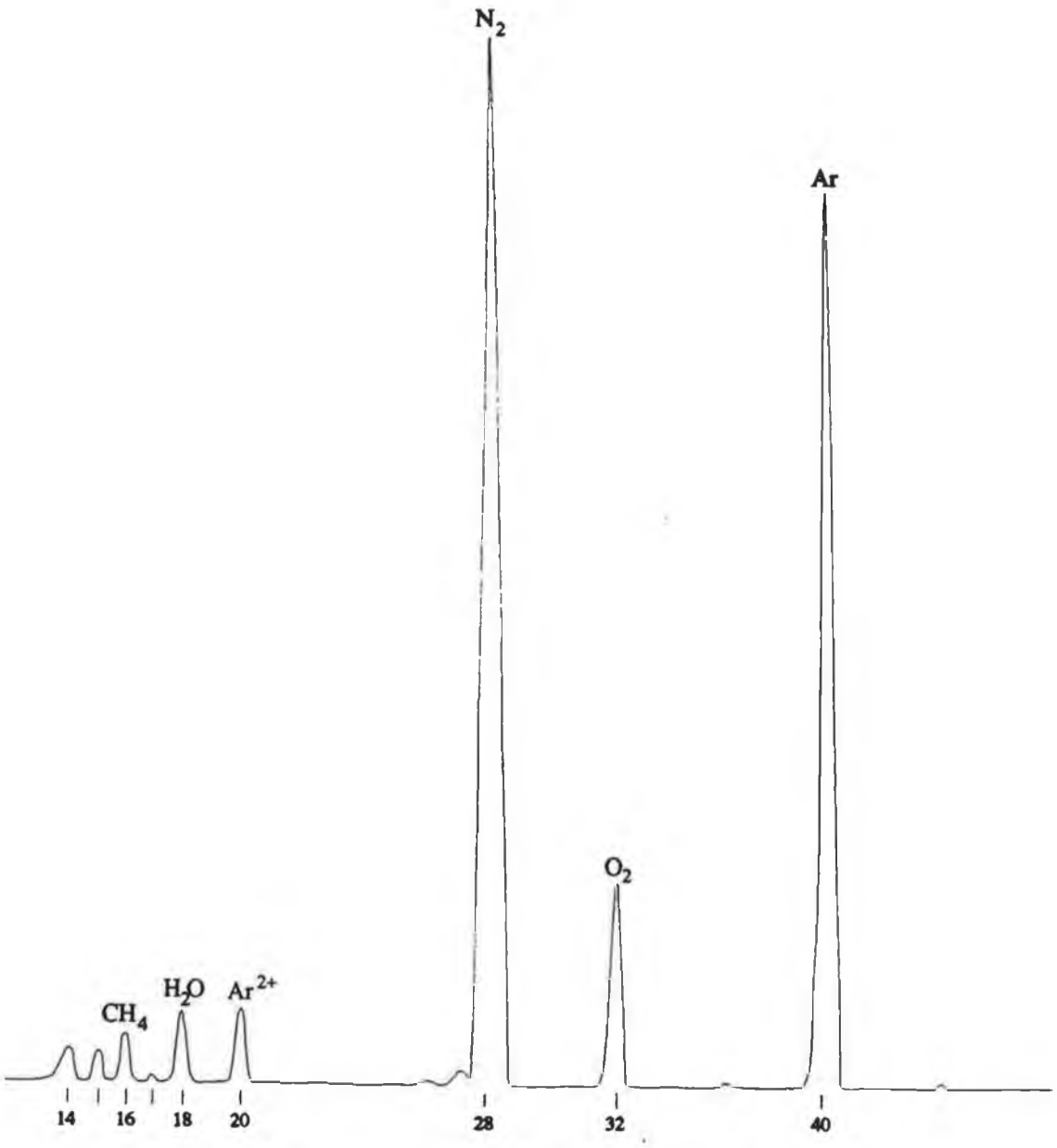

Spectrum # 6

The mass spectrum of 90% Ar, 10% CH_4 and air at $3.5x10^{-5}$ mbar

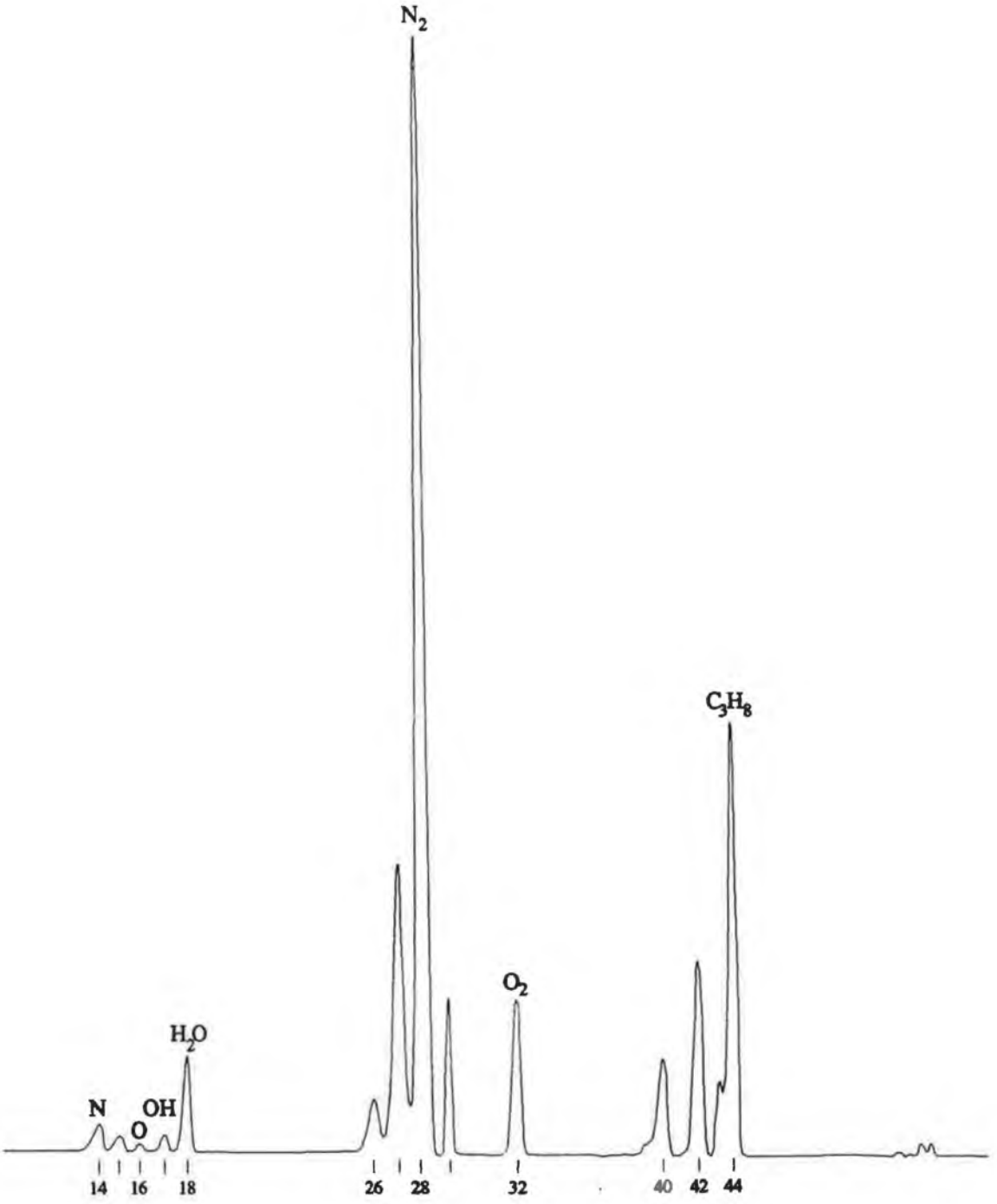

Spectrum # 7

The mass spectrum of Butane/Propane and air at $3x10^{-5}$ mbar

(Calor Kosangas : C_4H_{10} / C_3H_8)

Resolution and Abundance sensitivity of spectra

The full width of the peaks at half maximum is 0.4 amu and seems generally independent of atomic mass. Thus the resolution by definition (atomic mass divided by 2.08 times the FWHM) increases with atomic mass from a value of 18.8 at 15 amu to a value of 50 at 40 amu which is more than sufficient for residual gas analysis.

The abundance sensitivity can be examined as follows. From the isolated peak of argon at 40 amu in *spectrum # 4* it can be seen that the width of the base is approximately 1.2 amu across and it has quite distinctive edges. Since the base extends ±0.6 amu about its center position its value at ±1 amu can be considered as zero and so the abundance sensitivity is infinite by definition.

As mentioned above the peaks have an almost un-naturally sharp cut-off, especially on the right hand side. This is because the actual spectrum signal drops below zero on this side of the peaks, as can be seen in oscilloscope trace, so the overshoot compensation circuit cuts this off replacing what was a negative value with zero and in this sense the abundance sensitivity is artificially enhanced. There is also an associated "dead time" after a peak which is the time taken for the negative overshoot to reach its maximum value (see chapter 3). During this time the compensation circuits output is held at zero volts. The effect of this can be seen in *spectrum # 1* where the peak of the nitrogen isotope at 29 amu is sharper than its 27 amu counterpart. What has happened here is that part of the 29 amu peak has been obscured while the negative overshoot of the 28 amu peak was reaching maximum. This is not a problem as long as the height of mass 29 is not adversely affected, otherwise the abundance sensitivity could not be considered as infinite.

CONCLUSION

There is no doubt that the mass spectrometer described in this thesis is well capable of resolving mass peaks of as little as one atomic mass unit apart. Although this was only tested with gases of atomic mass up to 40 amu, there is no reason to suspect that it wouldn't work up as far as the required 100 amu, needed for residual gas analysis. This can be demonstrated using the computer model which in fact suggests that with modification, length of tube, frequency of voltage etc., it could probably be used for a much larger range of masses. The rôle of the computer model was not stressed much in the text but it played a very important part at the beginning of the research, most notably in the discovery of ion bunching. The good agreement between experimental and calculated values of breakthrough times makes the model a reliable indicator of what to expect.

The construction of the spectrometer is very simple and because of its very lax requirements on tolerances, especially since any variation in one parameter can be compensated with another (see figure 2.10, p.22), it could be easily manufactured for a fraction of the cost of a quadrupole of equal performance. However the quadrupole is capable of operating with a Faraday cup at pressures in the range 10^{-4} to 10^{-7}mbar, whereas an electron multiplier is needed at all pressure ranges with the new time-of-flight spectrometer and so takes away from this advantage somewhat. The length of the spectrometer is extended by approximately 150mm by the electron multiplier to an overall length of approximately 450mm which is very compact for a time-of-flight and compares favorably with a typical quadrupole.

Possible problems could arise in the presence of very heavy ions that take more than one cycle of the tube frequency to travel down the tube, as discussed in the text and such things as having to adjust peak heights by a calibration factor (HAF), having to shape the peaks to compensate for overshoot and adjust the mass scale to make it linear, are a little awkward. It should be noted that

the height adjustment factor only corrects for the abnormalities in the heights of peaks due to the fundamental operation of the mass spectrometer and does not include factors such as the initial divergence or defocusing of the ion beam (figure 3.3, p.32), the efficiency of the ion source for different gases or the detection efficiency of the electron multiplier for different ion masses etc.. As there was no available method for comparing the heights of peaks, it in not known if these factors are significant and need to be included, so the computer calculated peak heights, HAF etc. should be taken with this in mind.

The fact that pulses of ions are being detected rather than a continuous ion beam make it necessary to use high-frequency high-gain high- bandwidth amplifiers (a problem shared with conventional time-of-flight spectrometers). As a result the spectrum is noisy and needs to be averaged electronically if all but the largest peaks are to be observed. While this in itself does not present much difficulty, it means that considerably more expensive and elaborate circuitry is needed compared to other mass spectrometers, the main competitor for residual gas analysis being quadrupoles, which simply measure a dc current.

Apart from the above problems, which are quite easily overcome, the spectrometer functions very well and is a definite competitor to the older types for residual gas analysis, where its combination of low cost materials and general simplicity make it a good choice.

Future Developments

As mentioned in the text, the potential for this mass spectrometer could be greatly improved by the digital control of its components, such that it could be controlled by a computer, where the necessary adjustments such as peak height, mass scale and overshoot compensation could be achieved with greater ease and a lot more versatility. The automatic control of DC voltage, AC amplitude, frequency etc., would also allow a computer to adjust the parameters of the spectrometer to optimise

performance for a particular mass peak or range of mass peaks. Improvements could also be made in the computer model to include such things as the efficiency of the ion source, electron multiplier, electrostatic lenses etc., as mentioned above, so that a more accurate height adjustment factor could be calculated to include all the relevant variables.

There is a possible alternative to the one economic drawback of this spectrometer, the electron multiplier / high speed electronics and it is shown in the diagram below. It consists of replacing the electron multiplier tube with a Faraday cup and a grid G_3. This grid can be the same grid that is used at present to reduce field penetration caused by the high voltage on the front end of the electron multiplier (see figure 2.8, p.21), since field penetration will not be a problem with this configuration

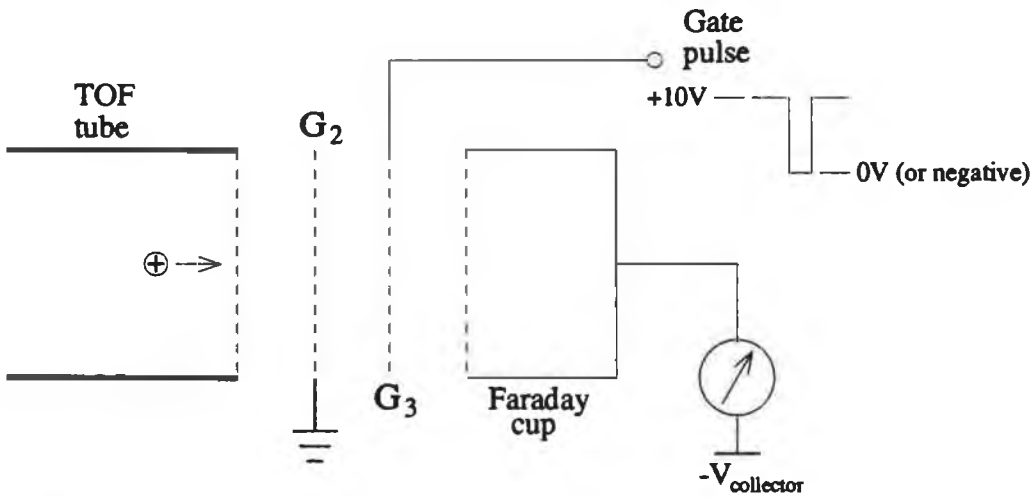

Figure: future 1
Schematic diagram of a possible alternative to an electron multiplier detector

The idea is to apply a 10 to 20nS negative pulse to G_3 at a particular time during the tube cycle that is of interest, while keeping the grid at +10V or greater at all other times (initial ion energy = 10eV). Thus only the ions that cross grid G_2 at the time the pulse is applied to G_3 will go on to reach the Faraday cup. By using a measuring device with a slow response compared to the frequency of pulses on G_3, an average current for that point in the spectrum will be obtained. It is much easier

electronically, to measure the magnitude of what in effect is a small dc current, than the present technique; measuring the height of a 10 or 20nS pulse of current (even if it is magnified by 10^6 times by an electron multiplier).

A mass spectrum can be obtained by changing the timing of the pulse with respect to the tube voltage, similar to what is done electronically at present. The pulse depth is a matter of convenience, although it must at least equal the voltage on G_2 (0V) if it is to allow all ions passing G_2 to cross into the detector. Very sharp and accurate pulses can be obtained by using a length of transmission line terminated with a short circuit, the length determining the pulse width (10nS per meter). The Faraday cup can be directly replaced with an electron multiplier at very low pressures if necessary, to increase sensitivity, similar to what is needed when using a quadrupole or other types of mass spectrometers.

REFERENCES

[1] White, F.A. & Wood, G.M. 1986. "Mass Spectrometry, Applications in Science and Engineering". Wiley: New York

[2] Dempster, A.J., Phys. Rev., 11, 316 (1918).

[3] Bainbridge, K.T., Phys. Rev., 44, 123 (1933).

[4] Nier, A.O., Rev. Sci. Instr., 11, 212 (1940).

[5] Davis, W.D., in Trans. of the 10th National Symposium of Vacuum Technology, Pergamon, New York (1962), p.363.

[6] Roboz, J. 1979. "Introduction to Mass Spectrometry, Instrumentation and techniques". Wiley: New York

[7] Bennett, W.H., J. Appl. Phys., 21, 143 (1950).

[8] Stephens, W.E., Phys. Rev., 69, 691 (1946).

[9] Wiley, W.C., and McLaren, I.H., Rev. Sci. Instr., 26, 1150 (1955).

[10] Harting, E & Read, F.H. 1976. "Electrostatic Lenses" Elsevier

[11] V.G. Quadrupoles Ltd., Nat Lane, Winsford, Cheshire CW7 3QH, England. (1986).

[12] Thorn EMI Electron tubes Ltd., Bury Street, Ruislip, Middlesex HA4 7TA, England. (1988).

[13] Philips/Mullard Ltd., Mullard House, Torrington Place, London WC1E 7HD, England. (1987).

[14] Horowitz, P. & Hill, W. 1980. "The Art of Electronics" Cambridge University Press: Cambridge

[15] Smith, R.J., 1976. "Circuits, Devices and Systems". Wiley: New York

[16] Handbook of Chemistry and Physics, 70th edition, 1989-1990, section B-277.

ACKNOWLEDGEMENTS

To my supervisor, Dr. Joe Fryar, for his excellent guidance and support during the course of this research.

To the rest of the academic staff for their advice and encouragement.

To Eolas for their substantial funding of this research.

To the other members of the Atomic and Nuclear Group; Neil o'Hare, Charles Markham and Kieran McCarthy, for their advice, friendship and company, providing a cheerful pleasant atmosphere in the Lab, and to Mike Sheehy, who I took over from, for guidance when starting this research.

To the other postgraduate students, who have made working here so pleasant and enjoyable, namely; Kev McGuigan, Kev Devlin, Paul Jenkins, John Scanlon, Colin Potter, Adrian Geissel, Jim Brilly, Colin Kelly, James Molloy, Jim Campion, Simon McCabe, Gerry Shaw, Richie Corcoran, Marggie Jones, Liam Roberts, Kev Mellon, Siobhan Daly, Hugh Grimely, Brian Hurley, Ciaran o'Morain, Ger Ennis, Mark Daly, Brian Finigan, Dave Evans, Tony Murphy, and Ena Prosser, the only non-physics member of the "Breakfast club".

APPENDIX A

Below is the periodic table of elements showing the atomic mass and number for each element. The table overleaf is a list of nuclidic masses and relative abundances of isotopes, of the elements that occur in the mass spectra in chapter 4.

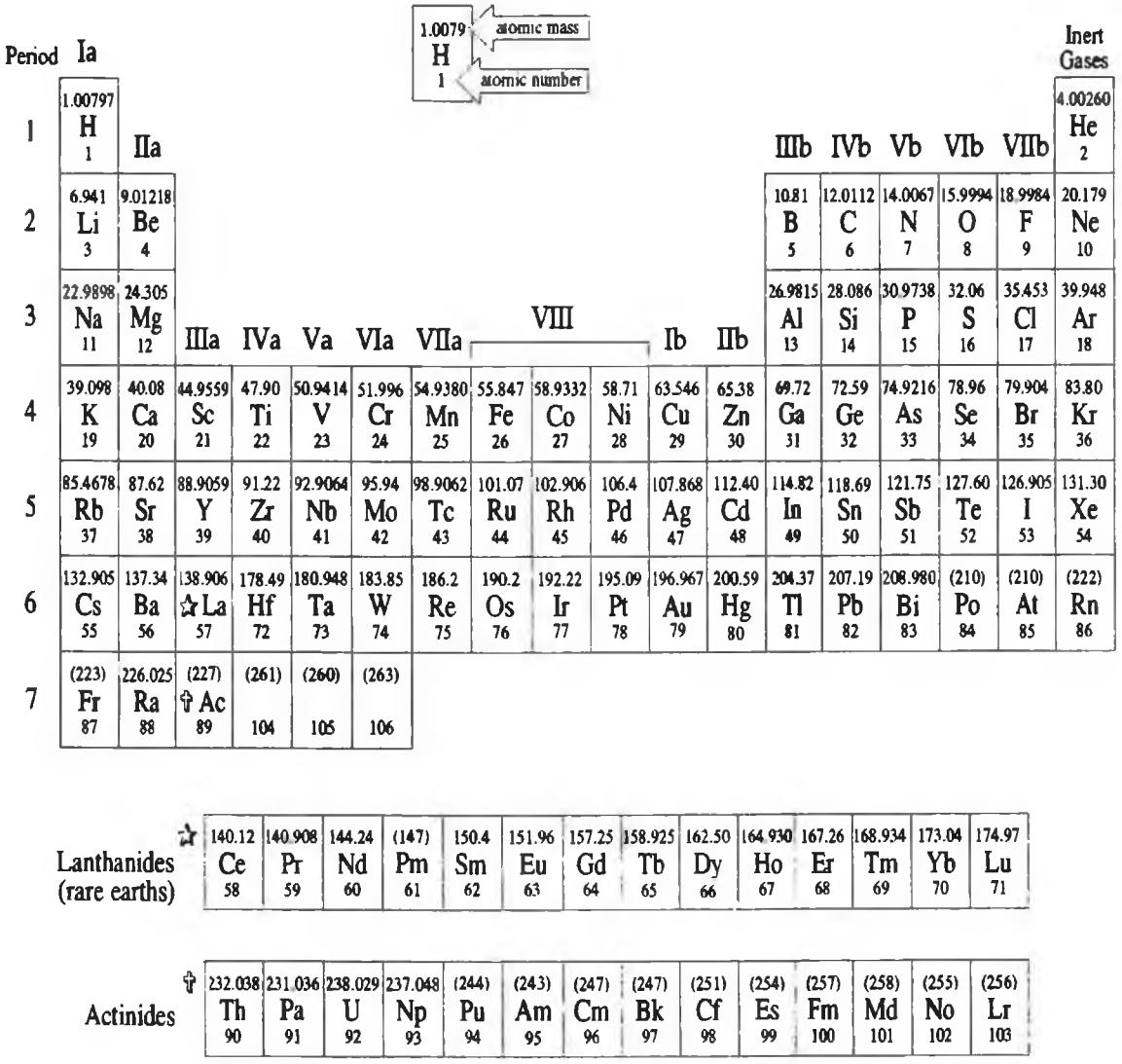

The following designations are conventional for a chemical element **X** [6]:

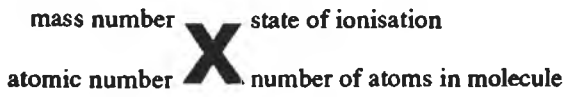

Below is a table showing the elements, and their isotopes, which appear in mass spectra presented in chapter 4 [16].

Table of elements and their isotopes, which appear in the mass spectrum of air

Element	atomic number	mass number	percentage natural abundance	nuclidic mass	half life	atomic mass
Hydrogen	1					1.00797
		1	99.985%	1.007825		
		2	0.015%	2.0140		
		3		3.01605	12.26 yr	
Helium	2					4.002603
		3	0.000138%	3.01603		
		4	99.999862%	4.00260		
		5		5.01222		
		6		6.018886	0.808 s	
		8		8.03392	0.122 s	
Carbon	6					12.0111
		9		9.031039	0.127 s	
		10		10.01686	19.3 s	
		11		11.01143	20.3 min	
		12	98.90%	12.000000		
		13	1.10%	13.003355		
		14		14.003241	5730 yr	
		15		15.010599	2.45 s	
		16		16.014701	0.75 s	
Nitrogen	7					14.0067
		12		12.018613	0.011 s	
		13		13.005738	9.97 min	
		14	99.63%	14.003074		
		15	0.37%	15.000108		
		16		16.006099	7.13 s	
		17		17.008450	4.17 s	
		18		18.014081	0.63 s	
		19		19.017040	0.42 s	

Continued overleaf.....

.....continued

Element	atomic number	mass number	percentage natural abundance	nuclidic mass	half life	atomic mass
Oxygen	8					15.9994
		13		13.02810	0.009 s	
		14		14.008595	70.6 s	
		15		15.003065	122 s	
		16	99.76%	15.994915		
		17	0.04%	16.999131		
		18	0.2%	17.999160		
		19		19.003577	26.9 s	
		20		20.004075	13.5 s	
		21		21.008730	3.14 s	
Argon	18					39.948
		32		31.997660	≈0.1 s	
		33		32.989930	0.017 s	
		34		33.980269	0.844 s	
		35		34.975256	1.77 s	
		36	0.337%	35.967545		
		37		36.966776	34.8 days	
		38	0.063%	37.962732		
		39		38.964314	269 yr	
		40	99.60%	39.962384		
		41		40.964501	1.83 hr	
		42		41.963050	33 yr	
		43		42.965670	5.4 min	
		44		43.96365	11.9 min	
		45		44.968090	21 s	
		46		45.968090	3.8 s	

APPENDIX B

The diagrams of a proposed vacuum chamber for the mass spectrometer are shown below. It is intended that the spectrometer be a self contained unit with all the electrical connections being brought out at the back, such that it could be attached to a vacuum system via a single flange connection, like present commercial residual gas analysers. It should then be a simple matter of connecting the mass spectrometer to the vacuum chamber, connecting the vacuum components via a single cable to the electronics (all contained in one unit), to set up the spectrometer.

The present layout of the spectrometer is shown full in figure B.3 on page 3. The ion source and electron multiplier are drawn approximately to scale.

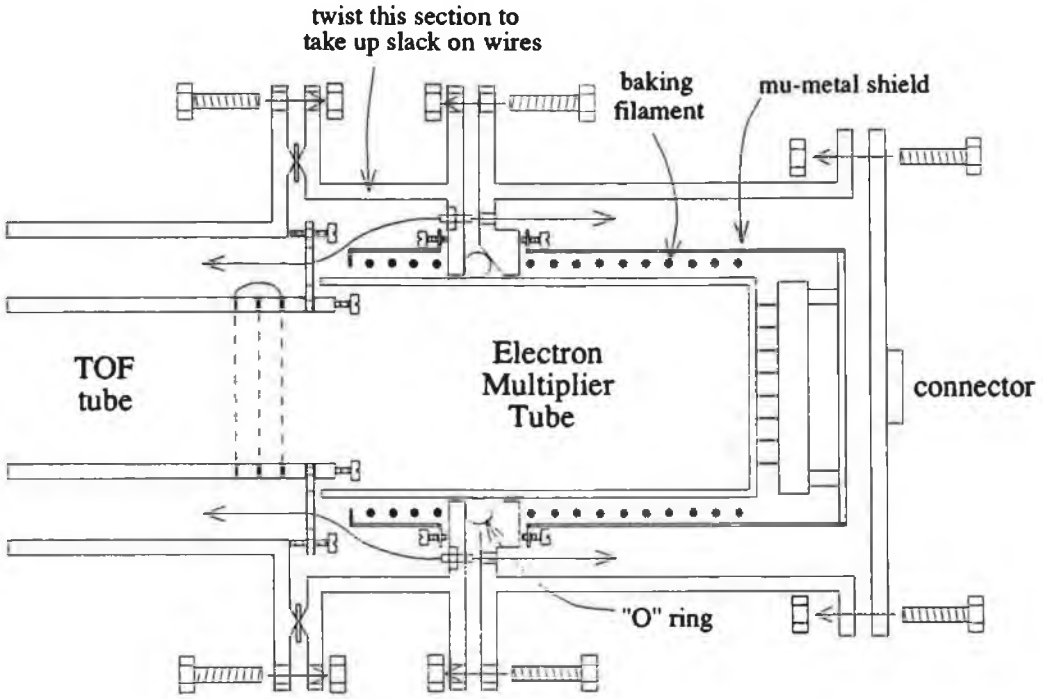

Figure B.1
Diagram of proposed vacuum mounting of the electron multiplier tube showing the connections to both the time-of-flight tube and the ion source

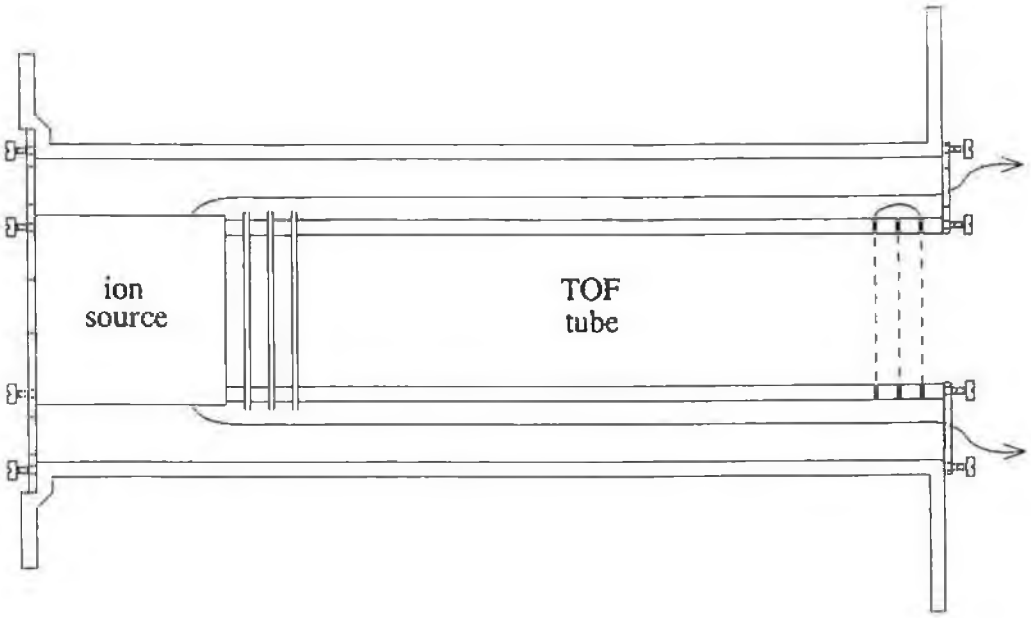

Figure B.2
Diagram of proposed vacuum chamber for time-of-flight tube and ion source

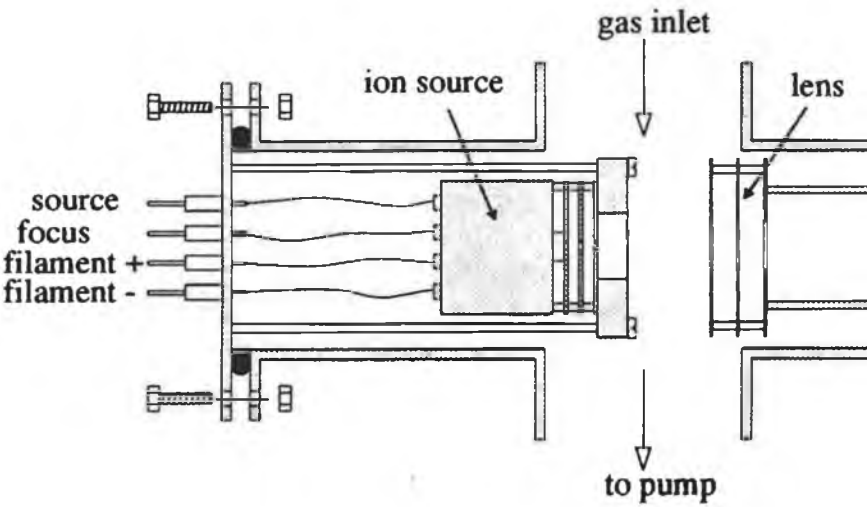

Figure B.3

Full diagram of the present mass spectrometer

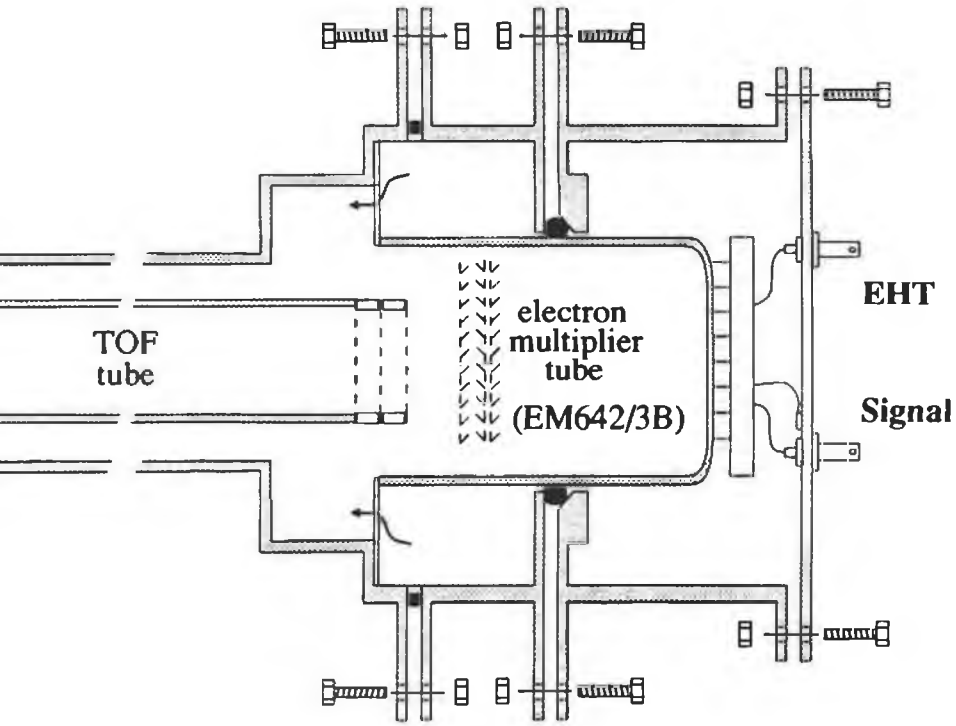
TOF
tube
electron
multiplier
tube
(EM642/3B)
EHT
Signal

APPENDIX C

Part 1

The first part of this appendix deals with circuits that were not given fully in chapter 3 for reasons of clarity. The first of these circuits is a three stage low-pass "Butterworth" active filter, shown below in figure C.1. it is a standard circuit, the details of whose operation are given in most textbooks on electronics and so it was not deemed necessary to show in detail in Chapter 3. The figure in which it appeared was figure 3.11.

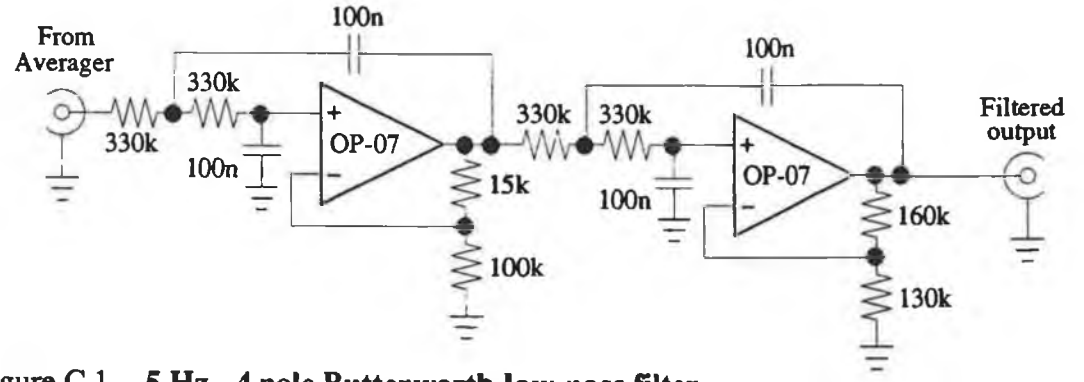

Figure C.1 **5 Hz - 4 pole Butterworth low-pass filter**

Also included here is the actual circuit for overshoot compensation. The circuit shown in figure 3.15 differes slightly from the actual circuit in that the compensation capacitor C1 and resistor VR1 are in fact biased to a small positive voltage via IC6, shown in a dashed box in figure C.2 overleaf. This makes no difference to the operation of the circuit as explained in chapter 3, it simply allows for a constant DC component that is inserted into the input signal by the leakage current from the FET switch. The compensation circuit will now be activated by an input signal below this unwanted DC voltage (usually below 100mV) instead of zero volts.

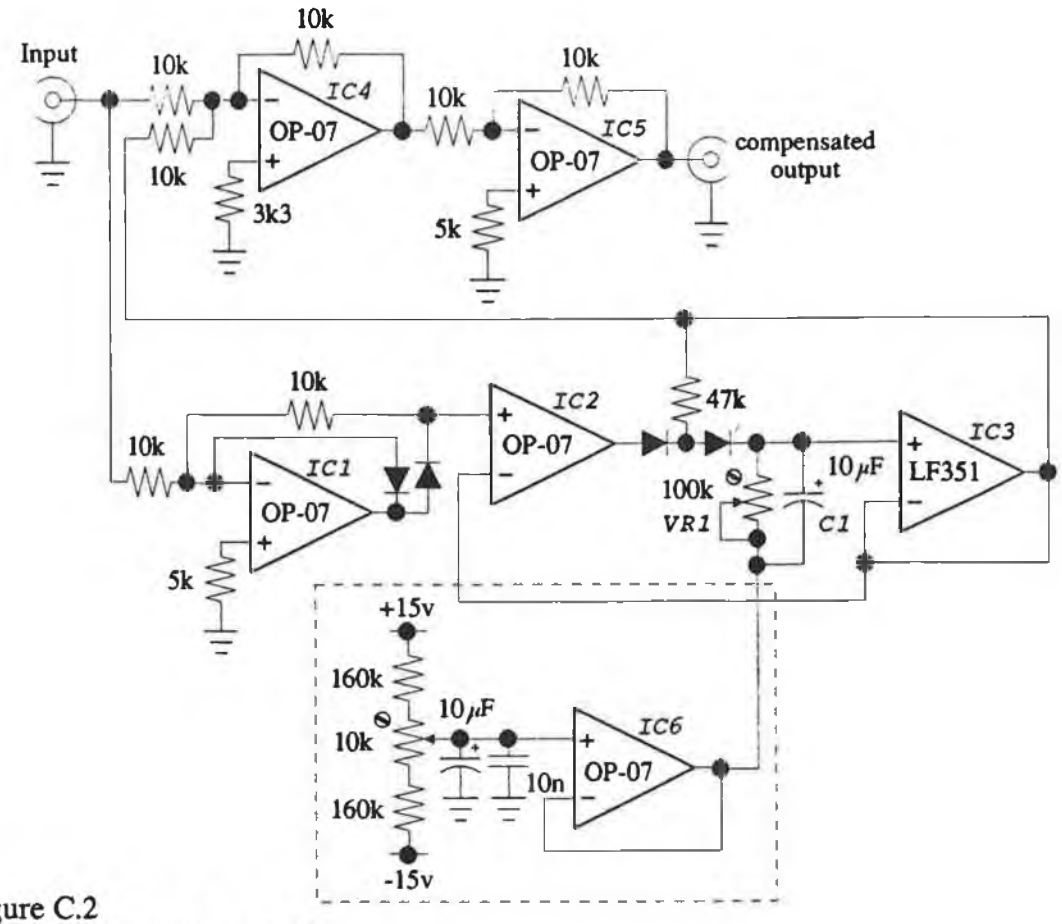

Figure C.2
Modification to figure 3.15

Figure C.3 on page 3 is the complete circuit of the mass spectrometer, showing all but the circuitry that controls the ion source. This circuit is of no importance to the operation of the mass spectrometer except in controlling the initial ion energy.

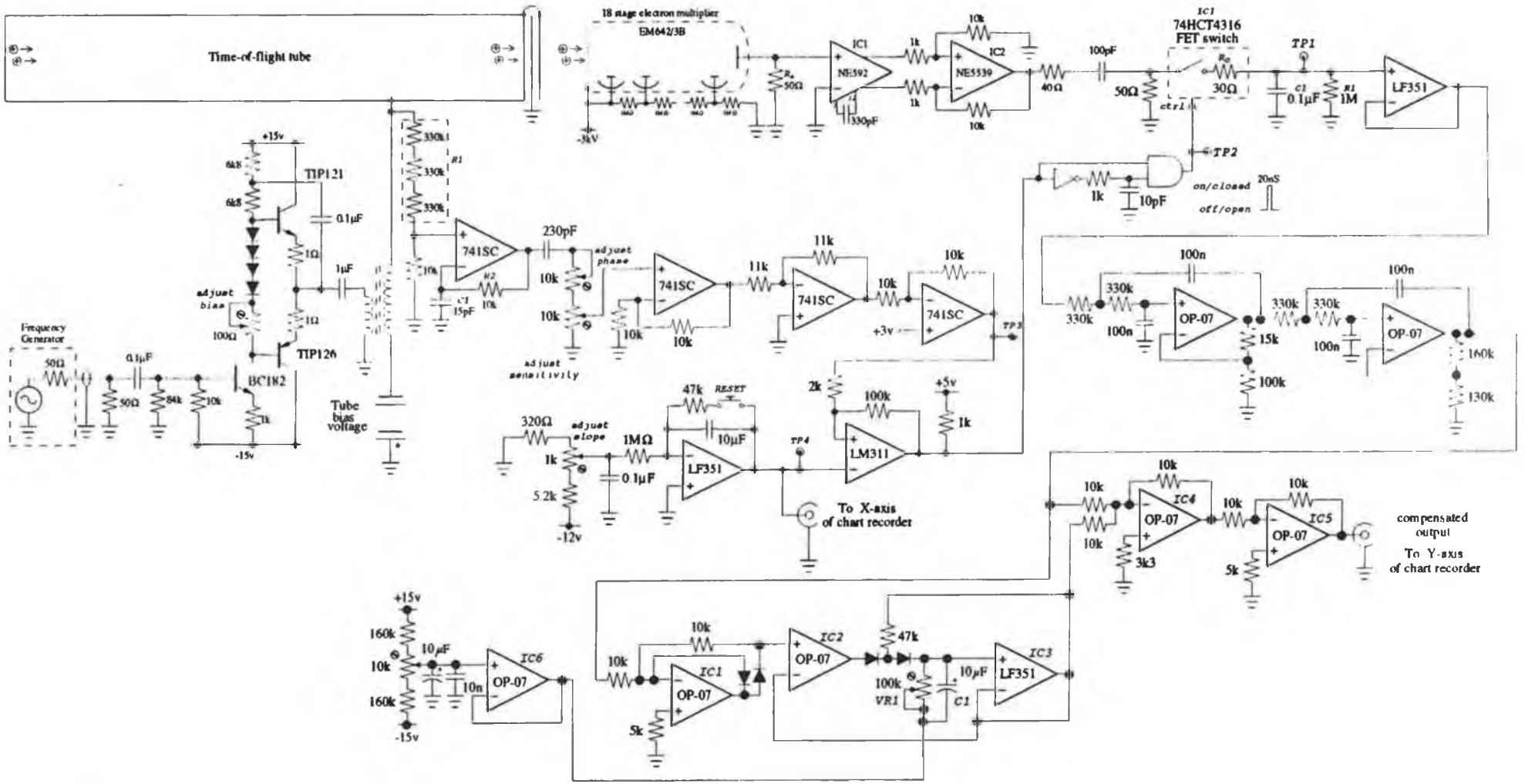

Figure C.3

The complete circuit of the mass spectrometer used to obtain results for this thesis

Part 2

The second part of this appendix concerns circuits that were designed for the mass spectrometer but for various reasons were never built.

The first of these is a programmable waveform generator that requires direct access to an 8-bit data line, a 1MHz clock, a $\overline{\text{write}}$ line and 6 address lines. The circuit, figure C.4, is shown overleaf. It produces an output waveform of any shape (programmable) at any frequency between 5kHz and beyond 100kHz. It also provides a trigger pulse whose position can be programmed to any point in the waveform within 10nS. It will also provide two auxiliary, fixed phase, trigger pulses if needed. The waveform amplitude is also programmable in 256 steps.

The waveform generator works by having a high speed digital to analog converter connected to RAM chips which have the waveform stored within them. The memory address of the RAM (2k, 16 bit) is clocked sequentially at 10MHz so that the output stream of numbers is converted into an analog equivalent. The waveform is written into the RAM by the controlling computer by disabling the 10MHz clocking signal and addressing the RAM via 2 of the 6 allocated computer addresses. The addresses and their functions are given below.

AD0 & AD1:

These are the addresses of the function generator memory and also contain convenient ways of altering the adjustable trigger pulse in 10nS steps.

AD0: D_7 - increment trigger phase by 10nS (write 1 into this line, it clears automatically).

D_6 - direction of trigger phase increment (0:increase 1:decrease).

D_5 - load a preset phase delay into the trigger phase adjustment counters.

D_4 - not connected.

D_3 - 0:enable waveform output 1:write to RAM.

D_2 - RAM address $_{10}$ (RD_{10})

D_1 - RD_9

D_0 - RD_8

Figure C.4
Circuit diagram for a computer controlled function generator

AD1: D_7 - RD_7

D_6 - RD_6

D_5 - RD_5

D_4 - RD_4

D_3 - RD_3

D_2 - RD_2

D_1 - RD_1

D_0 - RD_0

AD2 & AD3:

These addresses are the way of writing the data into the RAM. D_7 to D_0 of AD2 hold the 8 most significant bits of the RAM data and D_7 to D_0 of AD3 hold the 8 least significant bits.

Note: since the digital to analog converter, which the RAM supplies with numbers, is only 12-bit, only D_7 to D_0 of AD2 and D_7 to D_4 of AD3 are used to program in the actual waveform i.e. D_3 to D_0 of AD3 do not contain data for the converter instead they are used to control the operation of the waveform generator. D_3 is an important line with regard to the working of the generator. Because the waveform data will more often than not use only a small part of the 2k of memory a pulse is needed to tell the circuit when the waveform data ends so that it can reset the address of the memory and repeat the waveform. This pulse is supplied by writing 1 into D_3 when the final waveform point is being written into the RAM and zero at every other point. D_2 is usually set to zero when writing to the RAM. It is only set to 1 at the point in the waveform where the user wants to define the point t=0 on the waveform (usually at the very first data point). The signal from D_2 is sent to the programmable trigger adjustment circuit and so phase zero is defined to be the point in the waveform that this line goes high. If it goes high twice or more during the waveform, two or more trigger pulses are generated at the specified delays. D_1 and D_0 are not important, they merely provide two extra trigger pulses (for an oscilloscope etc.) which the phase of which the user can set by writing 1 into these lines at the appropriate part of the waveform.

AD4:

This address sets the peak to peak amplitude of the output waveform from 0 to 100 mV in steps of ≈0.4 mV.

AD5 & AD6:

These two addresses allow the user to preset the delay between t=0 on the waveform and the output of the trigger pulse. The preset is loaded by writing 1 into D_5 of address AD0 as mentioned above. The delay can be adjusted between 0 and 9999, 10nS increments i.e. between 0 and 100μS. The delay is specified in BCD format as follows:

AD5:	D_7 - MSB		AD6:	D_7 - MSB	
	D_6			D_6	
	D_5	1000's		D_5	10's
	D_4 - LSB			D_4 - LSB	
	D_3 - MSB			D_3 - MSB	
	D_2			D_2	
	D_1	100's		D_1	1's
	D_0 - LSB			D_0 - LSB	

Figure C.5 overleaf shows another circuit which was designed to replace the averaging circuit in chapter 3. It is fully computer controlled and the spectrum data is outputted in the form of an optional 12 or 8 bit binary word. It requires an 8 bit data line, a 1MHz clock, a $\overline{\text{read}}$ line, a $\overline{\text{write}}$ line and 4 address lines. The addresses are as follows:

AD7:

Sets the number of samples per data point (minimum: 16, maximum: 271).

AD8:

Sets the gain of an analog amplifier (after averaging) so that weak signals may be amplified to improve height resolution when read off the ADC. The amplifier range is

Figure C.5
Circuit diagram for a computer controlled analog sampling and averaging circuit

X1 to X256. This was designed particularly for the situation where only one small peak is being examined. The input signal amplitude cannot exceed 5V peak, since any larger voltage would damage the FET switches, so any large peak in the spectrum would mean the small peak could not cover the input range of the ADC and if it was 4096 times smaller than the large peak it would not be seen. With the amplifier present this threshold drops to 1/1048576! The amplifier also allows the mass spectrometer to give the same size peaks over a pressure variation of 2.5 orders of magnitude.

AD9 & AD10:

Location of the analog to digital converter and flags connected with the conversion process.

AD9: Holds the most significant 8 bits of the ADC data

AD10: D_7, D_6, D_5, D_4 — Least significant 4 bits of ADC data (if ADC is set to 12 bit mode)

D_3 - not connected

D_2 - $\overline{\text{end of nulling}}$ / start conversion*

D_1 - $\overline{\text{end of sampling}}$

D_0 - $\overline{\text{end of conversion}}$ / start conversion*

*data line has a dual function (when written to it does one thing and when read from it indicates another).

The last three data lines of AD10 are used in controlling the various analog processes that take place. When 1 is written into D_2 it causes the analog circuit to automatically null itself (trimming its output to zero volts for whatever voltage is present at the input at the time of nulling). This process takes approximately half a second and when finished is indicated by D_2 going low. Writing 1 to D_0 starts the data collection process. It sets D_1 and D_0 high, waits for a trigger pulse and samples the input for the pre-programmed number of samples (AD7). When this is completed it sets D_1 low. The track and hold amplifier is triggered and after a short delay to let it's output settle ($\approx 1\mu S$) the ADC starts converting. When this

is completed D_0 is set low. Note: writing to any other data line has no effect.

The last circuit in this appendix, figure C.6, is not connected with the above two but designed as a replacement for the circuit given in figure 3.12. Instead of providing a trigger pulse that gives a mass spectrum with a mass scale relative to the TOF tube voltage, it gives the mass scale with respect to time. The advantage of this is that phase delays in the various circuits are no longer relevant.

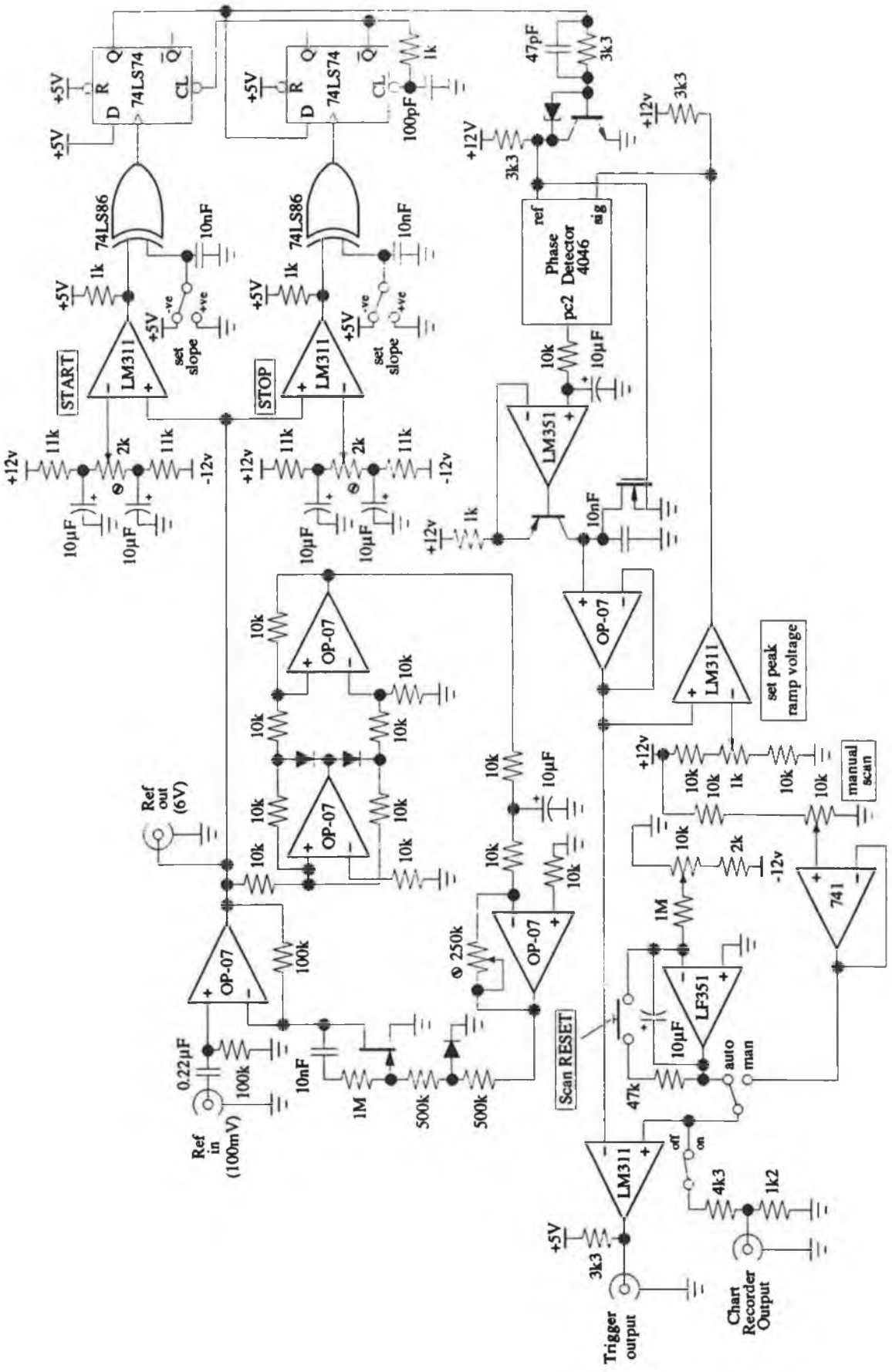

Figure C.6
Circuit diagram for an alternative trigger generator circuit with phase increasing linearly with respect to time

APPENDIX D

The following is a listing of five computer programs which were used to calculate the results and present the computer simulations used in this thesis. They were all written in the high level language "C" and all written to run on an Acorn Archimedes micro-computer.

All the programs below incorporate a file called EXITTIME which is fundamental to the simulation of the spectrometer. It is a special file called an include file which is not a program in itself but is written as if it was part of a main program. When a program is compiling and calls an include file, the text of the include file is simply placed in the program where it was called and the whole thing is then complied together. EXITTIME contains a subroutine which calculates the time an ion reaches the detector (if at all) when given the time the ion enters into the mass spectrometer from the ion source. Thus, passing a value for time to this subroutine will return a value for the time the ion comes to rest, negative if it doesn't reach the detector and positive if it does. The include file EXITTIME is given overleaf:

```
/*************************************************************

Include file:     exittime.h

requires a number of variables to be defined before it is
called in the main program.  These are:

f == frequency of tube voltage
m == mass of ion (in amu)
ac == amplitude of the AC tube voltage
dc == the magnitude of the DC component
e0 == the initial ion energy (in eV)

*************************************************************/

double exit_time(double);
double distance(int,double,double,double,float)
double velocity(int,double,double,double,float)

int dca;

double exit_time(time)
double time;
{
     int adc;
     float mas;
     double tinc,t0,t1,t2,tf,u,v,s,err;

     mas=m*1.66057e-27;
     v=u=pow(2*10.0*1.60219e-19/mas,0.5);
     tf=t0=time; s=0.0; adc=dca=dc;

     for(tinc=1.0e-9;s<4.5e-3 && v>0;tinc*=2.0)
     {
        tf+=tinc;
        s=distance(1,t0,tf,u,4.5e-3);
        v=velocity(1,t0,tf,u,4.5e-3);
     }

     if (v<0 && s<4.5e-3) tf=t0;

     if(s>4.5e-3)
     {
        t1=tf-tinc/2.0; t2=tf;
        do
        {
          tf=(t1+t2)/2.0;
          s=distance(1,t0,tf,u,4.5e-3);
          err=fabs(s-4.5e-3);
          if(s<4.5e-3) t1=tf; else t2=tf;
        }
        while(err>1.0e-6);
        v=velocity(1,t0,tf,u,4.5e-3);
     }

     if(v>0) tf+=0.2545/v;

     t0=tf; u=v; s=0.0;
     for(tinc=1.0e-9;s<4.0e-3 && v>0;tinc*=2.0)
     {
```

```
    tf+=tinc;
    s=distance(-1,t0,tf,u,4.0e-3);
    v=velocity(-1,t0,tf,u,4.0e-3);
  }

  if (v<0 && s<4.0e-3) tf=t0;

  if(s>4.0e-3)
  {
    t1=tf-tinc/2.0; t2=tf;
    do
    {
      tf=(t1+t2)/2.0;
      s=distance(-1,t0,tf,u,4.0e-3);
      err=fabs(s-4.0e-3);
      if(s<4.0e-3) t1=tf; else t2=tf;
    }
    while(err>1.0e-6);
    v=velocity(-1,t0,tf,u,4.0e-3);
  }

  t0=tf; u=v; s=0.0;
  for(tinc=1.0e-9;s<3.5e-3 && v>0;tinc*=2.0)
  {
    tf+=tinc;
    s=distance(1,t0,tf,u,3.5e-3);
    v=velocity(1,t0,tf,u,3.5e-3);
  }

  if (v<0 && s<3.5e-3) tf=t0;

  if(s>3.5e-3)
  {
    t1=tf-tinc/2.0; t2=tf;
    do
    {
      tf=(t1+t2)/2.0;
      s=distance(1,t0,tf,u,3.5e-3);
      err=fabs(s-3.5e-3);
      if(s<3.5e-3) t1=tf; else t2=tf;
    }
    while(err>1.0e-6);
    v=velocity(1,t0,tf,u,3.5e-3);
  }

  t0=tf; u=v; s=0.0;
  if(v>0)
  {
    dca=2600-adc;
    for(tinc=1.0e-9;s<1.0e-2;tinc*=2)
    {
      tf+=tinc;
      s=distance(-1,t0,tf,u,1.0e-2);
    }

    t1=tf-tinc/2.0; t2=tf;
    do
    {
      tf=(t1+t2)/2.0;
      s=distance(-1,t0,tf,u,1.0e-2);
```

```
            err=fabs(s-1.0e-2);
            if(s<1.0e-2) t1=tf; else t2=tf;
          }
          while(err>1.0e-6);
          tf+=7.0e-8; /* EM tube & amplifier delay ≈ 70nS */
        }

        if(v<0) tf*=-1;

        return tf;
}


double distance(dir,t1,t2,u,grid)
int dir;
double t1,t2,u;
float grid;
{
        double s,w,mas;
        w=2*3.14159265358*f;
        mas=m*1.66057e-27;

        s=u*(t2-t1)
          -dir*1.60219e-19*dca*(t2*t2-t1*t1)/(2*grid*mas)
          +dir*1.60219e-19*dca*t1*(t2-t1)/(grid*mas)
          +dir*1.60219e-19*ac*(cos(w*t2)-cos(w*t1))
                                          /(w*w*grid*mas)
          +dir*1.60219e-19*ac*sin(w*t1)*(t2-t1)/(w*grid*mas);

        return s;
}


double velocity(dir,t1,t2,u,grid)
int dir;
double t1,t2,u;
float grid;
{
        double v,w,mas;
        w=2*3.14159265358*f;
        mas=m*1.66057e-27;

        v=u
          -dir*1.60219e-19*dca*(t2-t1)/(grid*mas)
          -dir*1.60219e-19*ac*(sin(w*t2)-sin(w*t1))
                                          /(w*grid*mas);

        return v;
}
```

```
/*************************************************

Program name:      singraph

Plots the ion exit curves on screen after inputing
various parameters.

*************************************************/

#include <stdio.h>
#include <math.h>
#include <Arthur.h>
#include <float>
#include <stdlib.h>

#define e 1.60219e-19
#define pi 3.14159265358
#define e0 10

void setup(void);
double voltage(double);
int xcoor(float);
int ycoor(float);

int m,dc,ac;
long f;
float c;

#include <exittime.h>

void main()
{
     int ml,mlflag,z,mas[10],x,flag;
     double t0,tl;

     mode(15);
     colour(133);
     cls();

     /**********  question time  **********/

     tab(2,4);
     printf("What is the frequency (kHz)?");
     scanf("%d",&f);   f=f*1000;

     tab(2,6);
     printf("What is the bias voltage (V)?");
     scanf("%d",&dc);

     tab(2,8);
     printf("What is the peak AC amplitude (V)?");
     scanf("%d",&ac);   abs(ac);

     mlflag=0;  z=2;
     do
     {
        tab(2,10);
        printf("What atomic mass lines do you ");
        printf("want displayed (amu)?");
        scanf("%d:,&ml);
```

```
            tab(53,10);
            printf("          ");
            if(ml>0 && mlflag<10)
            {
              mas[mlflag]=ml;
              mlflag++;
              tab(z,12);
              printf("%d",ml);
              z+=2+log10(ml);
            }
         }
         while(ml>0);
         for(x=mlflag;x<10;x++) mas[x]=0;
         mlflag--;

         tab(2,14);
         printf("How many cycles do you want displayed?");
         scanf("%f",&c);

         /**********  start graph  **********/

         cursor(0);
         setup();
         for(flag=0;flag<=mlflag;flag++)
         {
            m=mas[flag];
            do; while(inkey(-74));
            for(t0=0.0;t0<=c/f;t0+=c/(f*1268))
            {
              t1=exit_time(t0);
              if(t1<0)
              {
                 gcol(0,2);
                 t1*=-1;
              }
              else gcol(0,1);
              plot(69,xcoor(t1),ycoor(voltage(t0)));
              system("*fx21,0");
              if(inkey(-74)) break;
            }
         }
         cursor(1);
         printf("\n");
}

void setup()
{
         int uplimit,lolimit;
         float t0;

         mode(12);

         gcol(0,128);
         clg();
         colour(6);
         colour(128);
         cls();

         palette(8,16,50,50,50);
         palette(9,16,100,100,150);
```

```
        gcol(0,8);
        move(11,ycoor(dc));
        draw(1279,ycoor(dc));
        gcol(0,9);
        move(0,ycoor(0));
        draw(1279,ycoor(0));

        uplimit=(int)floor((dc+ac)/10)*10+10;
        lolimit=(int)floor((dc-ac)/10)*10-10;
        do
        {
           uplimit-=10;
           move(5,ycoor(uplimit));
           draw(15,ycoor(uplimit));
        }
        while(uplimit>lolimit);

        move(10,0);
        draw(10,1023);
        gcol(0,7);
        for(t0=0.0;t0<=c/f;t0+=c/(f*1268))
        {
           plot(69,xcoor(t0),ycoor(voltage(t0)));
        }
}

double voltage(time)
double time;
{
        double v;
        v=dc+ac*cos(2*pi*f*time);
        return v;
}

int xcoor(time)
float time;
{
        int x;
        x=(int)(time*1268.0*f/c+11);
        return x;
}

int ycoor(voltage)
float voltage;
{
        int y;
        y=(int)((voltage-(dc-ac))*1023/(2*ac));
        return y;
}
```

```
/*******************************************************

Program name:      sinfile

Plots the ion exit curve into a file "graphdata" in
subdirectory john, after inputing parameters from the
keyboard (also plots on the screen - similar to
"singraph").  The file "graphdata" may be imported
directly into GRAPHBOX for storage as a drawing.

*******************************************************/

#include <stdio.h>
#include <math.h>
#include <Arthur.h>
#include <float>
#include <stdlib.h>

#define e 1.60219e-19
#define pi 3.14159265358
#define e0 10

void setup(void);
double voltage(double);
int xcoor(float);
int ycoor(float);

int m,dc,ac;
long f;
float c;
FILE *fp;

#include <exittime.h>

void main()
{
     int ml,mlflag,z,mas[10],x,flag;
     double t0,t1;

     fp=fopen("$.john.graphdata","w");

     mode(15);
     colour(133);
     cls();

     /**********  question time  **********/

     tab(2,4);
     printf("What is the frequency (kHz)?");
     scanf("%d",&f);   f=f*1000;

     tab(2,6);
     printf("What is the bias voltage (V)?");
     scanf("%d",&dc);

     tab(2,8);
     printf("What is the peak AC amplitude (V)?");
     scanf("%d",&ac);   abs(ac);

     mlflag=0;  z=2;
```

```
      do
      {
         tab(2,10);
         printf("What atomic mass lines do you ");
         printf("want displayed (amu)?");
         scanf("%d:,&ml);
         tab(53,10);
         printf("          ");
         if(ml>0 && mlflag<10)
         {
           mas[mlflag]=ml;
           mlflag++;
           tab(z,12);
           printf("%d",ml);
           z+=2+log10(ml);
         }
      }
      while(ml>0);
      for(x=mlflag;x<10;x++) mas[x]=0;
      mlflag--;

      tab(2,14);
      printf("How many cycles do you want displayed?");
      scanf("%f",&c);

      /**********  start graph  **********/

      cursor(0);
      setup();
      for(flag=0;flag<=mlflag;flag++)
      {
         m=mas[flag];
         do; while(inkey(-74));
         for(t0=0.0;t0<=c/f;t0+=c/(f*1268))
         {
           t1=exit_time(t0);
           if(t1<0)
           {
              gcol(0,2);
              t1*=-1;
           }
           else gcol(0,1);
           plot(69,xcoor(t1),ycoor(voltage(t0)));
           fprintf(fp,"%d,%d\n",xcoor(t1),
                                ycoor(voltage(t0)));
           system("*fx21,0");
           if(inkey(-74)) break;
         }
      }
      cursor(1);
      printf("\n");
      fclose(fp);
}

void setup()
{
      int uplimit,lolimit;
      float t0;

      mode(12);
```

```
        gcol(0,128);
        clg();
        colour(6);
        colour(128);
        cls();

        palette(8,16,50,50,50);
        palette(9,16,100,100,150);

        gcol(0,8);
        move(11,ycoor(dc));
        draw(1279,ycoor(dc));
        gcol(0,9);
        move(0,ycoor(0));
        draw(1279,ycoor(0));

        uplimit=(int)floor((dc+ac)/10)*10+10;
        lolimit=(int)floor((dc-ac)/10)*10-10;
        do
        {
           uplimit-=10;
           move(5,ycoor(uplimit));
           draw(15,ycoor(uplimit));
        }
        while(uplimit>lolimit);

        move(10,0);
        draw(10,1023);
        gcol(0,7);
        for(t0=0.0;t0<=c/f;t0+=c/(f*1268))
        {
           plot(69,xcoor(t0),ycoor(voltage(t0)));
        }
}

double voltage(time)
double time;
{
        double v;
        v=dc+ac*cos(2*pi*f*time);
        return v;
}

int xcoor(time)
float time;
{
        int x;
        x=(int)(time*1268.0*f/c+11);
        return x;
}

int ycoor(voltage)
float voltage;
{
        int y;
        y=(int)((voltage-(dc-ac))*1023/(2*ac));
        return y;
}
```

```
/*************************************************************

Program name:      peakgraph

This program calculates the outline of the detected ion
current and outputs the curve into a data file called
"iondata", in subdirectory john, in a format that is
acceptable to GRAPHBOX.

*************************************************************/

#include <stdio.h>
#include <math.h>
#include <Arthur.h>
#include <float>
#include <stdlib.h>

#define e 1.60219e-19
#define pi 3.14159265358
#define e0 10
#define f 45000
#define dc -50
#define ac 150

int abs(int);
int xcoor(double);

int m;

#include <exittime.h>

void main()
{
     int ml,mlflag,z,x,flag,mas[20],output[1001];
     FILE *fp;
     double t0,tl,tb;

     mode(15);
     colour(133);
     cls();

     mlflag=0;  z=2;
     do
     {
        tab(2,4);
        printf("What atomic mass lines do you ");
        printf("want displayed (amu)?");
        scanf("%d:,&ml);
        tab(53,4);
        printf("          ");
        if(ml>0 && mlflag<20)
        {
          mas[mlflag]=ml;
          mlflag++;
          tab(z,6);
          printf("%d",ml);
          z+=2+log10(ml);
        }
     }
     while(ml>0);
```

```
        cls();

        for(x=mlflag;x<20;x++) mas[x]=0;
        mlflag--;

        /**********   start calculations   **********/

        for(x=0;x<=1000;x++) output[x]=0;

        tab(0,0);printf("Mass =      amu");
        tab(0,1);printf("tstart =         uS");
        tab(0,2);printf("%%time =");
        tab(0,3);printf("tfinish =         uS");
        tab(0,4);printf("tbreak =         uS");

        for(flag=0;flag<=mlflag;flag++)
        {
           m=mas[flag];
           tab(7,0);printf("%3d",m);
           do; while(inkey(-74));

           for(t0=0.0,tb=1.0/f;t0<=1.0/f;t0+=1.0e-9)
           {

             tab(10,1);printf("%2.3f",t0*1e6);
             tab(8,2);printf("%3.1f",f*t0*100);

             t1=exit_time(t0);
             if(t1<tb && t1>0) tb=t1;

             tab(10,3);printf("%2.3f",t1*1e6);
             tab(10,4);printf("%2.3f",tb*1e6);

             if(inkey(-74)) break;
             if(t1<0) continue;
             if(xcoor(t1)>0 && xcoor(t1)<1000)
             {
                output[xcoor(t1)]++;
             }
           }
        }

        fp=fopen("$.john.iondata","w");
        tab(0,6);
        printf("Writing to file \"$.john.iondata\"");
        for(x=0;x<=1000;x++)
        fprintf(fp,"%d,%d\n",x,output[x]);
        fclose(fp);

        printf("\n\n");
}

int xcoor(time)
double time;
{
        int t;
        float tl,tu;    /**  tu-tl :== view window **/

        tl=1.1e-5;  tu=3.3e-5;
```

```
        t=(int)((time-tl)*1000/(tu-tl));
        return t;
}
```

```
/*************************************************************

Program name:       HAFtable

Calculates the density of ions exiting the tube at
breakthrough by injecting ions of different mass every
1nS, over the period t=0 to t=3/4(tube period) and
counting the number of those that appear at the
breakthrough times.  It writes this number (Y co-ordinate)
with the corresponding atomic mass (X co-ordinate) into a
file "HAFlist" in a format suitable for GRAPHBOX.

*************************************************************/

#include <stdio.h>
#include <math.h>
#include <Arthur.h>
#include <float>
#include <stdlib.h>

#define e 1.60219e-19
#define pi 3.14159265358
#define e0 10
#define f 45000
#define dc -150
#define ac 50

int abs(int);
int xcoor(double);

int m;

#include <exittime.h>

void main()
{
     int x,haf[100],output[1000];
     FILE *fp;
     double t0,t1;
     fp=fopen("$.john.HAFlist","w");

     mode(15);
     colour(133);
     cls();

     /**********   start calculations   **********/

     for(x=0;x<=100;x++) haf[x]=0;

     tab(0,6);
     printf("Writing to file \"$.john.HAFlist\"");

     for(m=1;m<=100;m++)
     {
        printf("\nmass = %d amu",m);
        for(x=0;x<=1000;x++)
        {
          output[x]=0;
        }
        for(t0=0.0;t0<=0.75/f;t0+=1.0e-9)
```

```
            {
              t1=exit_time(t0);
              if(t1<0) continue;
              if(xcoor(t1)>0 && xcoor(t1)<1000)
              {
                 output[xcoor(t1)]++;
              }
            }
            for(x=0;x<=1000;x++)
            {
              if(haf[m]<output[x]) haf[m]=output[x];
            }
            fprintf(fp,"%d,%d\n",m,haf[m]);
         }
         fclose(fp);
         printf("\n\n");
}

int xcoor(time)
double time;
{
         int t;
         float t1,tu;    /**  tu-t1 :== view window **/

         t1=7.0e-6;  tu=2.3e-5;

         t=(int)((time-t1)*1000/(tu-t1));
         return t;
}
```

```
/************************************************************

Program name:    Exptcomp

Calculates the breakthrough times for a preset list of
atomic masses and compares the calculated times with the
experimental times.

************************************************************/

#include <stdio.h>
#include <math.h>
#include <Arthur.h>
#include <float>
#include <stdlib.h>

#define ac 150
#define f 45000

int m,dc;

main()
{
     int mflg,mls[15];
     float brkt[15];
     double ts,ts1,ts2,ts3,tf,p;

     mls[0]=14;mls[1]=15;mls[2]=16;mls[3]=18;
     mls[4]=20;mls[5]=28;mls[6]=32;mls[7]=40;

     mls[8]=14;mls[9]=15;mls[10]=16;mls[11]=18;
     mls[12]=20;mls[13]=28;mls[14]=32;mls[15]=40;

     brkt[0]=14.2;brkt[1]=14.3;brkt[2]=14.4;
     brkt[3]=14.79;brkt[4]=15.15;brkt[5]=16.33;
     brkt[6]=16.91;brkt[7]=17.89;

     brkt[8]=15.15;brkt[9]=15.37;brkt[10]=15.59;
     brkt[11]=16.07;brkt[12]=16.47;brkt[13]=17.87;
     brkt[14]=18.51;brkt[15]=19.6;

     for(mflg=0;mflg<=15;mflg++)
     {
     if(mflg<=7) dc=-50; else dc=0;
     m=mls[mflg];
     p=2.0/f+0.5;
     for(ts=0.0;ts<=1/(f*2.0)+0.5e-6;ts+=1.0e-7)
     {
        tf=exit_time(ts);
        if(tf<=0) continue;
        if(p>tf) { p=tf; ts1=ts; }
     }

     ts2=ts1;

     for(ts=ts1-1.0e-7;ts<=ts1+1.0e-7;ts+=1.0e-8)
     {
        tf=exit_time(ts);
        if(tf<=0) continue;
        if(p>tf) { p=tf; ts2=ts; }
```

```
        }

        ts3=ts2;

        for(ts=ts2-1.0e-8;ts<=ts2+1.0e-8;ts+=1.0e-9)
        {
           tf=exit_time(ts);
           if(tf<=0) continue;
           if(p>tf) { p=tf; ts3=ts; }
        }
        if(mflg==0) printf("\n\nDC component = -50V");
        if(mflg==8) printf("\n\nDC component = 0V");
        if(mflg==0 || mflg==1 || mflg==2 || mflg==15)
        {
           printf("\nMass = %3d amu",m);
           printf("  T expt = %3.1f uS",brkt[mflg]);
           printf("  T calc = %3.2f uS",(p+5.0e-9)*1e6);
        }
        else
        {
           printf("\nMass = %3d amu",m);
           printf("  T expt = %3.2f uS",brkt[mflg]);
           printf("  T calc = %3.2f uS",(p+5.0e-9)*1e6);
           printf(" ( %3.0f nS )",((p+5.0e-9)*1.0e6
                                   -brkt[mflg])*1.0e3);
        }
        }
        printf("\n\n");
    }
```

APPENDIX E

The transformer used in the time-of-flight tube driver was specially wound and this appendix outlines its electrical equivalent circuit. Several computer programs were written to simulate its response at various frequencies.

In general, a transformer can be represented electrically by the following circuit [15]:

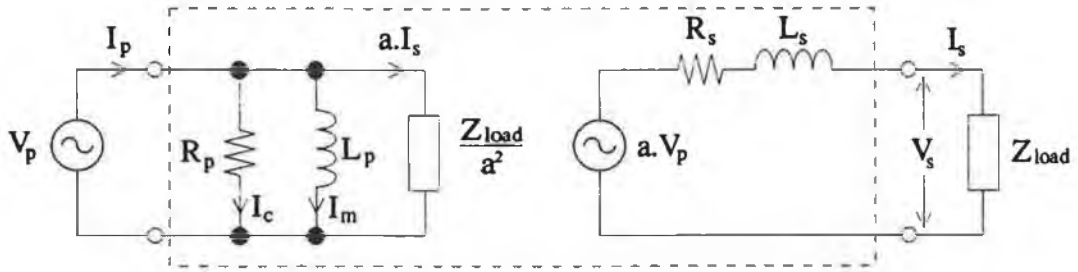

Figure E.1 **Electrical equivalent circuit of a transformer**

where

I_c is the core loss current, representing power dissipated in hysteresis and eddy current loss. I_c is in phase with voltage V_p so that the product is power.

R_p is the resistance accounting for the power loss.

I_m is the magnetising current. It is this current that establishes the magnetic flux. It lags the voltage by 90° and is in phase with the magnetic flux which it produces.

L_p is the inductance accounting for energy storage in the magnetic field.

R_s is the resistance, including the effects of both windings, that accounts for power loss in the resistance of windings due to the presence of I_s.

L_s is the inductance representing energy stored in leakage fields, i.e. magnetic flux lines set up in the secondary due to I_s that do not intersect the primary coil due to the non-ideal shape of the magnetic core.

a is the ratio of the secondary voltage V_s, to the

primary voltage V_p, with the secondary unloaded.

By leaving the secondary unloaded (open circuit test) the primary current is simply the excitation current of the transformer, i.e. $I_c + jI_m$, and from measuring its magnitude and phase relative to the applied voltage V_p, R_p and L_p may be determined.

Connecting zero ohms across the secondary terminals (short circuit test) and increasing the primary voltage until the rated secondary current is reached will allow the values R_s and L_s to be determined, by observing the magnitude and phase of the secondary current with respect to "a" times the primary voltage.

The equivalent of the mass spectrometer's transformer is shown below

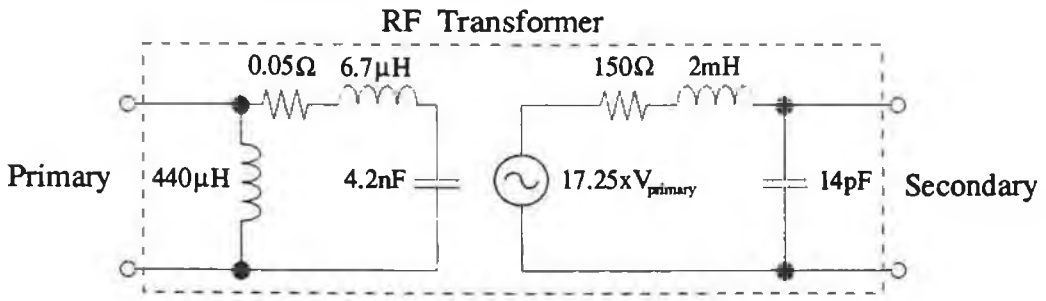

Figure E.2 **Mass spectrometer radio-frequency transformer**

The 14pF across the secondary represents the capacitance between the windings in the secondary which looks like 4.2nF at the primary (a=17.25) and was found by observing the frequency at which the primary circuit resonates with the secondary unloaded. R_p was so large relative to the impedance of L_p that it was immeasurable.

Figure E.3 overleaf shows the equivalent circuit of the primary with the secondary loaded with a 300pF capacitor (the TOF tube) in parallel with a 2.5MΩ resistor (the oscilloscope probe).

$$Z_T = \left[R_1 + \frac{\omega G L_1 (F+\omega L_1) - \omega G F L_1}{G^2 + (F+\omega L_1)^2} \right] + j \left[\frac{\omega G^2 L_1 + \omega F L_1 (F+\omega L_1)}{G^2 + (F+\omega L_1)^2} \right]$$

where

$$G = R_2 + \frac{R_2}{(R_3\omega C_1)^2 + 1} \quad \text{and} \quad F = \omega L_2 - \frac{R_3^2\omega C_1}{(R_3\omega C_1)^2 + 1}$$

This equation was used in a computer to calculate, among other things, the phase of V_s with respect to V_p for different frequencies, because it was originally proposed to use the transformer in a negative feedback loop so that its output voltage could be set accurately by computer control and be in phase with a computer generated reference signal.

Figure E.4 overleaf shows the experimental and computer calculated response curves for the transformer and demonstrates the accuracy of the model.

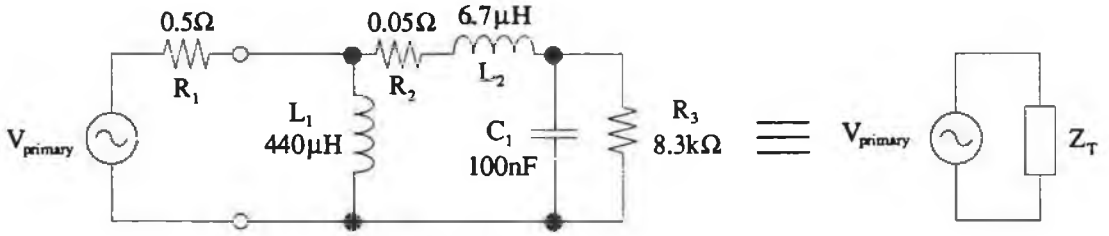

Figure E.3 **Electrical equivalent circuit of primary with a 300pF||2.5MΩ load on the secondary**

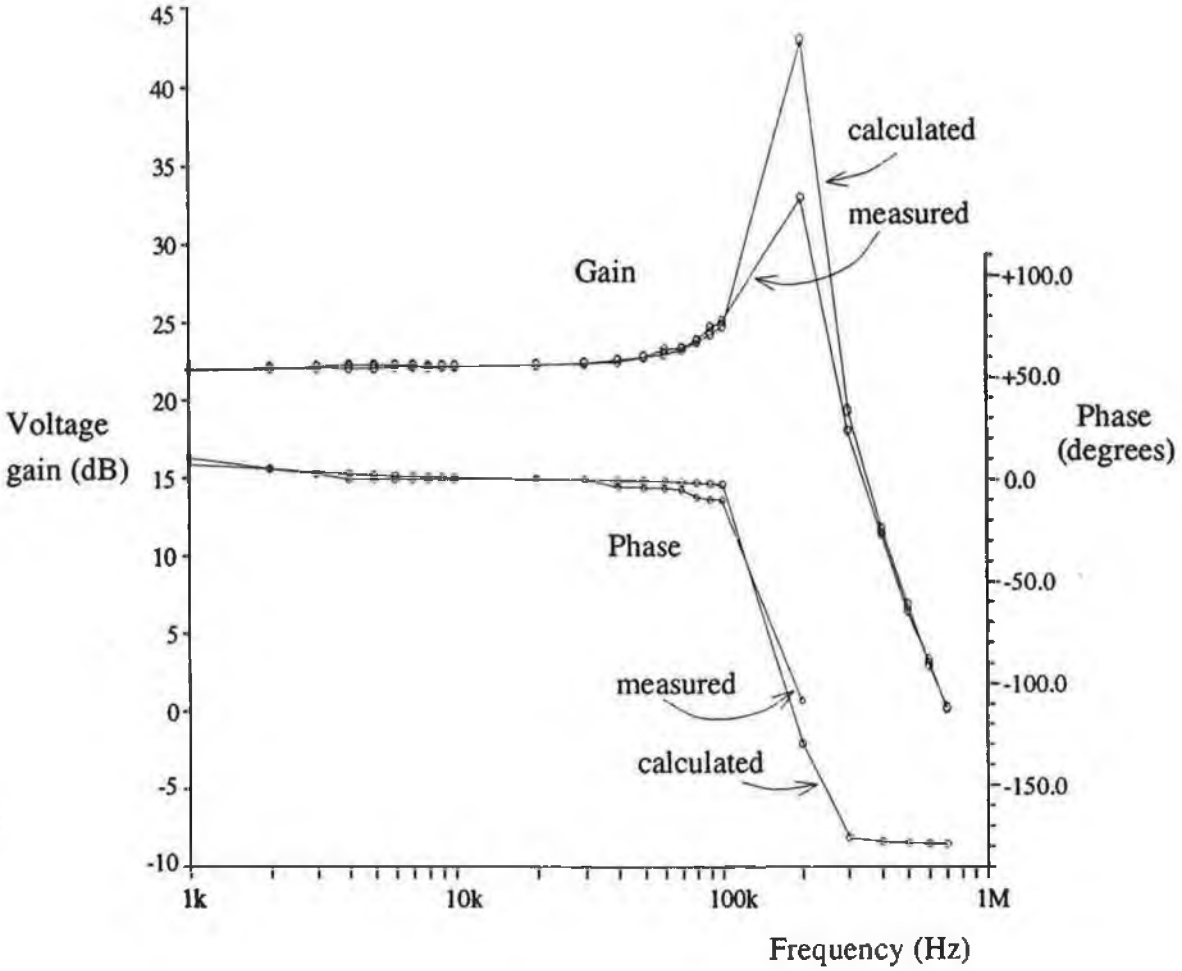

Figure E.4 **Calculated and measured response curves for the RF transformer**

APPENDIX F

Figure F.1 below is a computer simulation of the exit curve of an ion of mass 100 amu, as shown previously in figure 2.11. As mentioned in chapter 2, the detected ion current can be obtained from the slope of the ion exit curve and in this appendix the relationship between the two is examined.

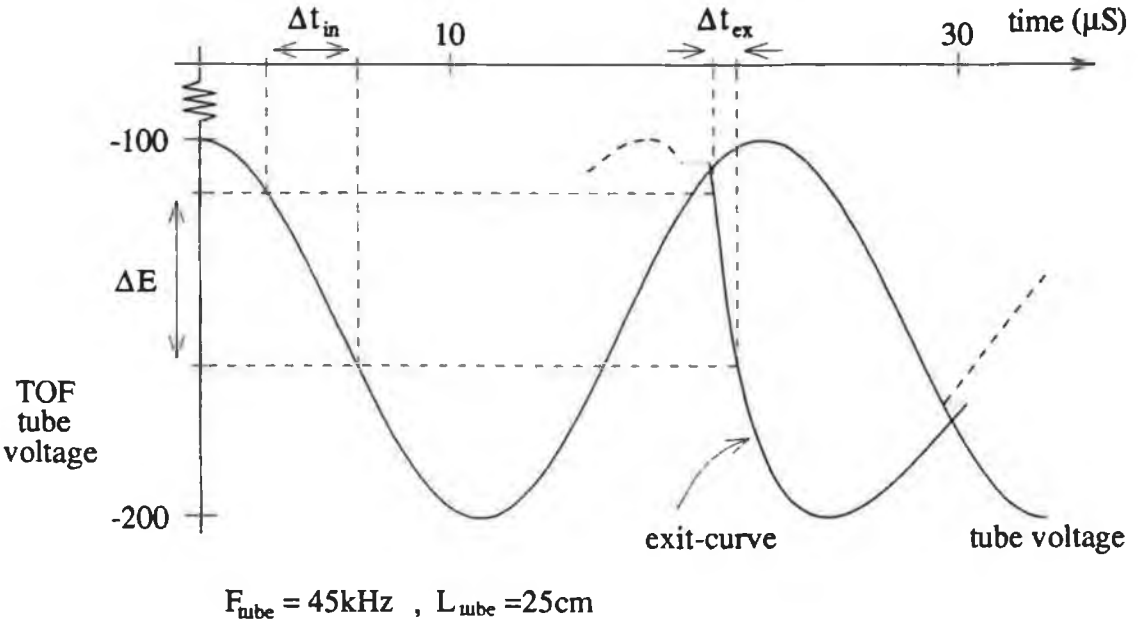

Figure F.1 **Computer simulation of the exit-curve for 100 amu**

Consider a small increment in time Δt_{ex}, shown in the figure, from which the slope is to be determined, via;

$$M_{slope} = \frac{\Delta E}{\Delta t_{ex}} \qquad eV\ s^{-1}$$

Now, the ion current during the time Δt_{ex} is simply the number of ions entering the tube with an energy within the range ΔE divided by Δt_{ex} i.e.

$$i_{exit} = \frac{N_{ions}(\Delta E)}{\Delta t_{ex}}$$

The number of ions with an energy within the range ΔE is the number that entered during the time Δt_{in}. The slope of the co-sinusoidal curve is

$$M_{cos} = \frac{\Delta E}{\Delta t_{in}} \qquad eV\ s^{-1}$$

i.e.

$$\Delta t_{in} = \frac{\Delta E}{M_{cos}}$$

Assuming that the ion input is constant, the number of ions entering the tube is simply proportional to Δt_{in}, i.e.

$$N_{ions}(\Delta E) = k \cdot \Delta t_{in}$$

$$\Rightarrow \quad N_{ions} = \frac{k}{M_{cos}} \cdot \Delta E \quad = \frac{k \cdot M_{slope}}{M_{cos}} \cdot \Delta t_{ex}$$

$$\Rightarrow \quad i_{exit} = \frac{k \cdot M_{slope}}{M_{cos}}$$

Taking the limit where Δt_{ex}, ΔE and Δt_{in} tend toward zero, this equation becomes

$$I_{exit} = I_{in} \left| \frac{M_{slope}}{-\omega B \cdot \sin(\omega t_{in})} \right|$$

where the AC component of the tube voltage is given by $B \cdot \cos(\omega t)$ and t_{in} is the time at which the ion has to enter the mass spectrometer in order to exit at the point in the exit curve, for which I_{exit} is being calculated. The modulus is taken because the sign of the equation has no meaning; I_{exit} is the number of coulombs of charge being detected per second (1 coulomb = 6.24×10^{18} singly charged ions) and it makes no sense to detect a negative number of ions.